Australian Government
Geoscience Australia

4th Biennial Conference on Asian Current Research on Fluid Inclusions ACROFI IV

10 – 12 August 2012, Brisbane, Australia

ABSTRACTS

Record
2012/50

GeoCat #
74234

Terrence P. Mernagh, Steffen G. Hagemann, and Vadim S. Kamenetsky (Editors)

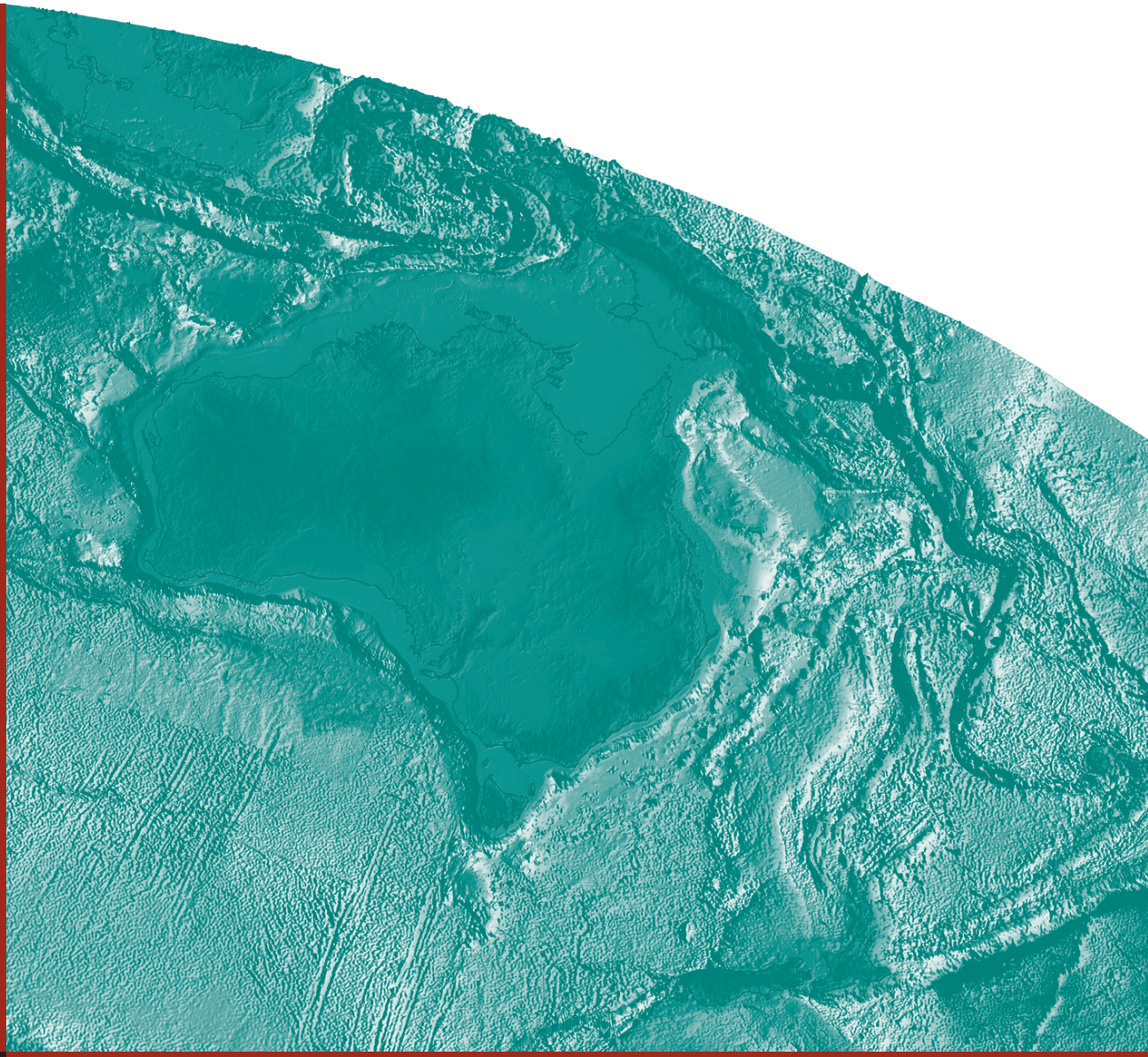

4th Biennial Conference on Asian Current Research on Fluid Inclusions ACROFI IV

10 – 12 August 2012, Brisbane, Australia

ABSTRACTS

GEOSCIENCE AUSTRALIA
RECORD 2012/50

Terrence P. Mernagh[1], Steffen G. Hagemann[2], and Vadim S. Kamenetsky[3] (Editors)

Australian Government
Geoscience Australia

1. Geoscience Australia, GPO Box 378, Canberra, ACT 2601, Australia
2. Centre for Exploration Targeting, The University of Western Australia, Crawley, Western Australia 6009, Australia
3. ARC Centre of Excellence in Ore Deposits, University of Tasmania, Hobart, Tasmania, 7001 Australia

Department of Resources, Energy and Tourism
Minister for Resources and Energy: The Hon. Martin Ferguson, AM MP
Secretary: Mr Drew Clarke

Geoscience Australia
Chief Executive Officer: Dr Chris Pigram

This paper is published with the permission of the CEO, Geoscience Australia

ISSN 1448-2177
ISBN 0 642 978-1-922103-52-9

GeoCat # 74234

Bibliographic reference: Mernagh, T.P., Hagemann, S.G. and Kamenetsky, V.S. (eds) 2012. 4th Biennial Conference on Asian Current Research on Fluid Inclusions ACROFI IV. Record 2012/50. Geoscience Australia: Canberra.

Contents


ECROFI-XXII
22ND BIENNIAL CONFERENCE
EUROPEAN CURRENT
RESEARCH ON FLUID INCLUSIONS
5-9 JUNE 2013
ANTALYA
Cumhuriyet University
Istanbul University
Turkey
www.ecrofi2013.org

Preface

The Asian Current Research on Fluid Inclusions (ACROFI) is the biannual meeting of fluid-inclusion researchers from Asian countries. It has the same format as its highly successful counterparts, the European ECROFI and the Pan-American PACROFI. The conference provides an international forum for exchange of the latest research results and ideas between geoscientists from academia, government and industry from Asian countries and the rest of the world. It focuses on studies of fluid- and silicate-melt inclusions. Students are also encouraged to come to ACROFI to present their results and meet other experts in this field of research.

The inaugural ACROFI meeting (ACROFI I) was held at the Nanjing University, China on 26–28 May 2006. The meeting was well represented by all the Asian countries and Australia with delegates from America and Europe in attendance. The second meeting (ACROFI II) took place at the Indian Institute of Technology, Kharagpur, India 12–14 November 2008. The third meeting (ACROFI III) took place at the Institute of Geology and Mineralogy of SB RAS, Novosibirsk, Russia 15–20 September, 2010. Australia was chosen to host the ACROFI IV meeting which was held at the Queensland University of Technology in Brisbane, 10–12 August 2012.

ACROFI IV has been organised around the following themes:

1. New developments for the study of fluid and melt inclusions
2. Magmatic melts and fluids
3. Metamorphic fluids
4. Subsurface and basinal fluids
5. Fluid and melt inclusions associated with ore deposits and mineral exploration
6. Novel fields of fluid inclusion research

The following abstracts are printed in author alphabetical order following the standard practice although during the conference they will be presented according to the above mentioned themes. A large number of fluid inclusion studies are carried out to gain a better understanding of how various mineral systems form and the challenge is how to better use this information for mineral exploration. The study of silicate melt inclusions has also gained prominence in recent years and is providing new information on fluid immiscibility and partitioning of various elements between melts and fluids. Experimental studies are also important for understanding how fluid and melt inclusions form and for providing information on the chemical systems of relevance to fluid and melt inclusion research. An interesting theme emerging from the abstracts submitted for this conference is that our traditional understanding of how fluid inclusions form may not always be correct. Several abstracts discuss the possibility that inclusions may initially form in non-crystalline silica or from colloidal solutions. This could be the start of a paradigm shift in our understanding of how fluid inclusions form under certain conditions and highlights the need for more research on this subject.

The study of fluid inclusions was pioneered by H.C. Sorby, A.P. Karpinsky, P. Nakken, and G.G. Lemmlein. Our understanding of fluid inclusions in the subsequent 154 years has expanded enormously. However, just as the invention of the microscope kick started the study of fluid inclusions, the recent development of sensitive microanalytical techniques will enable a much greater understanding of geological fluids.

Terrence P. Mernagh

Conditions of VMS, Mn- and Au-bearing hydrothermal systems formation from the Magnitogorsk Paleo-island Arc System, Southern Urals: Fluid inclusion data

N.N. Ankusheva, V.V. Zaykov
Institute of Mineralogy, Urals Branch, Russian Academy of Sciences, Miass, Russia

The formation of the VMS, Mn- and Au-bearing deposits is caused by hydrothermal fluids and their study is a key to understand ore-forming processes. The aim of this abstract is an overview of results from a fluid inclusion study of VMS and Au hydrothermal systems from the Magnitogorsk paleoisland arc system. Fluid inclusion data were obtained with using criometry and thermometry on barite, calcite and quartz. The Magnitogorsk paleoisland arc system consists of the Eifelian West-Magnitogorsk (WM) paleo-island arc, Sibay inter-arc basin and Givetian East-Magnitogorsk (EM) paleoisland arc (Puchkov, 2000).

The lower part of the WM paleoisland arc hosts gold-polymetallic type VMS deposits associated with the rhyolite-basalt complex of the Baymak ore area. Hydrothermal systems of the *Tash-Tau* and *Vishnevka* deposits consist of stringer-disseminated ores, feeder channels with calcite and quartz, and quarts veins in supra-ore dacites. NaCl with $MgCl_2$ and $CaCl_2$ prevail in salt composition and fluid salinity is 2–8 wt. % NaCl-eq. The homogenisation temperatures (T_{hom}) are 250–300 °C for sulphide-quartz veins from the Tash-Tau deposit, 160–170 °C for feeder channels and 120–200 °C for quartz and calcite veins in dacites, andesites and rhyolites from the Vishnevka deposit.

For the *Balta-Tau* deposit fluid inclusion data were obtained for stringer-disseminated ores (Holland et al., 2003). Homogenisation temperatures (T_h) of fluid inclusions in quartz and barite are 140–180 °C. First melting temperatures (T_{fm}) indicate NaCl–H_2O and NaCl–KCl–H_2O salt systems with salinity of 3–4.5 wt. % NaCl-eq.

Fluid inclusions in gangue minerals were studied in the *Severny Uvaryazh* (Au-bearing sulphide-barite ores in rhyodacites), *Utrenneye* (Au-bearing stringer-disseminated chalcopyrite-sphalerite and sphalerite ores with calcite in brecciated rhyolites), *Zvezdnoe* (sulphide veinlets with quartz and barite in sericite-quartz metasomatites) deposits. Au-bearing veins were formed due to hydrothermal fluids with salinities of 1.8 (Utrenneye) up to 11.9 wt. % NaCl-eq. (Severny Uvaryazh). T_{fm} indicate NaCl-Na_2SO_4–H_2O (Severny Uvaryazh), NaCl–H_2O и NaCl–$MgCl_2$–H_2O (Utrenneye and Zvezdnoe) salt systems. T_{hom} is 145–170 °C.

The *Yanzigitovo* Mn-bearing deposit (Sibay inter-arc basin) is located at the southern flank of an anticline structure which hosts numerous VMS deposits. A hematite-quartz edifice 20 m thick and 15–200 m long is situated at the top of the rhyolite-basalt sequence (Telenkov and Maslennikov, 1995). Fluid inclusions in quartz from dendritic, net-shaped and zonal hematite-quartz veins were studied. It was established that veins were formed from NaCl-fluids with salinity of 2.7–6 wt. % NaCl-eq and temperatures 200–230 °C.

The lower part of the EM paleoisland arc contains Cu-Zn VMS deposits of the Verchneuralsky ore region (Uzelga, Chebach'e, Talgan, Zapadno-Ozernoe). Fluid inclusion data in barite, quartz, carbonates, and sphalerite indicate that chloride-hydrocarbonate-sulphite ore-forming fluids have temperatures of 110–360 °C and salinities of 1–10 wt. % NaCl-eq (Karpukhina and Baranov, 1995). The *Lis'i Gory* Au-bearing ore field is located within andesite-basalt and siliceous sequences at the top part of the EM paleoisland arc. It includes Au-bearing siliceous zones and hematite-quartz

edifices which were formed from NaCl-fluids with salinity of 1.5–7 wt. % NaCl-eq. T_h is 120–290 °C.

Thus, fluid inclusion data allowed us to describe the history of hydrothermal activity provided for the formation of sulphide and gold mineralisation in the Magnitogorsk paleoisland arc system. The fluids which formed massive sulphide deposits at the lower part both of the WM and EM paleoisland arcs, are similar in homogenisation temperatures, salinities and complex salt composition with NaCl, KCl, $MgCl_2$ and $CaCl_2$. These fluids are characterised by widely varying salinities (1.8 to 11.9 wt. % NaCl-eq.) that are probably related to magmatic input.

Fluid inclusion data of minerals from hydrothermal systems of the Magnitogorsk paleoisland arc system are comparable with those from Au-bearing hydrothermal sulphide fields from island arc systems of the Pacific Ocean; e.g., ranges of fluid salinities (wt % NaCl-eq.) are 3.4–5.8 (Binns et al., 1993) and 2.7–6.9 (Bortnikov et al., 2004) in barite from barite-silica-sulphide chimneys from the Franklin Seamount, Woodlark Basin; 5.3–7.2 – in barite and anhydrite and 1.6–4.2 – in silica from the sulphide edifice from the Vienna Wood, Manus Basin (Bortnikov et al., 2004); 5 – in sphalerite from barite-sulphide chimney of the Vai Lili field, Lau Basin (Herzig et al., 1993); 2.2 (liquid) and 1.74–1.98 (vapour) – in the Brandon field, Rapa Nui, 21°S, EPR (Von Damm et al., 2003). The homogenisation temperatures vary from 128 ºC in silica from the Vienna Wood field up to 316 ºC in barite of the Franklin Seamount (Bortnikov et al., 2004). Salt composition also includes NaCl with $MgCl_2$ (Lau basin; Lecuyer et al., 1999) or $CaCl_2$ (Guaymas basin, Peter, Scott, 1988).

Based on the homogenisation temperatures, salinity, and salt composition of mineral-forming fluids the VMS deposits from the Southern Urals paleoisland arc structures are similar to modern analogues. The salinity values are lower and higher than that of seawater, suggesting a magmatic contribution to the hydrothermal systems.

This study was supported by Ministry of Education and Science of Russian Federation, (programs no. ГК П 237 and ГК № 14.740.11.1048), and Urals Branch of RAS (project no. 11-5-НП-554).

REFERENCES

Bortnikov, N.S., Simonov, V.A., Bogdanov, Yu.A., 2004. Fluid inclusions in minerals from modern sulfide edifices: physic-chemical conditons of formation and fluid evolution. *Ore Deposits Geology*, 1, **46**, p. 74–87.

Karpukhina, V.S., Baranov, E.N., 1995. Physic-chemical conditions of VMS deposits formation of Verkhneuralsky ore area, South Urals. *Geochemistry*, **1**, p. 48–63.

Puchkov, V.N., 2000. Paleogeodinamics of South and Middle Urals. Ufa, Dauria, 146 p.

Telenkov, O.S., Maslennikov, V.V., 1995. Automatized expert system of siliceous-ferrugenous sediments typization from paleohydrothermal fields, South Urals, Miass, 200 p.

Binns, R.A., Scott, S.D., 1993. Actively forming polymetallic sulfide deposits associated with felsic volcanic rocks in the eastern Manus back-arc basin, Papua New Guinea, *Economic Geology*, **88**, p. 2122-2153.

Herzig, P.M., Hannington, M.D., Fouquet, Y. et al., 1993. Gold-rich polymetallic sulfides from the Lau back arc and implications for the geochemistry of gold in sea-floor hydrothermal systems of the Southwest Pacific, *Economic Geology*, **88**, p. 2182–2209.

Holland, N.G., Roberts, S., Herrington, R.J., Boyce, A.J., 2003. The Balta Tau VMS deposit: An ancient gold-rich white smoker?, *Mineral Exploration and Sustainable Development*, Rotterdam, Millpress, **1**, p. 123–126.

Lecuyer, C., Dubois, M., Marignac, C. et al., 1999. Phase separation and fluid mixing in subseafloor back arc hydrothermal systems; a microthermometric and oxygen isotope study of fluid inclusions in the barite-sulfide chimneys of the Lau Basin, *J. of Geophysical Research.*, **104**, p. 911–928.

Peter, J.M., Scott, S.D., 1988. Mineralogy, composition, and fluid inclusion microthermometry of sea-floor hydrothermal deposits in the southern trough of Guaymas Basin, Gulf of California, *Can. Miner.*, **26**, p. 567–587.

Von Damm, K.L., Lilley, M.D., Shanks, W.C. et al., 2003. Extraordinary phase separation and segregation in vent fluids from the southern East Pacific Rise, *Earth and Planetary Science Letters*, **206**, p. 365–378.

Sulphur isotope and fluid inclusion studies of the Tasik Chini VHMS deposit, Pahang District, Peninsular Malaysia

Mohd Basril Iswadi Basori[1, 2], *Khin Zaw*[1], *Ross R Large*[1] *and Wan Fuad Wan Hassan*[2]
[1]*CODES ARC Centre of Excellence in Ore Deposits, University of Tasmania, Australia.*
[2]*Geology Programme, National University of Malaysia, Selangor, Malaysia*

The Tasik Chini Volcanic Hosted Massive Sulphide (VHMS) deposit is located in the Pahang district of central Peninsular Malaysia. The deposit is hosted by a Permo-Triassic volcano–sedimentary succession of submarine origin and has been exploited from Bukit Botol and Bukit Ketaya deposits. At both Bukit Botol and Bukit Ketaya, the host rocks are felsic volcanic rocks and show geochemical characteristics of arc tectonic settings. Mineralisation occurs as distinct ore zonation forming a stringer to massive sulphide zone at the footwall followed by barite lenses and exhalite layers (Fe-Mn ore) at the top. The mineralisation consists of pyrite as major sulphide mineral, with subordinate chalcopyrite, sphalerite and rare galena. Traces of gold are also present in the massive sulphide and barite ores. Sulphides show a narrow range of sulphur values from -2.87 ‰ to 8.30 ‰ which can be interpreted to be derived from reduction of seawater sulphate. Sulphate in barite yields a $\delta^{34}S$ range between 11.58 ‰ and 22.61 ‰ which are comparable to Permian-Triassic seawater sulphate. Preliminary fluid inclusion measurements in barite and quartz samples from the Tasik Chini VHMS deposit show that the primary inclusions contain two phase, liquid-vapour inclusions and range in size from 5 to 10 μm. Salinities for the primary inclusions range between 3.8 and 6.0 wt% NaCl equivalent and homogenisation temperatures range from 190 ^{o}C to 300 ^{o}C. In addition, preliminary laser Raman spectroscopic analysis of fluid inclusions in barite detected the presence of CO_2. Sulphur isotope and fluid inclusion results obtained for the Tasik Chini VHMS deposit suggest a seawater-dominated fluid with probably minor magmatic fluid input as the source of ore fluids.

Fluid regime in the Ramagiri-Penakacherla Granite-Greenstone ensemble of Eastern Dharwar Craton: Implications for gold metallogeny

Sourabh Bhattacharya and M. K. Panigrahi
Department of Geology & Geophysics, Indian Institute of Technology, Kharagpur, WB, 721302, India

INTRODUCTION

The Eastern Dharwar craton (EDC) is host to a number of auriferous greenstone (schist) belts namely Kolar, Hutti-Maski, Jonnagiri and Ramagiri-Penakacherla. They occur amidst the Peninsular gneiss in close spatial association with late-Archean younger granitoids. A sulfurous mixed aqueous-carbonic fluid generated by devolatilization of the greenstone volcanosedimentary pile is ascribed as the main carrier of gold for most occurrences albeit suspected magmatic signature of sulfur and involvement of fluid of diverse sources (Bhattacharya and Panigrahi, 2011 and references therein). Phase separation of such a homogeneous fluid with drop in P-T conditions possibly brought about deposition of gold in these deposits. Irrespective of the different suggested mechanisms of gold deposition, there seems to be a general agreement on the reduced nature of the fluid at the depositional regime evident from the dominance of methane. The efficiency of fluid derived from felsic magma in transporting gold is quite well known in many porphyry and epithermal systems and such fluids as alternate sources of ore fluid in orogenic gold deposits is being debated for quite some time (Ridley and Diamond, 2000). The auriferous Ramagiri-Penakacherla Schist Belt (RPSB) with extensive granitic activities in close proximity is the ideal ensemble to examine this alternate hypothesis on the source of auriferous ore fluid. Samples of quartz veins from the auriferous RPSB (QVS), quartz veins from the granitoids (QVG) and matrix quartz from the same domain (QG) were taken up for fluid inclusions studies. In RPSB, there are both smoky and milky white quartz vein types. whereas in the granitoid domain no such discrimination could be made.

RESULTS

In all the types of samples, aqueous biphase (type-I), pure-carbonic (type-II), aqueous-carbonic (type-III) and aqueous polyphase (with halite daughter crystal) (type-IV) inclusions occur mostly in the form of clusters, and locally in intra-grain trails. Based on Tm(ice), the type-I inclusions show a broad range of salinities (0 to 35 wt% NaCl equivalent) in all the three types of samples. Values of T_h for type-I inclusions in QVS and QG range between 100 to 300 °C. However, veins from the granitoid units have type-I inclusions, for which Th ranges up to 413 °C. Tm_{CO2} for type-II and type-III inclusions show a marked difference, based on the nature of the samples. For QVS, Tm_{CO2} for carbonic phase in type-II or type-III inclusions range from the melting point of pure CO_2 to -64.7 °C. The overall content of methane in type-II and type-III inclusions for QVS is much higher when compared to QVG and QG (confirmed by laser Raman microprobe (LRM) studies). Also, in contrast to type-III inclusions, the type-II inclusions are richer in methane, as evident from the recorded values of Tm_{CO2}. In addition, the type-II and type-III inclusions from the smoky quartz veins show much lower values of Tm_{CO2} than those from the white/milky white veins. The CH_4:CO_2 ratio for type-II inclusions varies from 0 to 0.25 and 0.05 to 0.71 from white and smoky quartz veins, respectively. Type-II inclusions of pure-CH_4 were detected from smoky quartz veins during LRM studies. For samples from the granitoid domain, type-II and type-III inclusions show narrow range of Tm_{CO2} values that cluster around the melting point of pure-CO_2, which is -56.6 °C. The melting point of CO_2-clathrate allows the determination of salinity for the aqueous phase in type-III inclusions. It ranges between 0 to 24 wt% (NaCl equivalent) for QVS and QVG and 0 to 4 wt% for QG.

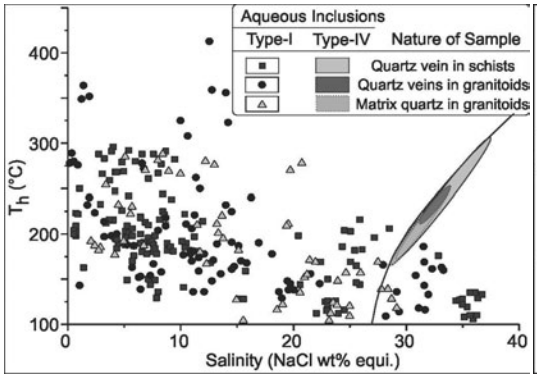

Figure 1. *Paired Th-salinity plots of type-I and type-IV inclusions from all types of quartz samples in the*

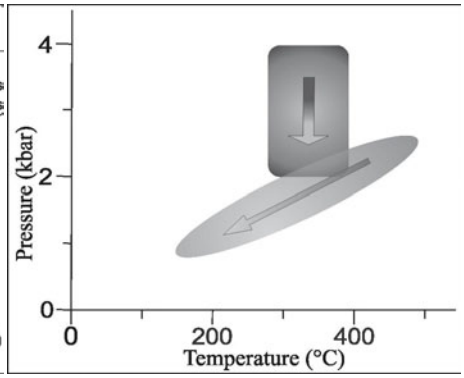

Figure 2. *P-T path of evolution of ore fluid in the QVS domain from RPSB.*

The values of Th $_{CO2}$, are much lower in case of type-II inclusions from QVS and particularly for those from the smoky quartz veins. Type-III inclusions from QVG show the broadest range of Th(tot), ranging between 214 and 431°C. For QVS it ranges between 250 and 390 °C. On the other hand, the same parameter for type-III inclusions in QG is restricted within 370 to 390 °C. Type-IV inclusions are most recurrent in QVS, and show maximum range of Th(tot), up to 300 °C. In contrast, the same type of inclusions in the quartz veins or matrix quartz from granitoid units shows Th(tot) to be always lower than 250 °C. Fig. 1 is the combined fluid evolution diagram reconstructed from type-I and type-IV inclusions from all the three types of samples. Fig. 2 is the P-T path of evolution of fluid in QVS reconstructed from type-I, II and III inclusions. The shaded elliptical regions represent unmixing regime (intersecting isochores of coexisting type-I and II inclusions), whereas the rectangular region represents the field for homogeneous aqueous-carbonic fluid.

DISCUSSION

In the absence of fluid boiling in any of the domain of study, the observed relationship between temperature and salinity could only be visualised as being the result of mixing of fluids from different sources. Considering the QVS scenario only, three different fluids – low-T high salinity (to the right of the halite saturation curve), high-T high salinity (along the halite saturation curve), and low to moderate salinity and moderate temperature, were delineated. Although source tracking for these fluids would be speculative at this stage Figures 1 and 2 indicate that the ore fluid was quite heterogeneous. The reconstructed P-T path of evolution is schematic and mostly conforms to the widely held view of phase separation. However, from the limited data, it is observed that the immiscible regime extends beyond the miscible regime in terms of temperature. This also further corroborates the heterogeneity and involvement of fluid of multiple sources rather than a single metamorphogenic fluid that carried gold.

The fluids in the granitoid domain are characterized by their methane-poor nature. As pointed out by Ridley and Diamond (2000), the CO_2:CH_4 ratio in the fluid is a result of interaction with host rocks rather than the source character. Therefore, the absence of CH_4 in the granitoid domain is not enough reason to rule out a genetic link between gold mineralisation and granitic activity in this segment of EDC.

REFERENCES

Bhattacharya, S. and Panigrahi, M.K., 2011. Heterogeneity in fluid characteristics in the Ramagiri-Penakahcerla sector of the Eastern Dharwar Craton: implications to gold metallogeny. *Russian Geology and Geophysics*, **52**, 1436p.

Ridley, J.R., Diamond, L.W., 2000. Fluid chemistry of orogenic lode gold deposits and implications for genetic models. *SEG Reviews*, **13**, 141p.

Native sulphur in fluid inclusions from quartz ore veins of the W–Mo Kalguta deposit

Borovikov A.A., Borisenko A.S.,
Institute of Geology and Mineralogy, SB RAS, Russia, Novosirsk.
Email: borovik@igm.nsc.ru

The Kalguta W-Mo deposit is situated in the SW part of the Gorny Altai (Russia) and restricted to the rare-metal granitoid massif of the same name. It is composed of granite-leucogranite igneous rocks, acid dykes and small intrusions of the Eastern Kalguta complex. The deposit is represented by NE striking and steeply south-east dipping, subparallel veins which contain complex oxide-sulphide W, Mo, Cu, Bi, Be mineralisation and Mo greisen ore formation in an explosive breccia. The ore body at the Kalguta deposit is crosscut by dykes of the Eastern Kalguta complex (granite-porphyry, elvan, ongonite, ultra rare-metal elvan) during several stages (Potseluev et al., 2008).

Fluid inclusions (FI) containing native sulphur as a solid phase were found in the quartz phenocrysts of altered granite porphyry which are crosscut by quartz veins with pyrite, sphalerite and molybdenite. Fluid inclusions with native sulphur are closely associated in space with gaseous CO_2 inclusions and fluid inclusions containing chalcopyrite and molybdenite as solid phases. The sphalerite- molybdenite -chalcopyrite veinlets belong to the last sulphide stage (Potseluev et al., 2008). Native sulphur is a daughter phase only in mainly gaseous inclusions. In fluid inclusions with other phase composition native sulphur is a xenogenic phase and characterized by different proportions of water-salt and gas phases (Fig. 1). Native sulphur solid phase usually has close to ideal spherical shape, is transparent and characterized by yellow color in fluid inclusions, melts easily under the influence of the laser during Raman spectroscopic analysis.

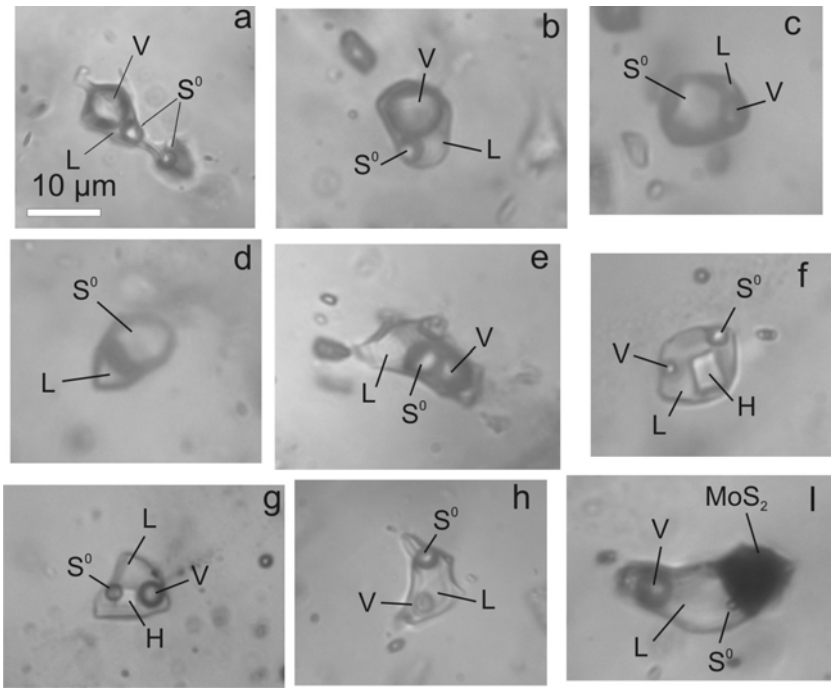

Figure 1. *Fluid inclusions containing native sulphur as solid phase. Essentially gaseous inclusions with sulphur daughter phase (a, b); other fluid inclusions containing xenogenic sulphur phase in different volume proportions with other phases (c-i). V – gas phase, L – water-salt solution, H – halite, S^0 – native sulphur. Scale: 10 micron.*

Native sulphur was indentified by the Raman spectroscopy analysis ("Ramanor U-1000" Jobin Yvon, laser Millenia Pro S2 (532 nm), detector HORIBA JOBIN YVON) using comparison of the 471.8 cm spectral line with sulphur spectrum from RRUFF database (http://www.rruff.info) (Fig. 2). The gas phase of these fluid inclusions is represented by CO_2 (96.8-86.9 mol %) and H_2S (13.1-3.2 mol %). Salt solutions contain dissolved CO_2, H_2S and HS^-. Essential quantities of HSO_4^- and SO_4^{2-} ions were not determined in the inclusion solutions. Heating of mainly gaseous fluid inclusions containing native sulphur leads homogenisation of the salt solution at 285-270ºC into the gas phase, however the

sulphur phase does not change its spherical shape and size. Under further heating, the size of the sulphur phase decreases, and its spherical shape is distorted at 340-365ºC, it disappears at 482-489ºC.

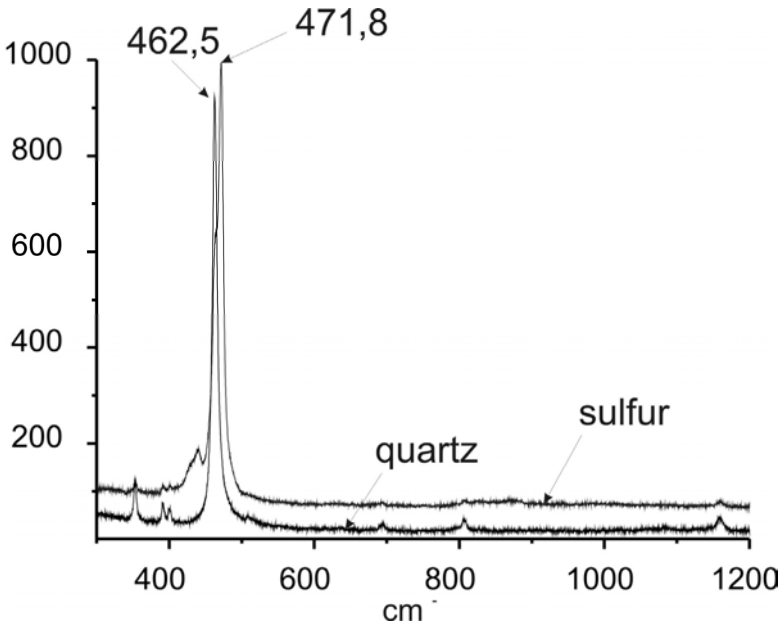

Figure 2. *Raman-spectrum of native sulphur in fluid inclusions of the Kalguta W-Mo deposit.*

Such behavior of native sulphur is probably a result of the sharp transition to the gas state or chemical reaction with other components of the inclusion. Homogenisation of the sulphur phase in the FI of different compositions was not observed. Sulphur was originally in the gas phase of the magmatic fluid. A temperature decrease led to the appearance of liquid emulsion phase in the hydrothermal fluid.

In addition, native sulphur was determined in FI trapped in halite from salt-bearing dolomite rocks of the Lena-Tungusska oil-gas province in Siberia, which were metamorphosed during the intrusion of dolerite dykes (Grishina and Dubessy, 1989); in quartz and fluorite from the Pb-Zn-F stratiform Sierra de Lushar deposits in Spain (Bény et al., 1982); in ruby from metamorphosed marble of the Luc Yen area in northern Vietnam (Giuliani et al., 2003); and in orthopyroxene from dunite in Italy (Frezotti et al., 2012). We explain the presence of sulphur as a separate phase in heterophase hydrothermal fluids by thermal reduction of sulphates at the presence of carbon. Besides, the presence of native sulphur in fluid inclusions from the Kalguta deposit may be due to sulphate reduction in oxidised and carbon-rich magmatic fluids which is suggested by the existence of amorphic carbon in the ore of the Kalguta deposit (Potseluev, 2004).
High sulphur contents in the ore-forming fluids increased the capability of hydrothermal fluid to extraction and transport of chalcophile elements that led to ore deposition of sulfide mineralisation of complex composition at the upper levels of the Kalguta ore-magmatic system.

The research work was supported by RFBR grants № 10-05-00730a and 12-05-00618a.

REFERENCES

Bény C., Guihaumou N., and Touray J.-C., 1982. Native sulphur-bearing fluid inclusions in the CO_2-H_2S-H_2O-S system. Microthermometry and Raman microprobe (MOLE) analysis. Thermochemical interpretations. *Chemical Geology*. **37**, 113-127.

Frezotti M.L., Tecce F., Casagli A., 2012. Raman spectroscopy for fluid inclusion analysis. *Journal of Geochemical Exploration*. **112**, 1-20.

Grishina S.N. and Dubessy J., 1989. Native sulphur in carbon dioxide inclusions. *Geokhimia*. **4**, 525-531.

Guiliani G., Dubessy J., Banks D., Hoàng Quang Vinh, Lhommeb T., Pironon J., Garnier V., Phan Trong Trinh, Pham Van Long, Ohnenstettere D., and Schwartz D., 2003. CO_2-H_2S-COS-S8-AlO(OH)-bearing fluid inclusions in ruby from marble-hosted deposits in LucYen area, North Vietnam. *Chemical Geology*, **194**, 167-185.

Potseluev A.A., Pikhvanov L.P., Vladimirov A.G., Annikova I.Yu., Babkin D.I., Nikiforov A.Yu., and Kotegov V.I., 2008. *In : The Kalgutincky rare-metal deposit (Gorny Altai): magmatism and ore genesis*. Tomsk: STT.

Potseluev A.A. and Kotegov V.I. 2004. Mineralogo-georchemical peculiarities of graphite from the Kalgutinsky greisen deposit. Izvestia of Tomsk Polytechnic University**. 307, No. 1**., 62-67.

Attributes of petroleum inclusion assemblages

J.Bourdet, R. Kempton, and P.J. Eadington
CSIRO Earth Science and Resource Engineering, 26 Dick Perry Ave., Kensington, 6151, WA, Australia.

A diversity of fluid inclusion techniques are established in the petroleum industry that involve measuring their abundance, fluorescence, PVT properties and geochemistry to constrain the state of the fluid, its composition, density, trapping temperature and pressure or gas saturation. This contributes to understanding basin-scale migration-accumulation processes. Because they trap palaeofluids, fluid inclusions offer unique insights into the filling of petroleum reservoirs. There is untapped potential for expanding the range of techniques or new interpretations of fluid inclusion data to make them more widely applied. Fluid inclusion techniques are a small part of the large data sets used in petroleum exploration and to be accepted the interpretations must be precise and accurate.

The GOI™ (Grains containing Oil Inclusions) technique (Eadington et al., 1996) is used widely to detect palaeo-oil zones or evidence for oil migration in currently oil-, gas- or water- saturated reservoirs. A difference between the depth and or attitude of fluid contacts is revealing of processes that operate during the preservation time of oil in reservoirs including displacement of oil by gas and leakage of oil through the seal (Lisk and Eadington, 1994; Lisk et al., 1997; Kempton et al., 2011). In addition to documenting the abundance of oil inclusions the GOI workflow documents selected attributes of oil inclusion assemblages (Figure 1) such as the petrographic superposition sequence, variance in the proportion of vapour, variability of the fluorescence colour of the oil, in datasets that reveal correlation and covariance between attributes that are useful for interpretation.
More recently, petrographic, experimental and spectroscopic studies of the attributes of oil inclusion assemblages (Bourdet et al., 2009a; 2009b; 2011) demonstrate that some of the variance in the appearance of oil inclusion assemblages is a consequence of in-reservoir fluid interactions. The known but controversial empirical relationship between UV-fluorescence colors of oil with its composition was used to calculate equations to derive the degree API of the oil as well of their saturates-aromatics-resins-asphaltene fractions. FT-IR spectra were used to measure and assess the variability of the CH_2/CH_3 ratio and methane content in different zones of a reservoir. Experiments were conducted to reproduce some of the natural variance.

These attribute and spectroscopic data show that in-reservoir fluid interactions contribute significant variance in the appearance of oil inclusion assemblages. It is necessary to separate the in-reservoir fluid interactions from those due to generation-migration processes to enable accurate understanding of petroleum systems at the basin scale.

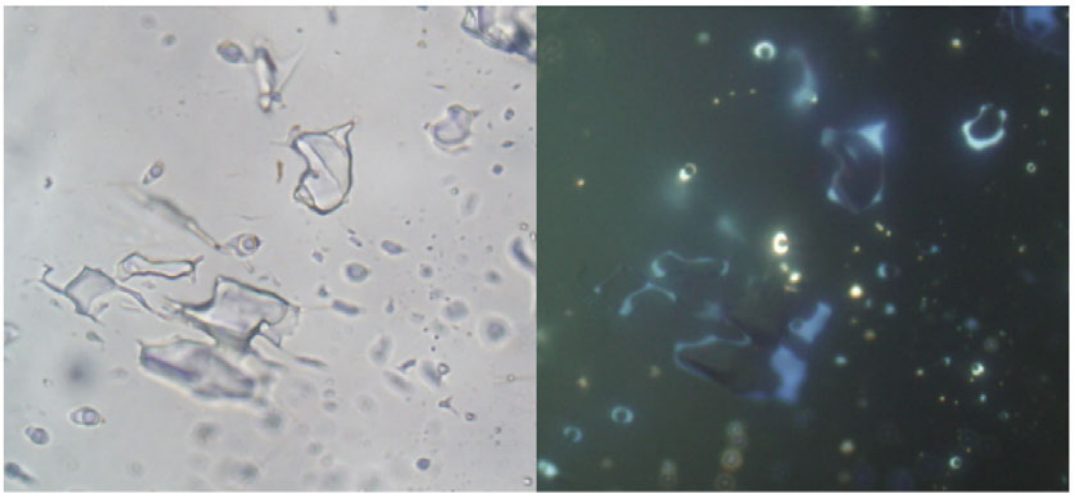

Figure 1*. Example of oil inclusion assemblage trapped at the quartz overgrowth boundary. This assemblage presents variability of the attributes such as the vapour-phase size and of the fluorescence colour of the oil. It results from the heterogeneous trapping of a residual oil and gas in a gas zone within a same oil inclusion assemblage.*

REFERENCES

Bourdet, J., Eadington P., Pironon, J., George S.C., Volk, H., Kempton, R., 2009. Progress on research about fluid inclusion assemblages attributed to water imbibition in an oil reservoir. *XX ECROFI*.

Bourdet, J., Eadington, P., Volk, H., Kempton, R., 2009. Fluorescence and FT-IR signature of a water imbibition process in an oil reservoir, VI *Geofluids*.

Bourdet, J., Eadington, P.J., Burruss, R.C., Chou I.-M., 2011. Alteration of oil by gas: experiments in fused silica capillary capsules. Goldschmidt 2011, 14-19 August, Prague, Czek Republic, Abstract.

Eadington, P.J., Lisk, M., Krieger, F.W. (1996). Identifying oil well sites. United States Patent No. 5543616.

Lisk, M., & Eadington, P. J., 1994. Oil migration in the Cartier Trough, Vulcan Sub-basin. In P. G. Purcell, & R. R. Purcell (Eds.), The Sedimentary Basins of Western Australia. Perth, WA: *Proceedings of the Petroleum Exploration Society of Australia*, pp. 301–312.

Lisk, M., O'Brien, G. W., & Brincat, M. P., 1997. Gas displacement: an important control on oil and gas distribution in the Timor Sea? *The Australian Petroleum Production and Exploration Association Journal*, **37(1),** 259–271.

Kempton, R.H., Gong, S., Kennard, J., Volk, H., Mills, D., Eadington, P., Liu, K., 2011. Detection of Palaeo-Oil Columns in the offshore northern Perth Basin: Extension of the effective Permo-Triassic Charge System. *The APPEA Journal*, **51**, 377–396.

Using fluid inclusions in opaque minerals; pyrite, magnetite and haematite

K. Burlinson[1], T. Mernagh[2], D. Gaboury[3], Jiuhua Xu[4] and Longhua Lin[4].
[1] *Burlinson Geochemical Services, Darwin, NT, Australia,*
[2] *Geoscience Australia, Canberra, ACT, Australia,*
[3] *University of Quebec, Chicoutimi, Quebec, Canada,*
[4] *University of Science and Technology Beijing, Beijing, China*

Just because we cannot observe fluid inclusions in opaque minerals does not mean they are absent or that we cannot use them to understand mineralisation events. In fact, opaque minerals are frequently more closely associated with economic mineralisation than is quartz and provide more relevant data.

The easiest technique to use on opaques is baro-acoustic decrepitation (http://appliedminex.com), which provides population measurements and approximate temperatures and is very useful for evaluation of suites of spatially related samples such as in mineral exploration. Complete gas analyses can be provided by an instrument which thermally decrepitates the sample in a vacuum and analyses the inclusion contents using an attached mass spectrometer (Gaboury et.al. 2008). Some opaque minerals are transparent to infra-red light, and normal observational methods can be used. Some pyrite samples can be examined in this way.

Baro-acoustic decrepitation of haematite and magnetite samples can quickly distinguish between sedimentary and hydrothermal deposits. Samples from magnetite skarns show intense decrepitation whereas stratigraphic magnetite has almost no decrepitation. This seemingly simple distinction is the subject of many controversies in these types of deposit. Haematite also can have high decrepitation counts, indicating a hydrothermal origin when many studies assume that haematite is merely a supergene alteration of magnetite, which would eliminate any fluid inclusions. The deposits at Tennant Creek, NT, Australia are a complex combination of hydrothermal and stratigraphic iron oxides which cannot readily be distinguished without fluid inclusion information provided by baro-acoustic decrepitation.

The origin of the Mengku iron deposits in the Altai area, Xinjiang, in far north west China are also the subject of much controversy. Samples from this area show low and variable decrepitation levels and indicate that there is a weak hydrothermal overprint on the mostly sedimentary stratigraphically controlled deposits. Magnetite samples decrepitated under vacuum showed no gas release. However, magnetite samples from skarns did show release of SO_2 and H_2S, without H_2O. This seems to be an unusual fluid type, but it is unlikely that these gases could have come from thermal decomposition of the sample in a vacuum.

Samples of pyrite from the Chessy base metal sulphide deposit, near Lyon in SE France show intense decrepitation which is consistent across some 20 samples and confirms the presumed origin of these deposits as hydrothermal alteration within an acid volcanic stratum. Pyrite samples from sedimentary deposits such as in the San Miguel pit, Rio Tinto area, Spain show no decrepitation. Pyrite from the Mt Charlotte gold mine, Kalgoorlie, WA, has also been examined for comparison.

REFERENCES

Gaboury, D., Moussa Keita, Jayanta Guha and Huan-Zhang Lu, 2008. Mass Spectrometric analysis of volatiles in fluid inclusions decrepitated by controlled heating under vacuum. *Economic Geology,* **103**, 439-443.

Mineralogical, fluid inclusion and Raman spectroscopic studies of Au-Cu mineralisation in the Delwara Group of rocks, Rajasthan, India – in a hydrothermal milieu

Sweta Chattopadhyay[1], Shyamal Kr. Sengupta [1] and Ramlal Jat[2]
1. Geological Survey of India, 15 A&B Kyd Street, Kolkata, India.
2. Geological Survey of India, NER, India

Gold – sulphide mineralisation has been observed in the Delwara Group (belonging to the Aravalli Super Group) rocks which are underlain by the rocks of the Banded Gneissic Complex (BGC), in Banswara district Rajasthan, India. The regional strike is N10°W to N20°W with moderately steep dips towards the east or west. The Delwara Group is represented by a volcano-sedimentary-carbonate sequence, comprising quartz-chlorite-muscovite schist, quartz-carbonate rock, dolomitic marble, calcitic marble, calc silicate rock, amphibole, quartzite, and fine-grained tourmaline –albite rock (Keratophyres?). Pegmatites, quartz veins, and quartz-carbonate veinlets pervade all the rock types**.** Gossans and malachite-azurite stains have been observed at a number of places along with tell-tale signs of panning.

These rocks are pervaded by opaque-rich veins showing entrapped patches of host rock material exhibiting a brecciated appearance in places. The calc–silicate, actinolite- biotite marble exhibits its typical granoblastic texture. Sheaf like aggregates of actinolite prisms in actinolite marbles are also noteworthy. The presence of a chlorite band within actinolite marble may define a wall- rock alteration feature. This chlorite band is sheared and crenulated and is composed of clinochlore. In the carbonate-bearing amphibolite rock, amphiboles show strong compositional zoning (from edenitic hornblende core to actinolitic rim). In the mineralised zone there is phlogopite while in the host rocks the mica composition is biotite. Such a change in composition of amphibole and biotite may reflect the nature of the hydrothermal alteration in the vicinity of the mineralised zone. Tourmaline occurring in tourmaline – albite rock and in the calc-silicate rock are of two types, Ti – poor (TiO_2 < 1%) and Ti rich (TiO_2 ~ 4 %.) and are dravitic in composition. The composition of feldspar varies considerably from the amphibolites to the albite – tourmaline rock ranging from Ab_{85} (amphibolites) to Ab_{97} (albite- tourmaline rock) .

The sulphide mineralisation is represented by pyrrhotite, arsenopyrite, chalcopyrite, and loellingite in decreasing order of abundance. In addition to the major sulphides, Native gold, Bi-Te and Au-Bi bearing phases and scheelite are associated with arsenopyrite/pyrrhotite. Au-Bi-Te veinlets pervade arsenopyrite grains in places. The subordinate oxide phases are magnetite, rutile, and ilmenite associated with the sulphides and silicate- carbonate gangue. Thick veins/veinlets of pyrrhotite, chalcopyrite and arsenopyrite pervade the host rock in an anastomosing manner. Arsenopyrite shows zoning in places with variable As/S ratio from core to rim (As/S in core = 1.12 and rim = 0.97). Zoning in arsenopyrite implies a local disequilibrium in the system. Native gold grains of approx. 100 µm have been recorded as inclusions within the fractured arsenopyrite. The maximum size of native gold is 184 µm x 110 µm. Native gold occurs within thin micro-veinlets of chalcopyrite and pyrrhotite pervading the host arsenopyrite. Loellingite occurs as inclusions within arsenopyrite both as discrete isolated grains and associated with native gold grains. Atomic % of 'As' in arsenopyrite (33.5 to 35 at %) when plotted in the pseudo-binary *T-X* section (after Kretschmar and Scott, 1976) falls along the pyrrhotite-arsenopyrite-loellingite join showing arsenopyrite composition as a function of temperature. The temperature of equilibrium of co-existing phases (po-asp-lo) shows a range from 350 °C to around 450 °C, which conforms to the studied ore mineral assemblages in the Delwara Block.

The Raman spectra suggests that the primary mono-phase fluid inclusions are dominantly CH_4-bearing along with other phases as H_2O, CO_2 and rarely N_2. Mono-phase $CH_4 \pm H_2O$ vapour inclusions also occur along secondary trails. Bi-phase primary inclusions show vapour phases with H_2O mainly and also with CH_4 and CO_2. The secondary bi-phase trails contain inclusions with only a CH_4-bearing vapour phase. Morphologically the CH_4- and CO_2 - bearing vapour phases are dark rimmed. The subordinately occurring, bi-phase inclusions with the dark rims have been identified as containing C (i.e. graphite + CH_4 + H_2O).

Banded tourmaline-albite and calcite-amphibole rocks are hosts for sulphide mineralisation. Petrographic studies indicate the mineralisation was strata-bound and then later remobilised. A vapour dominant, moderately high salinity and an appreciably higher temperature of homogenisation varying from 329.2 ° C to 430.7 °C is envisaged for the mineralising fluid which is also the minimum temperature of entrapment of the fluid. Homogenisation of the vapour bubble was largely into the liquid state, i.e. $L + V \rightarrow L$, thus implying that the ore bearing fluid was a liquid. The presence of CH_4 and CO_2 vapour phases in appreciable concentrations possibly attributes to Hydrolysis / Oxidation of the carbonaceous matter in the wall rocks, upon interaction with the hydrothermal fluid that was subsequently trapped during alteration and veining. $2C + 2H_2O = CO_2 + CH_4$ (Xavier et al, 2000). This temperature of homogenisation which is also the minimum temperature of entrapment of the mineralising fluid conforms with the As atomic % in arsenopyrite as a function of temperature, as studied for the ore mineral assemblages in Delwara Block.

When comparing a bivariate plot of T_h vs salinity with the schematic model depicting the theoretical evolution path of the parental fluids, the data is indicative of a combination of more than one trend and is attributed to mixing of fluids of contrasting salinity (Shepherd et al, 1985). In a bivariate plot of T_h vs pressure, pressure is calculated by the intersection of the fluid isochors (i.e. the equal density lines). The intersection is assumed to be an equivalent lithostatic load. The approximate pressure at the time of entrapment of the mineralising Cu-Au bearing fluid shows a range from 350 bars to 1400 bars approximately. The studies indicate that the remobilised native gold – sulphide bearing mineralising fluid was emplaced at hydrothermal conditions within the range (300 ^oC to 500 ^oC) at an approximate pressure range of 350 to 1400 bars.

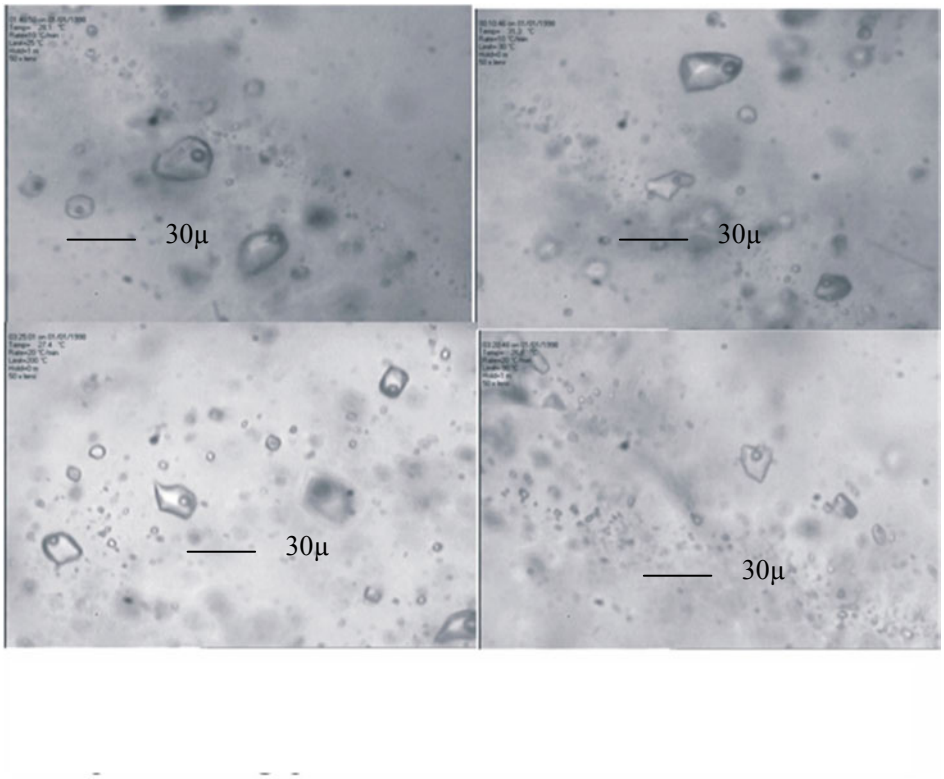

Figure 1. *Primary F.I. and Secondary F.I. Trails*

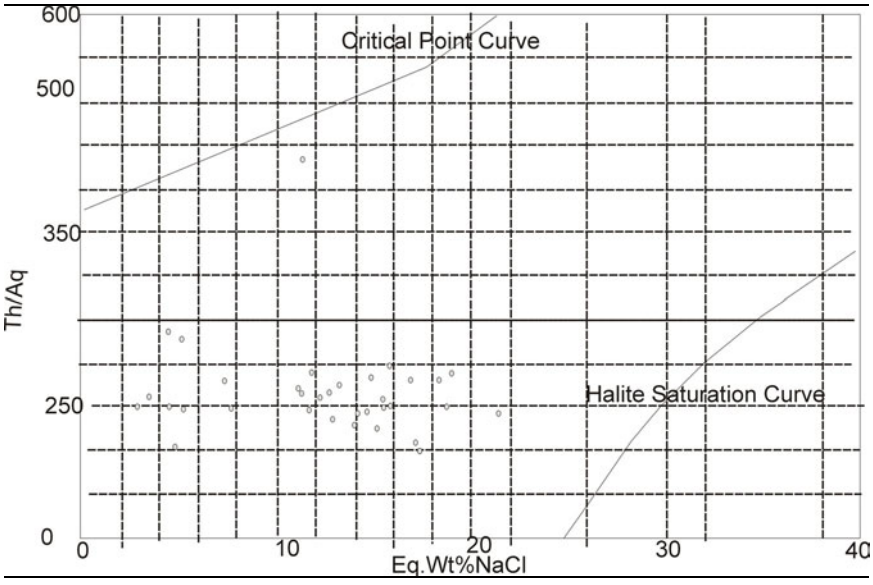

Figure2. *Bivariate plot of Th Vs Eq wt% NaCl*

Table 1: Morphological &Micro thermometric study of Fluid Inclusions.

L+ V ratio: 90:10, 85 : 15 (Primary & Secondary):	
size	5 to 25 µm in its max. length
Degree of Fill	0.71 to 0.96
Density	0.73 to 1.04
T_{fm} (Te)	-11.3° C to - 40.5° C (combination of dissolved salts of Na,K, Ca,Fe& Mg)
T_M	-2.8° C to -18.6° C
T_H	103 .8 to 430.7 C
Salinity (Wt% NaCl equivalent)	3.4 to 23.2
L + V + S ratio : 70:15: 15 , 80 : 10 : 10 (Primary: subordinate mode)	
Density	1.02 to 1.23
T_S NaCl	230.6 to 385 C (Probably Halite in composition)
Salinity (Wt% NaCl equiv.)	33.5 to 44.9

REFERENCES

Kretschmar and Scott, 1976. Phase relations involving arsenopyrite in system Fe-As-S and their applications. *Canadian Mineralogist.* **14**, 344-386

Shepherd, T., Rankin, A.H., and Alderton, D.H.M., 1985. A Practical Guide to Fluid Inclusion Studies. *Publ. Blackie & Sons, Glasgow,* 239 p.

Xavier R.P., Toledo, C.L.B., Taylor,B., and Schranki,A., 2000. Fluid Evolution and Gold Deposition at the Cuiaba Mine. SE Brazil: Fluid Inclusion and Stable Isotope Geochemistry of carbonates. *Revista Brasileria de Geociências,* **30(2),** 337-341.

Fluid evolution in various gneisses from the Chiplakot Crystalline Belt in northeast Kumaun Himalaya, India

Dinesh S. Chauhan[1*] *and Rajesh Sharma*[2]
[1]*Geological Survey of India, Northern Region, Lucknow, India*
**email: dinesh.chauhan@gsi.gov.in*
[2]*Wadia Institute of Himalayan Geology, Dehradun, India.*

The Chiplakot Crystalline Belt (CCB) represents one of the detached klippe of the Munsiari Formation in northeast Kumaun Himalaya, India (Valdiya, 1980). The CCB tectonically overlies the low grade metasedimentary sequence of the Lesser Himalaya along two thrusts termed as the South and North Chiplakot Thrust (SCT & NCT) in the south and north respectively. The CCB is mainly constituted of mylonitic granite gneiss, augen gneiss, granite-granodiorite gniesses, mica-schists with sericite-chlorite schist, biotite-sericite-quartz schist and quartz porphyry with bands of amphibolites. The granitic gneisses have been intruded by quartz veins, pegmatites, aplite veins of different and probably successive generations. These veins occur as both concordant and discordant bodies to the major foliation plane. The rocks in the CCB have attained amphibolite grade metamorphism. Patel and Kumar (2006) have identified the deformation mechanism in the area and proposed successive phases of deformation. They also believe that the two major geotectonic regimes viz. an early Himalayan ductile and a superimposed brittle deformation broadly acted for the entire evolution of the CCB. The granitic gneisses in the CCB are highly mylonitised near the thrust contact. Quartz in these gneisses occurs as stretched grains forming ribbon quartz. The complete recrystallisation of quartz grains is however, not evitable, as relict older grains are observed in the core of the ribbon quartz (Fig.1).

The fluid inclusion studies on the gneisses suggest that the relict grains host the earliest fluid inclusions with regular shapes which escaped re-equilibration during the shearing event. Fluid inclusions in the relict grains are reasonably different in terms of size, composition and occurrence than the fluid inclusions found in the recrystallised rim part of the quartz grains. In addition, newly crystallised quartz grains are also present as layers alternating with the micaceous minerals. The augen gneisses contain large porphyroblasts of feldspar with foliation wrapped around them. The later intrusion of micro-granite and aplitic veins consists of fine grained quartz and feldspar. The aplitic veins are parallel to the principle foliation planes. Sharma et al (2010) carried out a fluid inclusion study of the mineralised quartz veins at Gasku near the NCT. We focus here on the fluid inclusion study carried out on these granitic gneisses, augen gneisses and later intrusion of granitic material in these gneisses, and present the variation identified in the fluid circulation during shearing and later intrusion.

The main inclusions present in these granitic gneisses, augen gneisses and relatively un-deformed micro-granite and aplite veins are mixed CO_2-H_2O fluid inclusions with variable phase ratios. Two phase aqueous and halite bearing multiphase H_2O-CO_2 inclusions are also observed. Type I inclusions are halite bearing H_2O-CO_2 multiphase inclusions (Fig.2) wherein the halite crystal occupies about 20 vol% and the carbonic phase is about 20- 25 vol%. The cavity of such inclusions is regular and small. These inclusions occur as isolated inclusions and also in random distributions, strictly restricted within the relict quartz grains. They are considered to be primary inclusions. These inclusions never show complete homogenisation as the disappearance of the salt is never seen. Such inclusions are present both in granite gneiss and augen gneisses, but are absent in micro-granite and aplitic veins. Type II inclusions are H_2O-CO_2 inclusions with the aqueous phase

occupying nearly 70-90% of the cavity. These are distributed in isolation (Fig.3) as well as in small clusters both in the recrystallised quartz and the relict quartz grains. We consider that these inclusions were trapped during formation of the recrystallised quartz grains. The type III inclusions are aqueous biphase inclusions with a liquid-vapour ratio about 90:10. These aqueous fluid inclusions are dominant in the microgranite and aplite veins. Broadly, the thermometric data in granitic gneisses and augen gneisses are similar. The peak of the CO_2 melting histogram for Type I inclusions is at -57.2°C indicating only minor CH_4 as confirmed through its low intensity Raman band. The carbonic phase homogenised between 27° and 31° C to the liquid CO_2 phase. The complete homogenisation of these inclusions is never observed and inclusions leaked before the dissolution of salt. The partial homogenisation of the liquid and gas phase in these inclusions is in the range 268° to 290°C. The Type II inclusions show a triple point of CO_2 around -56.8°C to -57.8°C. The eutectic temperature was measured in a few inclusions between -22.2° to -25.6°C. These inclusions show clathrate melting between 7.0° to 7.6°C followed by complete homogenisation in a range between 270° and 385°C. The aqueous fluid phase trapped in micro-granite and aplitic veins provide eutectic temperature of about -31.2° to -26.0°C suggesting that the fluid is H_2O+NaCl+$MgCl_2$±$CaCl_2$. They completely homogenised between 180 and 210°C. However, those in the secondary plane (Fig.4) showed homogenisation from 140 to 150°C. Overall, a high salinity fluid is evident in the core part of the quartz representing the earliest fluid event preserved in the granite. The carbonic aqueous fluid present widely in these gneisses likely equilibrated with the major Himalayan syntectono-metamorphism, and a late with gneiss melt phase generation can also be inferred in the present study.

Fig.1 *Mylonitic granite gneiss showing a relict porphyroclast in the centre and recrystallised porphyroclastic quartz in tails.*

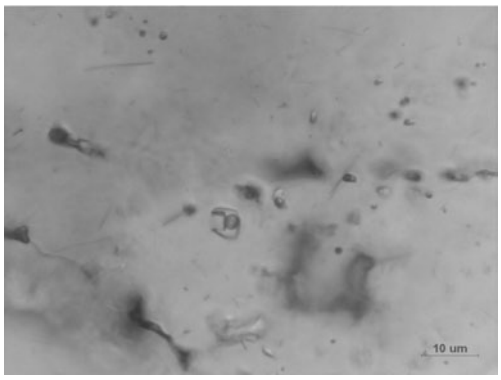

Fig.2 *Multiphase (aq-carb-salt) inclusion in relict quartz in mylonitic granitic gneiss*

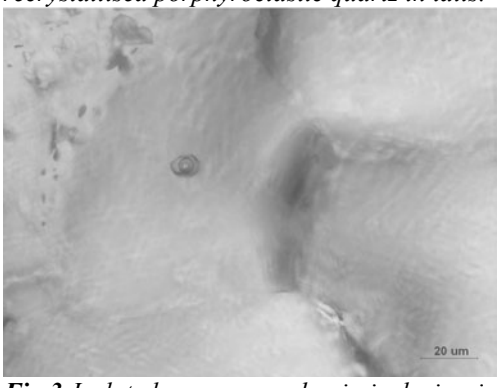

Fig.3 *Isolated aqueous-carbonic inclusion in recrystallised porphyroclastic quartz.*

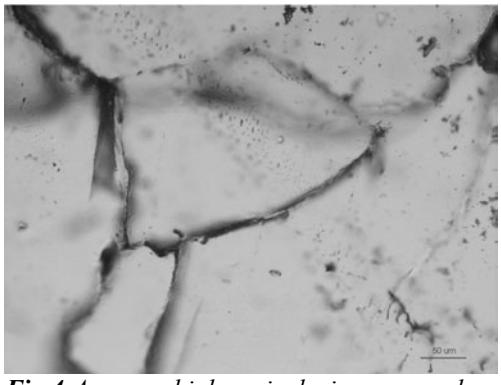

Fig.4 *Aqueous-biphase inclusions, secondary plane in aplitic vein*

REFERENCES

Patel, R. C. and Kumar, Y., 2006, Late-to-post collisional brittle-ductile deformation in the Himalayan orogen: evidences from structural studies in the Lesser Himalayan Crystalline, Kumaon Himalaya, India. *J. Asian Earth Sci.*, **27**, 735–750.

Sharma, R., Dinesh S. Chauhan and Rao, D. R., 2010, Polymetallic sulphide mineralization in Chiplakot crystallines, northeast Kumaun Himalaya, *Cur. Sci.,* **98**, 698-702.

Validya, K. S., *Geology of Kumaun Lesser Himalaya*, The Himachal Times Press, Dehradun, India, 1980, p. 291.

Ages and compositions of magmatic inclusions in zircon from Archean orthogneisses as evidence of origin and ages of protoliths

V.P. Chupin[1, 2], V.R.Vetrin[3], S.A. Sergeev[4], N.G. Berezhnaya[4], and N.V. Rodionov[4]
[1]*Institute of Geology and Mineralogy SD RAS, Novosibirsk, Russia*
[2] *Novosibirsk State University, Russia*
[3]*Geological Institute KSC RAS, Apatity, Russia*
[4]*Center of Isotopic Research, VSEGEI, St. Petersburg, Russia*

INTRODUCTION

Silicate melt inclusions (glassy and completely crystallized) in cores of zircon from Archean orthogneisses provide direct information about the compositions of ancient magmas and the volcanic or plutonic origin of gneiss protoliths (Chupin et al., 1994, 1998). Ancient ages of magmatic cores of zircon from orthogneisses are traditionally interpreted as a protolith age of these rocks. In the study presented here, we showed that the magmatic cores of zircons from Archean metavolcanites were being crystallized in considerable time interval. Protolith ages of these rocks correspond to the youngest ages of zircon cores. This data were obtained for the first time by study of age and genesis of zircon from metavolcanic tonalitic-trondhjemitic gneisses (TTG) which dominate among the Archean rocks intersected by the Kola Superdeep Borehole at a depth of –6842 to –12262 m**.** These gneisses are among the oldest rocks of the continental crust within the northwestern part of Baltic Shield.

METHODS

To obtain the direct information about origin of zircon we have used for the first time data on composition (phase and chemical) and age (trapping time) of primary melt and fluid inclusions (Chupin et al., 2006). The results of inclusions study along with data on morphology, geochemistry and cathodoluminescence of zircon made possible to identify genetic types and generations of this mineral. Glass phase in unheated melt inclusions have been confirmed optically, thermometrically and by Raman-spectroscopy. The chemical composition of melt inclusions was determined using a "JEOL JXA-8100" electron microprobe. The time of inclusion trapping was defined by in-situ isotope $^{207}Pb/^{206}Pb$ age of the host zircon (near the inclusion) using a SHRIMP-II ion microprobe (at the Center of Isotopic Research of VSEGEI, St. Petersburg).

RESULTS AND DISCUSSION

Primary magmatic (glassy and cogenetic CO_2-rich) inclusions occur in the cores of prismatic zircons and are absent in their metamorphic overgrowths and in isometric grains with a complex crystal shape. The melt inclusions in inner parts of crystal cores have plagiorhyodacitic-plagiorhyolitic compositions, while inclusions located closer to the edge of cores have mainly rhyolitic compositions (Table). The old concordant $^{207}Pb/^{206}Pb$ ages for the zircon cores form an continuous time interval from 2887 to 2812 Ma for TTG of 8th Unit (depth 10601-11411 m) and from 2883 to 2830 Ma for TTG of 10th Unit (depth 11708-12262 m). These data and the presence of glassy inclusions indicate that the zircon cores represent relict-magmatic mineral of volcanic protoliths of gneisses. The presence of melt and cogenetic liquid CO_2 inclusions in inner parts of crystal cores suggests the crystallisation of early zircons in the deep-seated chamber from CO_2-saturated magmas.

The obtained results revealed that the Archean zircons from TTG of the Kola Superdeep Borehole belong to relict-magmatic and metamorphic genetic types. According to their radiogenic ages relict-

Table 1. Chemical compositions (wt.%) and ages of melt inclusions in zircons from TTG of 8th Unit (sample 26) and 10th Unit (samples 90 and 43) of the Kola Superdeep Borehole

Inclu-sion no.	SiO_2	TiO_2	Al_2O_3	FeO	MgO	CaO	Na_2O	K_2O	Cl	F	Total	$^{207}Pb/^{206}Pb$ Age, Ma
26-8 c	74.59	0	13.74	0.55	0	1.85	3.83	1.02	0	n.a	95.58	2874±9
26-6 c	72.81	0.17	13.68	0.1	0.02	1.84	5.12	2.28	0.01	n.a»	96.03	≥2865±9
26-7 c	73.39	0.10	14.04	0.29	0.08	1.48	4.74	1.71	0	н.а	95.83	2842±13
26-11 i	77.07	0.03	8.98	0.01	0.02	0.73	2.85	2.72	0	n.a	92.41	<2853±8
26-10 e	75.18	0	12.73	0.24	0	1.56	3.32	2.78	0	n.a	95.81	≥2812±11
26-12 e	73.31	0	13.77	0.19	0	1.55	2.69	3.77	0	0	95.28	n.a
26-9 e	72.03	0.02	15.53	0.14	0.01	1.23	3.43	3.37	0	0	95.76	n.a
43-9 c	73.78	0.04	14.13	0.01	0.02	1.34	2.90	1.94	0.05	0.20	94.41	2854±5
43-9 i	76.88	0.09	11.83	0.11	0.02	1.33	1.73	1.93	0.07	n.a	93.99	≤2854±5
43-1 e	74.39	0.06	12.30	0.02	0.01	1.26	3.25	3.33	0.03	n.a	94.65	<2842±7
43-5 i	69.03	0.78	13.09	0.29	1.66	1.96	4.37	3.33	0.07	0.26	94.84	2826±11
90-1 c	77.72	0.19	10.91	0.14	0.03	2.77	2.31	1.91	0.11	n.a	96.09	≤2854±10
90-11 c	73.97	0.01	15.13	0.13	0.04	1.25	3.08	2.10	0.03	0.14	95.88	≤2850±10
90-11 e*	72.71	0	14.93	0.07	0	1.07	8.12	2.61	0	0.16	99.67	2823±14
90-3 i	75.55	0.11	12.14	0.17	0.24	1.44	3.69	2.84	0.07	n.a	96.25	≤2849±6
90-10 i	72.72	0.05	14.18	0.87	0.05	2.19	3.61	2.16	0.03	0.17	96.03	≤2833±6
90-7 i	70.66	0.10	13.50	0	0	1.54	5.68	4.35	0.03	0.26	95.62	≤2834±7
90-6 i	74.82	0.00	13.04	0.06	0.00	1.17	1.74	3.83	0.39	0.05	95.10	≥2827±8

(c, i, e) position of inclusions in crystal cores: c - central part, i - intermediate, e - edges.

magmatic zircons are divided into two generations. The early one has more than 70-My crystallisation history and probably crystallised in deep plagiorhyodacitic-plagiorhyolitic magma chambers. It is suggested that eruption and fast crystallisation of these magmas resulted in the formation of residual K_2O-rich rhyolitic melts. The latter were trapped on the final stages of crystallisation of the protolithic zircons at ~2830 Ma ago for 10^{th} Unit and ~2810 Ma ago for 8^{th} Unit.

CONCLUSION

In-situ dating of zircon (and its magmatic inclusions) from Archean metavolcanites of the Kola Superdeep Borehole showed that the protolith ages of these rocks correspond to the youngest ages of relict-magmatic zircons. Age of early generation of relict-magmatic zircons can be significantly (for more than 70 Ma) older relative to the age of volcanic protolithic zircons.

REFERENCES

Chupin V.P., Chupin S.V., Pospelova L.N., Kotov A.B., and Stepanyuk L.M., 1994. Melt inclusions in zircon from Archean gneisses as indicator of origin of protoliths and composition of ancient magmas. *Doklady AN SSSR*, **338**, 806-810.

Chupin S.V., Chupin V.P., Barton J.M., and Barton E.S., 1998. Archean melt inclusions in zircon from quartzite and granitic orthogneiss from South Africa: magma compositions and probable sources of protoliths. *Eur. J. Mineral.,* **10**, 1241–1251.

Chupin V.P., Vetrin V.R., Rodionov N.V., et al., 2006. Composition of melt inclusions and age of zircons from plagiogneisses of the Archean complex in the Kola Superdeep Borehole, Baltic Shield. *Doklady Earth Sciences,* **406, (1)**, 153-157.

Raman microspectroscopy study of carbonate ion in synthetic fluid inclusions in system Na_2CO_3 - H_2O

J.Y. Ding[1], P. Ni[1], J.Y. Pan[1], and L. Li[1]
[1] Institute of Geo-fluid, State Key Laboratory for Mineral Deposit Research, School of Earth Sciences and Engineering, Nanjing University, Nanjing, China

INTRODUCTION

Raman microspectroscopy is a useful non-destructive technique to analyse single fluid inclusions, and can applied to the qualitative and quantitative measurement of the fluid in inclusions (e.g., Dubessy et al., 1982; Burke, 2001). Carbonate ion is the major species in some natural aqueous fluid inclusions (Roedder, 1972, 1984). The aim of this work is to determine the carbonate ion in synthetic fluid inclusion in system Na_2CO_3-H_2O at ambient temperature (293 K) by Raman microspectroscopy, especially to quantify the concentrations of carbonate ion based on the characterisation of Raman spectra of fluid inclusions.

EXPERIMENTS

This study used the optical fused silica capillary, which was purchased from Polymicro® Technologies, LLC (http://polymicro.com), to synthesize the fluid inclusion (for details, see Ni et al., 2011). Capillary samples were prepared containing aqueous solutions with various concentrations of Na_2CO_3 (0.25 mol·L^{-1} ~ 2.0 mol·L^{-1}, in intervals of 0.25 mol·L^{-1}). All Raman spectra were collected on a Renishaw® RM2000 Raman spectrometer fitted with an air-cooled CCD detector and an air-cooled Ar^+ laser with excitation at 514 nm.

RESULTS

Raman spectra for Na_2CO_3-bearing aqueous solutions in capillary samples are shown in Figure 1. In all these spectra, the strongest band of CO_3^{2-} (1064 cm^{-1}) and O-H stretching bands of water (between 2800 $cm^{-1}$and 3800 cm^{-1}) are distinguished in the spectral range shown (900 ~ 4000 cm^{-1}) and it is noted that the intensity of the band of CO_3^{2-} becomes stronger with the increasing of the concentration of $NaCO_3$ in solution.

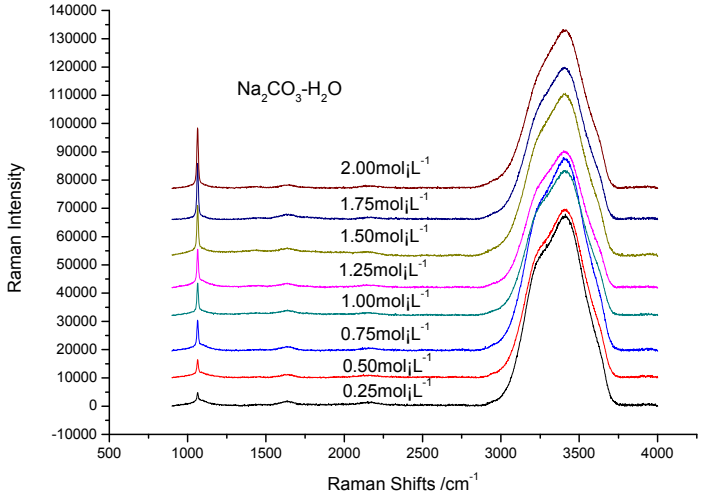

Figure 1: *Raman spectra of solutions in capillary samples with the various concentrations of CO_3^{2-} (900 ~ 4000cm^{-1})*

A parameter (*I*), the ratio of Raman intensity of CO_3^{2-} band (in 1064cm^{-1}) to that of water bands (between 2800 and 3800cm^{-1}), is introduced for detecting the relationship between the intensity of band of CO_3^{2-} and the concentration of $NaCO_3$ ($c(NaCO_3)$, in molarity) in solutions. In this work, the Raman spectra were analyzed using the Grams/32 computer program (provided by Renishaw®). The Raman spectra in 1000 cm^{-1} ~ 1200 cm^{-1} were first fitted into Gaussian sub-bands to remove the signal of capillary tube, then the area of CO_3^{2-} band and the area of water bands were obtained, and the parameter *I* was calculated. Figure 2 presents the correlation between *I* and $c(NaCO_3)$ and the data can be well fitted by the equation: $c(NaCO_3) = -1244(I)^2 + 132.4(I) + 0.042$.

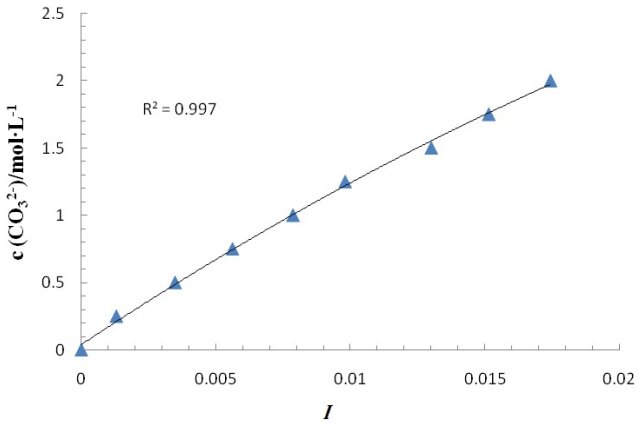

Figure 2: *Relationship between I and c(NaCO$_3$) (in molarity)*

CONCLUSIONS

The results reveal three conclusions. (1) There is a function relationship between the concentration of $NaCO_3$ ($c(NaCO_3)$) and the parameter of intensity of Raman band of CO_3^{2-} (*I*), where *I* is the ratio of Raman intensity of CO_3^{2-} band (1064 cm^{-1}) to that of water band (O-H stretching bands between 2800 and 3800 cm^{-1}). The relationship is expressed as: $c(NaCO_3) = -1244(I)^2 + 132.4(I) + 0.042$. (2) Using water as an internal standard can well correlate the concentration of species in fluid inclusions with the ratio of Raman intensity of bands of the species to that of water. (3) By removing the signal of the host mineral a precise concentration of carbonate ion in fluid inclusions can be obtained.

REFERENCES

Dubessy, J., Audeoud, D., Wilkins, R., and Kosztolanyi, C., 1982. The use of the Raman microprobe mole in the determination of the electrolytes dissolved in the aqueous phase of fluid inclusions. *Chemical Geology*, **37**, 137-150.

Burke, E.A.J., 2001. Raman microspectrometry of fluid inclusions. *Lithos*, **55**, 139-158.

Roedder, E., 1972. The composition of fluid inclusions. USGS, *Professional Paper*, 440p.

Roedder, E., 1984. Fluid Inclusions. Mineralogical Society of America, Michigan, USA, *Reviews in Mineralogy*, **12**, 644p.

Ni, P., Ding J.Y., Chou, I-M. and Dubessy, J., 2011. A new type synthetic "fluid inclusion": The technique of optical fused silica capillary. *Earth Science Frontiers*, **18**, 132-139.

REE-rich CO_2 fluids in the giant Bayan Obo deposit, China: Implications for REE mineralisation

H.R. Fan, F.F. Hu, K.F. Yang and S. Liu
Key Laboratory of Mineral Resources, Institute of Geology and Geophysics, Chinese Academy of Sciences, Beijing 100029, China

GEOLOGICAL SETTING AND MINERALISATION

The Bayan Obo REE-Nb-Fe deposit hosts the world's largest known light rare earth element (LREE) resource, as well as being a major Nb and Fe producer of China. LREE reserves in the deposit, which contains 70% of the world LREE resources, are 57.4 million metric tons (Mt) with an average grade of 5.17 to 6.19 wt percent REE_2O_3, and Nb reserves are approximately 2.2 million Mt with an average grade of 0.126 to 0.141 wt percent Nb_2O_5. The deposit consists of replacement bodies hosted in dolomite marble and of magnetite, REE fluorocarbonates, fluorite aegirine, amphibole, calcite and barite. The main-stage banded mineralisation shows a generalised paragenetic sequence of strongly banded REE and Fe ores showing alteration to aegirine, fluorite and minor alkali amphibole. These rocks are cut by aegirine-rich veins containing apatite, bastnaesite, fluorite and quartz, and later aegirine-rich veins and pods associated with barite, bastnaesite and Ba-REE-fluorocarbonates.

Fluid inclusions

Three types of fluid inclusions have been recognised on the base of their appearance at room temperature: (i) two phase aqueous liquid-vapor (L-V), (ii) two to three phase CO_2 (C), and (iii) three phase liquid-vapor-solid (L-V-S) inclusions. L-V inclusions occur in fluorite, quartz, barite and REE fluorocarbonates, and range up to 20μm in diameter. Primary L-V inclusions are most abundant in the latest coarse-grained fluorite veins which cut banded REE and Fe ores. These primary L-V inclusions are related to the latest fluids. Most other L-V inclusions in quartz and REE fluorocarbonates occur along secondary planes.

CO_2 inclusions occur in isolated cavities or planar arrays in healed microfractures in fluorite and quartz. The inclusions are generally less than 20μm in diameter and have three phases consisting of an aqueous liquid, a carbonic liquid and vapour with relatively constant phase ratios. Melting of the carbonic phase ($TmCO_2$) occurs either at the CO_2 triple point of -56.6°C, or over a small interval with depressed melting temperatures between -57.0 and -56.7°C. These measurements indicate that the carbonic phase in these inclusions is nearly pure CO_2. Melting of the CO_2 clathrate (Tmclath) in the presence of CO_2 liquid occurs between 4.1 and 8.5°C. Partial homogenisation ($ThCO_2$) of CO_2 liquid + CO_2 vapour to liquid CO_2 occurs between 20.2 and 29.5 °C. Upon heating, more than one-half of the studied inclusions decrepitated prior to final homogenisation, at temperatures from 200 to 280°C. Total homogenisation temperatures to liquid, obtained mainly from inclusions with lower CO_2 contents and smaller diameters, range from 250 to 320°C.

L-V-S inclusions are common in samples from Bayan Obo, and are concentrated mainly in fluorite, but are also found in quartz cores and in REE fluorocarbonates. They occur as isolated inclusions and are primary. During heating experiments some L-V-S inclusions decrepitated or stretched prior to total homogenisation. Only a few of them survived, and the hexagonal or irregular shaped daughter minerals (that may be REE fluorocarbonates) were nearly always the last phase left in the inclusions. With continuous heating and cooling, the hexagonal shaped daughter minerals displayed the following three behaviours: (1) complete dissolution at temperatures of 420~480°C, these are also the total homogenisation temperatures of the inclusions; (2) re-crystallised to one or more new hexagonal shaped daughter minerals at about 400~320°C. Cubic halite, if existing, dissolved from 220 to 250°C during heating and formed again at about 260 to 280°C during cooling. The

homogenisation temperatures might be considered to present the temperature of the mineralising fluid prior to ore deposition.

Solid phases trapped in the inclusions contain a complex and varied assemblage. The solid phases are encountered either singularly or, more commonly, in association with other solid phases. REE-carbonates, halite, sylvite, barite, calcite and pyroxene (?) have been identified on the basis of crystal habit (microscopic and SEM) and EDX analysis. Comparison of spectra of unknown daughter crystals with Raman spectra of reference REE-carbonate mineral crystals, indicates that the hexagonal or irregular shaped daughter minerals in L-V-S inclusions may be cebaite and bastnaesite. It is inferred that daughter minerals in multiphase inclusions in mineralising veins were crystallized from trapped fluids, and are real daughter minerals.

Conclusions

The presence of REE-carbonates as an abundant solid in the ore-forming veins shows that the ore-forming fluids are very rich in REE, and therefore, have the potential to produce economic deposits of REE at Bayan Obo without requiring large-scale convective fluid systems and high water-rock ratios typically envisaged for other magmatic-hydrothermal ore-forming environments.

Acknowledgements

The present study was supported by National Basic Research Program of China (Project No. 2012CB416605).

Thermobarogeochemical conditions for the Kuhilal Noble Spinel Area formation (Tajikistan)

A.R.Fayziev[1] and S.A.Elnazarov[1]
[1]Institute of Geology, Earthquake Engineering and Seismology, 734063. 267 Ayni, Dushanbe Tajikistan

The Kuhilal deposit in south-western Pamir has been the source of famous Badakhshan Lal (noble spinel) production for many hundreds years (from VII century). In addition, it also produces gem quality golden-yellow clinohumite, and commercial magnesium silicate minerals (talc, forsterite, enstatite) and Mg-carbonate (magnesite).

Kuhilal is a magnesian skarn deposit in the contact aureole of magnesium marble with an aluminosilicate gneiss-migmatite sequence formed under granulite and amphibolite facies metamorphism. In the early stage of skarn formation forsterite, spinel, and enstatite crystallised, while in the regressive stage tremolite, klinogummit, calcite, etc were formed.

Primary fluid solution-melt inclusions are found in all abovementioned minerals. Most of them are negative crystal-faceted. However, their form depends on the state of aggregation of host mineral. The needle-like tremolite and enstatite secretions have greatly elongated inclusions but granular aggregates of clinohumite and forsterite have isometric ones. Spinel hosts inclusions with perfect octahedral shapes. The size of inclusions in spinel, clinohumite and calcite are tenths and hundredths microns, and in forsterite, enstatite and tremolite - thousandths microns. They are mostly multi-phase fluid-crystal (crystallised), and rarely consist of single-phase gas. Inclusions have up to 8-10 crystalline phases, and a gas phase. The gas phase is usually deformed and located in interstices of "daughter" crystals. Often several separate gas phases can be observed. Only hexagonal crystals of phlogopite, needle-like crystals of rutile and irregular grains of graphite are diagnosed among solid phases. The inclusions in the studied minerals homogenised into liquid, except for inclusions in calcite. Inclusions in calcite homogenised exclusively to the gas phase, indicating a high fluid saturation of the mineral-forming medium at time of this mineral formation. Often, complete homogenisation can not be reached in crystallized inclusions because they explode soon after disappearance of the gas phase. Another feature of these inclusions is that when they are heated to 400-450°C the dissolution of solid phases does not occur, which may indicate a lack of well-soluble minerals between the solid phases.

The ranges of homogenisation temperatures of inclusions in minerals of the Kuhilal deposit are: forsterite 800-740°C, spinel 770-650°C, enstatite 690-650°C, calcite 690-670°C, clinohumite 680-600°C. Secondary inclusions in the studied minerals are two-phase fluid (gas-liquid), the range of temperature of homogenisation for these inclusions is 450-380°C. The pressure at the time of crystallisation of minerals was high and is in the kilobar range. The mineral-forming fluids were mainly chloride with a low HCO^{3-} content. The cations are dominated by Ca^{2+}, Na^{+}, K^{+} and Mg^{2+}. However, the presence of multiphase inclusions of insoluble solid phases suggests more complex compositions of mineral-forming melt-solution fluids. Carbon dioxide dominates the gas phase of inclusions. The homogenisation temperatures are generally consistent with the temperature conditions of regional metamorphism of the host rocks as calculated by the various mineral geothermometers: 700-900°C for granulite and 600-650°C for amphibolite facies. Actually, the skarn mineralisation stage could have occurred during the highest stage of regional metamorphism (granulite facies), and a regressive process at lower temperature (amphibolite facies). The pressure for skarns at Kuhilal did not exceed 5-6 kbar.

Fluid inclusion microthermometry and Raman spectroscopic analysis of the Chah Zard epithermal gold-silver deposit, west central Iran

Majid Ghaderi[1], Hossein Kouhestani[1], Khin Zaw[2] and Terrence Mernagh[3]
[1]Department of Economic Geology, Tarbiat Modares University, Tehran, Iran
[2]CODES ARC Centre of Excellence in Ore Deposits, University of Tasmania, Hobart, Australia
[3]Geoscience Australia, GPO Box 378, Canberra, Australia

The low- to intermediate-sulphidation epithermal Au-Ag deposit of Chah Zard is located in the central part of the Urumieh-Dokhtar magmatic arc, west central Iran. The host rocks are late Miocene calc-alkaline to high-K, calc-alkaline intermediate to felsic volcanic rocks with arc magma geochemical affinities. Gold and silver are hosted by hydrothermally cemented breccia bodies, veins, and disseminated sulphides and sulphosalts. The mineralogy of the veins and breccias is dominated by pyrite, marcasite, arsenian pyrite, arsenopyrite, chalcopyrite, galena, sphalerite and silver sulphosalts together with native gold and electrum. The gangue mineralogy includes quartz, adularia and clay minerals with minor carbonate. Fluid inclusion microthermometry with petrographic data on ore minerals constrains the stages of ore deposition in Chah Zard. At room temperature, the entrapped fluids are of four compositional types:

(1) three-phase inclusions, with vapour bubble, liquid, and cubic NaCl solid;
(2) aqueous liquid-rich, liquid-vapour inclusions (that homogenised into liquid phase);
(3) one-phase vapour inclusions;
(4) one-phase liquid inclusions.

All fluid types are present in quartz from the cement of the Au-Ag-bearing polymictic breccia. Type (2) and (3) or (4) fluids also occur within sphalerite from late base metal-rich veins and show consistent phase proportions. At Chah Zard, the type (2) fluid is the main ore-forming fluid. Microthermometric measurements show that quartz-hosted type (2) fluid inclusions homogenised within 197–345°C. The corresponding bulk salinities vary between 10–14 wt percent NaCl equiv. Laser Raman spectroscopy confirms that the vapour phase in these inclusions is dominated by CO_2. Sphalerite-hosted type (2) fluid inclusions show a distribution of $Th_{(total)}$ and bulk salinities between 262–311°C and 8–12 wt percent NaCl equiv, respectively. Based on the $Th_{(total)}$ of inclusions trapped from type 2 fluids, a minimum hydrostatic depth of 970 m to 440 m is estimated for the depth of mineralisation at Chah Zard. The salinities and homogenisation temperatures of the main-stage ores indicate that the hydrothermal fluids responsible for the epithermal gold–silver deposit at Chah Zard may have been derived from interaction of magmatic fluids with meteoric water under epithermal conditions.

Haftcheshmeh copper porphry deposit, Arasbaran Copper Belt, Northwestern Iran

Hassanpour, Sh.
Department of Geology, Payame Noor University, Tehran, Iran (Hassanpour@pnu.ac.ir).

INTRODUCTION

The Main Copper belt of Iran that corresponds with the Cenozoic Arasbaran magmatic belt (AMB) extends via Iran and Armenia, with an average width of 40 Km، from northwest to southeast of Ahar Quaderangle (GSI, 1992) NW Iran. This belt is characterised by dominantly calc-alkaline volcanic, pyroclastic and intrusive rocks. The belt, hosts numerous porphyry-type Cu ± Mo deposits but most notable are two world-class deposits, Haftcheshmeh (185 Mt of ore at 0.4% Cu and 350-400 ppm Mo) and Sungun (>500 Mt of ore at 0.69% Cu and ~250 ppm Mo) in the northwestern part of the Arasbaran Copper belt, respectively.

There is evidence (Hassanpour, 2010) that the northwestern part of Iran formed on a separate arc related to the southern Caucasusian subduction zone. The arc extends from northwest Iran to Armenia in the north and contains several porphyry-style deposits, including Sungun and Haftcheshmeh in Iran and Agarak, Kajaran and Dastakert in Armenia.

The Haftcheshmeh prospect is located in a magmatic suite of rocks. The compositions of the intrusions vary from gabbro to granodiorite. The granodiorite has intruded into the intrusion with Gabbroic composition. Drilling has indicated an ellipsoidal body of 500x700m dimension at >700m depth. Potassic, phyllic, propylitic and argillic alteration assemblages are well developed in Haftcheshmeh. Mineralisation is disseminated as well as occurring in stockworks in the granodiorite and the gabbro. Sillica A and D type veinlets are observed in this district.

With respect to the alteration and ore mineralogy, the homogenisation temperature and the salinity data, the Haftcheshmeh deposit can be classified as that of a porphyry system. Porphyry deposits associated with arc locations in a subduction zone, are characterised by oxidised and acidic fluids, Furthermore the rocks are hydrothermally altered and contain sulphates. The Haftcheshmeh prospect is a typical porphyry deposit in terms of its subduction related tectonic setting, association with felsic intrusions, and alteration and mineralisation characteristics.

FLUID INCLUSION STUDIES

Heating and freezing experiments were carried out on fluid inclusions in quartz veins from the main stage of mineralisation at *Haftcheshmeh*. The inclusions occur as rods and spindles, ellipsoids, circles, irregular elongate and oblate shapes, and negative crystal forms, and vary in size from <5 - 50 microns. Most measurements were performed on primary fluids inclusions, 5 - 20 microns in diameter. Four types of fluid inclusions are distinguished: 1) VLS; 2) LVS; 3) LV; 4) Vl. The liquid-rich inclusions homogenised by vapour bubble disappearance, and the vapour-rich inclusions homogenised to a vapour phase.

The temperature of homogenisation varies between 22 8- 440 ºC (mean= 355 ºC) in quartz veins. Salinities vary between 5.4 - 15.03 wt% NaCl equivalent in quartz veins (Fig. 1). The occurrence of secondary and pseudosecondary inclusions with the same Th and salinities as the primary inclusions supports the observation that ore fluids were introduced in more than one stage, so that secondary and pseudosecondary inclusions in one quartz and/or sphalerite generation represents primary inclusions in the next generations. The wide range in Th and salinity can be explained by boiling and fluid mixing. Boiling is supported by the coexistence of liquid- and vapor-rich inclusions, the occurrence of platy calcite pseudomorphs, and hydrothermal breccias. The stable isotope data suggest the involvement of a magmatic fluid component, and mixing of fluids (Hassanpour, 2010).

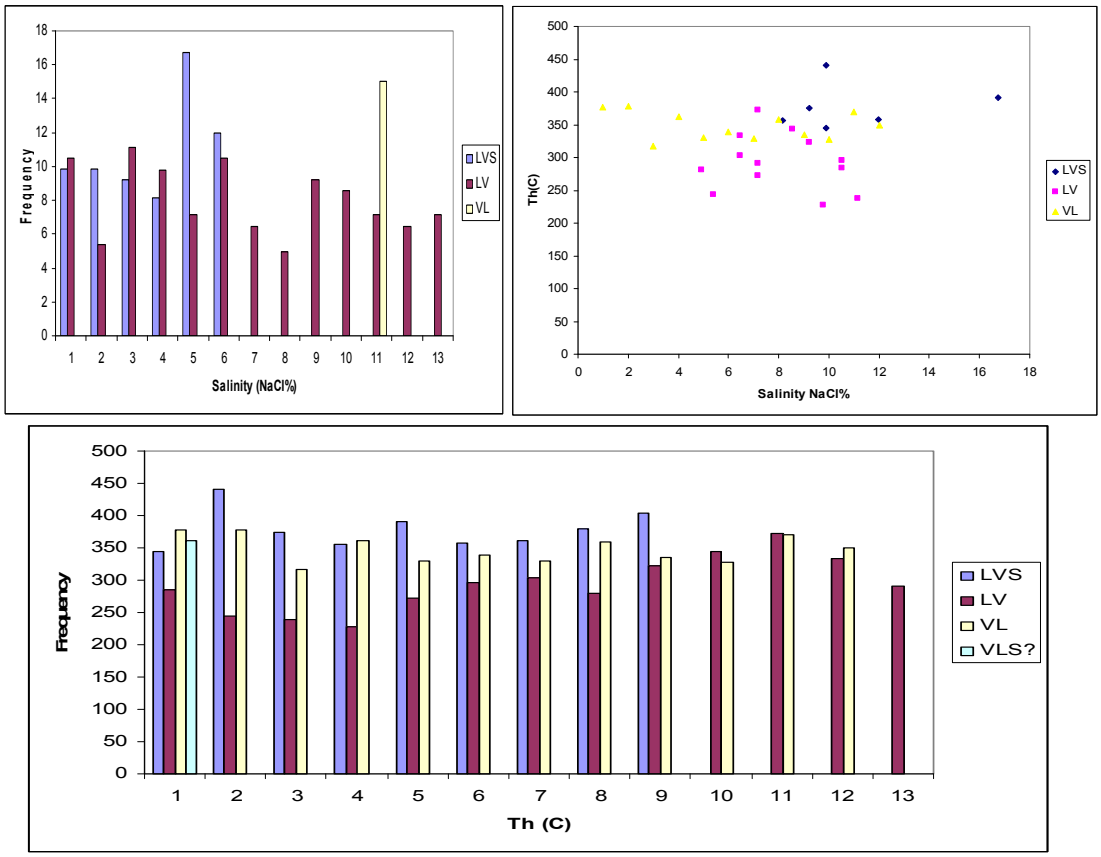

Figure 1. *Th, Salinity (equivalent wt%) and Th vs Salinity diagrams for the Haftcheshmeh Porphyry deposit*

DISCUSSION

With respect to the alteration and ore mineralogy, the Th and the salinity data, indicates that the Haftcheshmeh deposit can be classified as a porphyry system. The Haftcheshmeh porphyry deposit is associated with an arc location in a ubduction zone, metals are deposited from oxidised and acidic fluids, and are characterised by the occurrence of hydrothermal alteration including sulphates.

Acknowledgements

This research was funded by "Exploration Department" at NICICO (National Iranian Copper Industries Company). Supports by Mohammad Kargar and Mehrdad Heidari, administrators of "Exploration and Engineering Development Department", were a prerequisite for initiation and completion of the research.

References

Mehrparto,M., Aminifazl, A., Radfar, J., 1992, Varzeghan geological map, Geological survey of Iran.

Hassanpour, S., Alirezaei, S., Rasa, I., Selby, D.,Sergeev, S., 2010, SHRIMP U–Pb Zircon Geochronology Of The Sungun Cu-Mo Porphyry System; Evidence For An Early Miocene Porphyry-Style Mineralization In Northwest Iran, *in press*.

Hassanpour S (2010) Metallogeney and mineralization of Cu-Au in Arasbaran Zone, NW of Iran, *Unpublished PhD Thesis*, Shahid Beheshti University, Iran.

Fluid inclusion evidence for a hydrothermal origin for magnetite-apatite ores in the Chadormalu Iron deposit, Bafq District, central Iran

Heidarian, H.[1], *Padyar, F.*[1], *Alirezaei, S.*[1]
[1]*Faculty of Earth Sciences, Shahid Beheshti University, Tehran, Iran*

The Bafq district in Central Iran is host to many Kiruna-type Iron Oxide ± apatite deposits and occurrences including the world-class Choghart and Chadormalu mines. The district lies in the central part of the N-S trending Kashmar-Kerman volcanic-plutonic belt in Central Iran (Fig. 1) and the overall ore tonnage is estimated at ~2 Gt (NISCO, 1980).

The district is characterised by a Neoproterozoic metamorphic basement complex intruded by Early Cambrian felsic-intermediate intrusions, and overlain by an unmetamorphosed Early Cambrian volcanic-sedimentary unit (CVSU, Ramezani and Tucker, 2003). The volcanic rocks are dominated by rhyolite-dacite, associated with subordinate andesite, spilitic basalt, and less common nephelinitic to basanitic lava flows. The sequence is intruded by small, mafic-intermediate intrusive bodies and late doleritic dykes. The deposits are mainly hosted by CVSU and shallow felsic intrusions. The iron oxide ores are locally associated with REE-rich phosphate ± silicate ± carbonate assemblages, referred to as apatitite (Stosch et al., 2011). Individual apatitite bodies are uncommon. A detailed description of various generations of apatite is presented in Stosch et al. (2011).

The timing of ore formation at Choghart has been constrained at 515±21 Ma and 529±21 Ma (monazite Th/U- Pb method, Torab and Lehmann, 2007). Stosch et al. (2011) reported apatite U–Pb ages ranging from 527 to 539 Ma for five iron deposits in the Bafq district. The ages fall in the age range reported for the plutonic and volcanic rocks in the same district (525-545 Ma, zircon U-Pb, Ramezani and Tucker, 2003) as well as the widespread deposition of Late Proterozoic- Early Cambrian evaporites in Central Iran (Forster and Jafarzadeh, 1994). Ramezani and Tucker (2003) proposed an arc setting for the Early Cambrian magmatism in the Bafq district, whereas the predominantly alkaline and bimodal character of the magmatism led Samani (1998), Daliran (2002) and Daliran et al. (1999, 2010) to favour an extensional setting.

The deposits are associated with widespread Na- and Ca-metasomatism, represented by common occurrence of albite and actinolite, as well as subordinate potassic, silicic, and locally sericitic hydrothermal alteration. The genetic relation between alteration and mineralisation, however, has been a controversial issue.

Two main groups of iron ore have been distinguished in the Bafq iron district; one, represented by Mishdovan and Narigan deposits, consists of jaspillite associated with Infracambrian volcanic-sedimentary rocks, and is considered to be of sedimentary-exhalative origin (Daliran, 1990, 1999). The second group, represented by Choghart, Chadormalu, Chahgaz, and Sechahun deposits, is more important and more controversial. The proposed origins vary from ore magmas filling volcanic diatrems or lava flows (Forster and Jafarzadeh, 1994), magmatic segregations associated with carbonatites (Samani, 1988), hydrothermal alteration associated with large-scale brine circulation induced by felsic magmatism in the Early Cambrian (Torab and Lehmann, 2007), and metasomatic replacement of preexisting rocks by hydrothermal (deuteric) solutions charged with iron leached from cooling felsic plutons (Daliran, 1999). Moore and Modaberi (2003) suggested that segregation of an iron oxide melt and subsequent hydrothermal processes dominated by alkali metasomatism were both variably involved in the formation of iron ores in Choghart and possibly other iron deposits in the Bafq district.

The Chadormalu iron deposit lies to the north of the Bafq district and consists of several ore bodies enclosed in metasomatized volcanic and sedimentary rocks. A mafic intrusion, variably affected by sodic (albite) and calcic (actinlolite) alteration, occurs to the west of the deposit. Several post-ore doleritic dykes have been mapped. Apatite is a common accessory mineral and occurs as disseminated grains coexisting with magnetite, as well as discrete veins and veinlets commonly associated with magnetite, in actinlolite-rich rocks. Minor pyrite locally occurs in the ore and appears to be a late phase. Here we report fluid inclusion data for apatite from two samples, one from a vein type, and the other from a massive ore. In the former, apatite occurs intimately associated with magnetite in a vein, 12 cm wide, enclosed in an actinlolite-rich wall rock (Fig. 2-A). Apatite crystals, <1 to 4 cm long, display textures typical of open-space filling. The second sample consists of coarse apatite crystals, 0.5-2 cm long disseminated in massive magnetite (Fig. 2-B); no preferred orientation can be distinguished in the sample. The inclusions vary in size from <1µm to 25µm in the vein-type ore and <1-15 µm in the massive ore. They display faceted, rounded and irregular shapes. In both samples, most inclusions were found to be liquid-rich; they homogenised to liquid upon heating. Rare vapour-rich inclusions occur in the vein-type ore. Variations of T_h and salinities for the two types of apatite are shown in Figure 3. The preliminary data suggest that the vein-type ore formed from fluid(s) with higher salinity, but lower temperature. Further work on various apatite generations and their bearings to the ore formation is in progress.

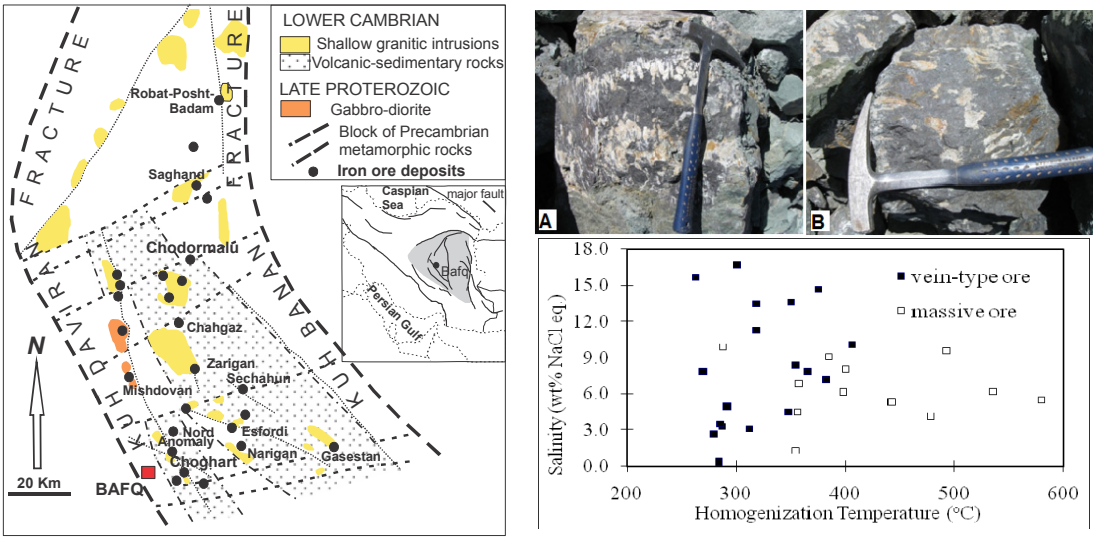

Figure 1 *(left). Simplified geological map of the Bafq District, showing the distribution of iron oxide–apatite deposits (after Stosch et al., 2011). Inset shows the location of the Bafq district in Central Iran in a sketch map of Iran.* ***Figure 2*** *(top right). A. Vein-type ore consisting of apatite (creamy white) and magnetite (dark grey) in actinolite-rich wall rock. B. Massive ore, consisting of magnetite and apatite.* ***Figure 3*** *(bottom right). Variations of T_h and salinities for the two types of apatite.*

Our fluid inclusion data suggest that magnetite-apatite ore in Chadormalu, and most likely in similar deposits in the Bafq district, was at least partly of hydrothermal origin, formed through circulation of a hot, low-moderate salinity fluid. The same fluid could have been involved in the widespread alkali-calcic alteration in the Early Cambrian volcanic-sedimentary rocks. Iron may have been leached from the country rocks, and redeposited in suitable structures.

REFERENCES

Daliran F., 1990. The magnetite-apatite deposit of Mishdovan, East Central Iran. An alkali rhyolite hosted, "Kiruna type" occurrence in the Infracambrian Bafq metallotect. Heidelberger Geowissenschaftliche Abhandlungen, *Ph.D. Thesis*, **37**, 248p.

Daliran F., 1999. REE geochemistry of Bafq apatites, Iran; implication for the genesis of Kiruna-type iron ores. In: Stancly et al. (Eds.) *Mineral Deposits; Processes to Processing*. Balkema, Rotterdam, pp. 631-634.

Förster H. and Jafarzadeh A., 1994. The Bafq mining district in Central Iran: A highly mineralized Infracambrian volcanic field. *Economic Geology*, **89**, 1697-1721.

Moore F., Modabberi, S., 2003. Origin of Choghart iron oxide deposit, Bafq District, Central Iran: New isotopic and geochemical evidence. *Journal of Sciences, Islamic Republic of Iran,* **14(3)**, 259-269

Ramezani J., Tucker R.D., 2003. The Saghand region, Central Iran: U–Pb geochronology, petrogenesis and implications for Gondwana tectonics. *American Journal of Science*, **303**, 622–66.

Samani B., 1998. Precambrian metallogeny in Central Iran. *AEOI Sciences Bulletin* **17**, 1–16 (in Farsi with English abstract)

Stosch H.G., Romer R.L., Daliran F., Rhede D., 2011. Uranium–lead ages of apatite from iron oxide ores of the Bafq District, East-Central Iran. *Mineraium Deposita*, **46**, 9–21.

Torab F.M., Lehmann B., 2007. Magnetite-apatite deposits of the Bafq district, Central Iran: apatite geochemistry and monazite geochronology. *Mineralogical Magazine*, **71**, 347-363.

Fluid inclusion variability of the basement rocks in Bangladesh

Ismail Hossain
Department of Geology and Mining, University of Rajshahi, Rajshahi 6205, Bangladesh
(ismail_gm@ru.ac.bd)

Despite the spatial and temporal association of pegmatite and aplite veins within dioritic rocks in the basement rocks of Bangladesh, the relation between the two lithotypes still has some disparities of opinion. Granitic pegmatite with intermittently aplite veins formation could be the result of thermal anomalies, which are predicted to cause fluid convection. Without doubt they have usually a genetic affinity to the rocks they intersect. Considering this view, fluid inclusion study of dioritic rocks with pegmatite and aplite veins have been carried out to understand physico-chemical conditions of Palaeoproterozoic (1.73 Ga) basement rocks in Bangladesh (Hossain et al., 2007), and constrain relationships with different types of fluids and to constrain their crystallisation history.

Petrographic and microthermometric investigations of fluid inclusions from the basement rocks in Bangladesh indicate that H_2O-rich fluids are trapped in quartz and plagioclase in dioritic rocks. Primary nature of occurrence of the inclusions in coarse-grained minerals in diorites indicates that the fluids were trapped during the crystallisation of the host minerals and that the trapped H_2O-rich fluid can be regarded as a trace of magmatic fluid. Microthermometric studies of fluid inclusions in pegmatite and aplite veins from the same basement rocks indicate their dominantly CO_2-rich composition with rare H_2O-rich fluids. Some H_2O-rich inclusions are hypersaline inclusions with equivalent NaCl concentrations of 0.17–22.95 wt.%. Previous studies on fluid inclusions in magmatic rocks suggest that occurrences of such CO_2 + hypersaline H_2O fluids and dominant CO_2-rich fluid in late-stage pegmatite and aplite are common (Roedder, 1979; Nabelek and Ternes, 1997). This is probably due to separation of magmatic fluid into two immiscible phases at low temperature, CO_2-rich gas and salt-rich liquid (brine) and/or the change in fluid compositions from H_2O-CO_2 to CO_2 during the crystallisation stage (Nabelek and Ternes, 1997).

On the other hand, in present dioritic rocks, a dense H_2O-rich fluid, with low salt content, depending on Cl and H_2O abundances in the original fluid, may separate at various stages directly from the normal liquid line of descent and its CO_2 content is sufficiently high, it too may separate off a new immiscible CO_2-rich phase in pegmatite and/or aplite veins. Another possibility that at continuing lower temperatures and/or pressures, a new CO_2-rich fluid may separate, form either the water-rich phase or possibly from hydrous saline melt (Roedder, 1992). However, in this case, different intrusion stages of dioritic rocks and veins as well as lack of H_2O-CO_2 mixed fluids in diorite samples suggest two-stage fluid activities (earlier H_2O-rich and by later CO_2-rich fluid), which have been reported for dioritic rocks elsewhere (Roedder, 1992; Hossain et al., 2009).

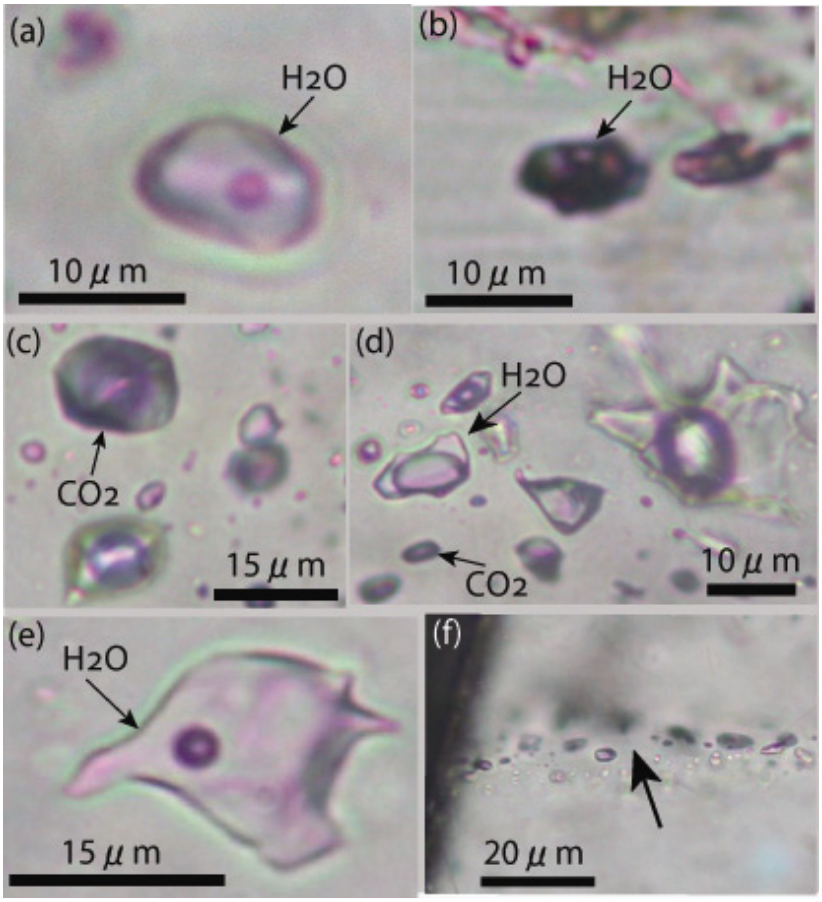

***Figure 1**: Different types of fluid inclusions in the basement rocks: primary aqueous fluid inclusions in quartz (a) and plagioclase (b) in dioritic rocks, primary CO_2 fluid inclusions in quartz (c) in pegmatite, cluster of fluid inclusions showing coexistence of primary CO_2 and aqueous fluid inclusions in quartz (d) in pegmatite, primary aqueous fluid inclusions in quartz (e) in aplite, and trails of very small secondary (indicated by arrow) fluid inclusions in quartz (f) in aplite, which are not suitable for microthermometric measurements.*

REFERENCES

Hossain, I., Tsunogae, T., Rajesh, H.M., Chen, B. and Arakawa, Y., 2007. Palaeoproterozoic U-Pb SHRIMP zircon age from basement rocks in Bangladesh: A possible remnant of Columbia Supercontinent. *C.R. Geoscience*, **339**, 979–986.

Hossain, I., Tsunogae, T. and Rajesh, H.M.. 2009. Geothermobarometry and fluid inclusions of dioritic rocks in Bangladesh: Implications for emplacement depth and exhumation rate. *Journal of Asian Earth Sciences*, **34**, 731–739.

Nabelek P.I. and Ternes, K., 1997. Fluid inclusions in the Harney Peak granite, Black Hills, South Dakota, USA: implications for solubility and evolution of magmatic volatiles and crystallization of leucogranite magmas. *Geochimica et Cosmochimica Acta*, **61**, 1447–1465.

Roedder, E., 1979. Origin and significance of magmatic inclusions. *Bulletin de Mineralogie*, **102**, 487–510.

Roedder, E., 1992. Fluid inclusion evidence for immiscibility in magmatic differentiation. *Geochimica et Cosmochimica Acta*, **56**, 5–20.

Fluid inclusions in different depths at Sanshandao gold deposit, Jiaodong Peninsula: Implication for ore genesis

F.F. Hu, H.R. Fan, X.H. Jiang and K.F. Yang
Key Laboratory of Mineral Resources, Institute of Geology and Geophysics, Chinese Academy of Sciences, Beijing 100029, China

GEOLOGICAL SETTING AND MINERALISATION

The Sanshandao gold deposit, with gold resources of more than 150 t, is located in the north western part of the Jiaodong Peninsula, which is currently the most important gold province in China, both in terms of gold production and gold ore reserves. The gold mineralisation is confined to a major fault zone (Sanshandao fault) that cuts the Mesozoic Sanshandao granodiorite and the Archaean Jiaodong Group gneisses and amphibolites. The deposit is a typical highly fractured and altered, disseminated gold system, characterised by strong silicification, sericitization, and sulphidation. Recent deeper drilling exploration (>2000m) gives a chance to compare nature of ore-forming fluids at different depths.

Fluid inclusions

Fluid inclusions in the altered wall rocks and gold ores from different depths were examined. Three compositional types of fluid inclusions, namely CO_2-H_2O±CH_4, H_2O-rich and pure-CO_2 inclusions, were identified based on their optical characteristics at room temperature.

The microthermometric study of fluid inclusions was carried out for the samples collected from near surface to about 2000m depth in the drilling hole. The homogenisation temperatures and calculated salinities from different stages are summarised in Figure 1.

The type of fluid inclusions in the early mineralisation stage are mainly CO_2-H_2O±CH_4. The calculated X_{CO2} varies from 0.1–0.0.32 0.32, and inclusions contain CH_4. Bulk densities of the inclusions range from 0.58 to 0.98 g/cm^3. The types of fluid inclusion in the main mineralisation stage are CO_2-H_2O±CH_4, and pure-CO_2 inclusions. The calculated bulk densities of the inclusions are 0.28–0.79g/cm^3 and 0.91–1.03g/cm^3, respectively, showing co-existing low and high density inclusions. The type of fluid inclusions in the late mineralisation stage are H_2O-rich inclusions with less CO_2 (X_{CO2}=0–0.07). Bulk densities of these inclusions are higher (0.89–1.05g/cm^3).

Homogenisation temperatures of fluid inclusions are 258–416°C in the early mineralisation stage, 180–321°C in the main mineralisation stage, and 112–231°C in the late mineralisation stage, showing temperatures gradually decreasing from the early to late stage. The variation of homogenisation temperatures of the same stage at different depths is nearly stable, showing no tendency for increasing temperature with increasing depth.

The ore-forming fluids are low salinity. Variations in the salinity of fluid inclusions in the same stage from different depths are not obvious. There also exists CH_4-bearing inclusions in the early and main mineralisation stages in the upper and lower drilling holes.

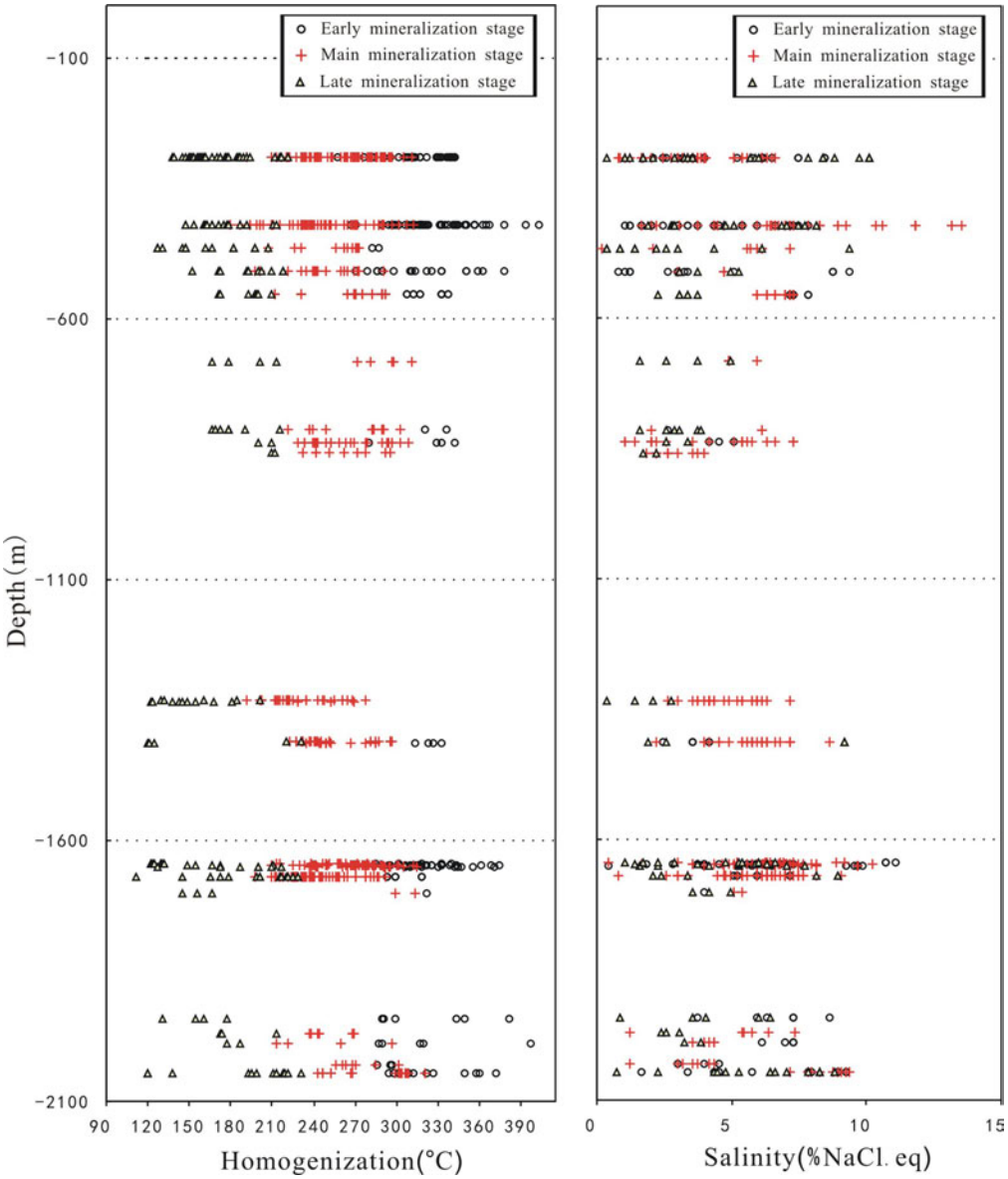

Figure 1: *Homogenisation and salinity of fluid inclusions vs. different depths in the Sansandao gold deposit*

Conclusions

Petrography and fluid inclusion studies indicate that the Sanshandao gold deposit is formed from similar gold-bearing fluids as in other deposits in the Jiaodong Peninsula, characterised by H_2O-CO_2-NaCl±CH_4 fluids and similar homogenisation temperature and pressure conditions during the main gold mineralising stage. The nature of the ore-forming fluids is nearly same over the 2000 m vertical depth. These stable circumstances are a prerequisite to the formation of this super-large gold deposit.

Acknowledgements

This study was financially supported by the Natural Science Foundation of China (41173056).

A mystery of hydrothermal fluids: Myths and facts about fluid inclusions

V. S. Kamenetsky[1] *and O. V. Vasyukova*[1]
[1] CODES, *University of Tasmania, Hobart, Tasmania, 7001 Australia*

MAGMATIC IMMISCIBILITY AND MELT/FLUID INCLUSION STUDIES

Orthomagmatic theories assume that many types of economic mineralisation relate to magmas and magma-derived fluids, however, the existing record of phases linking silicate melts and hydrothermal fluids is very poor. At least we know that a variety of phases form and disappear in the transition from magmas to "hydrothermal" fluids, and we believe that such phases represent widely operating immiscibility. The compositional divergence between unmixed phases is extreme, and even though the physical amounts of the new phase may be small, its separation and transport can be important.

It is traditionally believed that melt and fluid inclusions hosted in magmatic and hydrothermal minerals represent "snapshots" of melts or fluids at the time of crystallisation, i.e. parental to crystallising minerals. While the use of silicate melt inclusions in deciphering compositions of magmas is being well justified, the trapping mechanisms and compositions of fluid inclusions were not scrutinized enough to conclude that they directly apply to natural fluids.

Occurrence and composition of fluid inclusions

In our studies of quartz-hosted fluid inclusions we targeted their distribution within quartz, daughter phase assemblage, compositions and behaviours during thermometric experiments. Trails of inclusions are aligned with healed fractures crosscutting growth planes or randomly oriented through quartz crystals (Fig. 1). The fractures healed with later quartz are clearly visible in cathodoluminescence (CL). The trails and inclusions in them can be very abundant and so densely and randomly distributed that identification of truly primary inclusions is not possible. Three main types of inclusions are present in different or the same trails in a sinle quartz grains: (1) aqueous vapour rich with minor amounts of liquid, often containing a few euhedral crystals, (2) aqueous liquid-rich with a vapour bubble and (3) crystal-rich with variable amount of liquid and solids. The number of crystals is highly variable (up to 14 daughter minerals). The contents of fluid inclusions are metastable and prone to spontaneous recrystallisation followed by changes in the number, shape and volume ratios of phases.

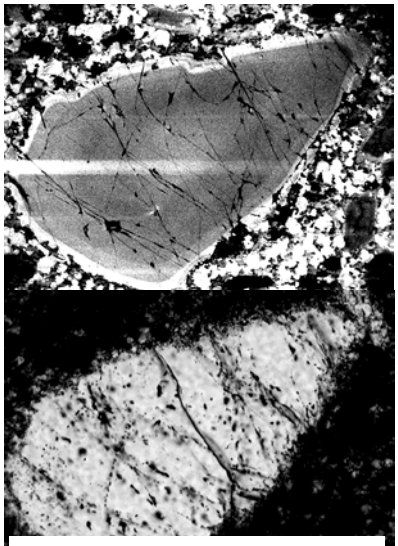

Figure. 1. *CL and transmitted light images of "quartz eye" showing healed fractures and distribution of trails of fluid inclusions*

Chlorine is a major anion, present in crystals and the aqueous solution of fluid inclusions, whereas the cations are dominated by Na, K, Fe, Mn, Cu, Zn and Pb. The compositions of fluid inclusions within healed fractures vary greatly in absolute concentrations, and although abundances of major elements are generally correlated, the element ratios deviate significantly (to 65%) from the average, suggesting vastly fluctuating fluid chemistry. The compositional heterogeneity among the inclusions supports the notion that ''*a hydrothermal fluid is . . . an evolving or changing entity*'' (Skinner, 1979, p. 12) and implies chemical variability among their parental fluids. Crystal-rich inclusions homogenise into liquid at 550–650°C. On cooling they remain homogeneous for ~100–150°C below homogenisation temperature, and then undergo spontaneous unmixing into at least two liquids and nucleation of several vapour bubbles. With further cooling the boundary between two liquids fades out, and spontaneous changes in the phase

composition in both phases occurs within a few degrees at <120–140°C. Such behaviour of inclusion is unlikely to represent crystallisation, but resembles cooling-induced changes in a colloid or gel (e.g. coagulation).

Chlorine vs silica in ore-forming fluids

Highly saline (hypesaline or brine) aqueous fluid inclusions are a priori considered to show properties of metal-transporting hydrothermal solutions. Notably, saline fluid inclusions provide compositional and temperature values that are characteristic of NaCl saturation in water ("*halite trend*", Cloke & Kesler, 1979). Thus halite and other chlorides should be the first minerals to crystallise from hydrothermal solutions, if the latter are indeed represented by fluid inclusions. Surprisingly, hydrothermal chloride minerals are missing completely from any orthomagmatic deposit.

On the other hand, quartz is the main gangue mineral, and its genetic association with ore minerals is unequivocal. Other forms of silica and silicate minerals also have a significant presence in mineralised rocks, thus demanding high concentrations of silica in hypothetical hydrothermal solutions and fluid inclusions that supposedly represent them. The amounts of magmatic H_2O and rates of the fluid flow, required for silica and metal transport into and within ore-forming systems, remain geologically unreasonable.

Quartz textures and possible origin

We studied shapes and textures (by optical, cathodoluminescence-CL and backscattered electron-BSE microscopy) of quartz grains, and the distribution of quartz-hosted fluid inclusions in different porphyries. Most quartz grains are round or even spherical in shape ("quartz eyes"), and have distinct zoning or layering in CL. The number of layers/bands varies from a few to several tens, and they have shapes from nebulous to ellipsoidal to perfect crystallographic (Fig. 2). The bands are randomly intersected by healed fractures, which are always decorated by aqueous saline inclusions (Figs. 1, 2). The fractures often cause rupture, displacement and inflection of some bands towards the core of grains (Fig. 2). Where large fractures intersect the grain surface the outermost bands are split and curved towards the fracture. The textures of quartz grains are inconsistent with their origin as phenocrysts. We envisage in-situ segregation of residual SiO_2- and H_2O-rich liquid (e.g. silica-gel) into blebs and globules during magma cooling and crystallisation. The solidification of globules was unlike crystallisation, as they were developing coeval banding and conchoidal fractures (Figs. 1, 2), and more likely as a result of coagulation. They perhaps remained in a plastic state even at low temperatures, when healing of fractures and trapping of chloride- and metal-rich substance, residual after coagulation of the silica-gel, as fluid inclusions occurred.

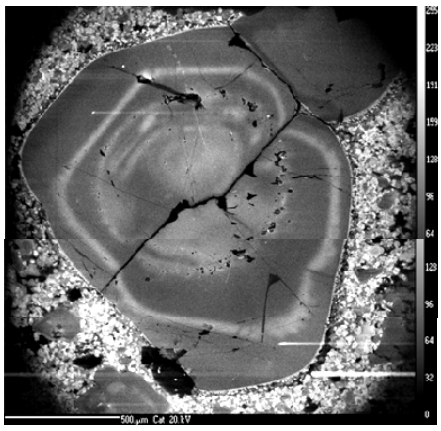

Figure. 2. *CL-structure of quartz "eye" from Panguna, PNG. Note deformation of bands in vicinity of healed fractures*

CONCLUSIONS

Liquid/fluid immiscibility at the brink of magma solidification is undoubtedly a starting point of mineralising processes. But the composition of immiscible phases, their evolution at cooling, and when and how these phases deposit economic metals and silica, remain unsubstantiated. Many years ago John Elliston called for a paradigm shift in petrology and economic geology "*It is time to recognise that developments in colloidal and surface chemistry and the rheology of aqueous pastes now enable us to resolve longstanding problems….provide an established basis for an alternative genesis for granites and orebodies*". It is time now to think and act accordingly.

References

Cloke, P.L. and Kesler, S.e., 1979. The halite trend in hydrothermal solutions. *Economic Geology*, **74**, 1823-1831.

Skinner, B.J., 1979. The many origins of hydrothermal mineral deposits. In: Barnes, H.L. (Ed.), *Geochemistry of Hydrothermal Ore Deposits*. Wiley & Sons, New York, NY, pp. 1-21

Datolite mineralisation of the Dalnegorsk borosilicate deposit: Formation conditions according to fluid inclusion data

Karas O.A., Pakhomova V.A.
Far East Geological Institute, Far Eastern Branch of Russian Academy of Sciences, Vladivostok, Russia

The Dalnegorsk borosilicate deposit is located in the central part of the Dalnegorsk Ore District, which contains diverse types of mineralisation. Here, besides the discussed large borosilicate deposit, there are tin-polymetallic ore deposits of vein-disseminated type, lead-zinc deposits of skarn and vein type, and gold-silver vein manifestations. They are confined to horsts of folded basement, which include large allochthonous units of Triassic limestone and are located in the points of intersection of regional shear zones controlled by distribution of alkaline basaltic dykes.

The borosilicate deposit is confined to a large limestone olistoplaka stretching for 3.5 km in the north-east direction and occurring within sedimentary melange of olistostrome strata overlaid by a cover of siliceous-terrigenous rocks of Gorbushinsky series. The thickness of the olistoplaka exceeds 600 m. Limestone and siliceous-terrigenous rocks are deposited subvertically and compose a southeastern wing of the Central Form [2]. Solid skarn massif with axinite-danburite-datolite mineralisation is confined to Middle-Upper Triassic riftogenic limestone strata and has a complex internal structure conditioned by a presence of units of unsubstituted rocks, faults, and diabase porphyrite dykes. The Dalnegorsk borosilicate deposit is a typical limestone skarn deposit with superimposed boron mineralisation. Metasomatic zonality occurs as diffusion-bimetasomatic zones within «granite-limestone» contact and infiltration zones outside of the contact. Datolite mineralisation and, to a lesser extent, datolite-danburite and axinite-datolite mineralisation were formed in the infiltration limestone skarns. Thickness of the datolite mineralisation depends on a degree of skarn modification and diminishes with depth. Hedenbergite, garnet, wollastonite and other skarns are spatially combined with the intrusive body that provided temperature conditions for metasomatism.

Skarn, borosilicate, and quartz-carbonic stages of mineralisation were established at the deposit [1]. Bulk of datolite and some of danburite were deposited during the main borosilicate stage. Datolite, the most common borosilicate at the deposit, develops, as a rule, within limits of skarn beds and is not recorded outside of them. It occurs deeply in the opencast in thin-banded aggregates consisting of pale-green datolite, pyroxene, and rarely wollastonite. In skarns, datolite occurs as separate bands and nodules, forming grain aggregates with granular size varying from shares of millimeters to 2-5 cm.

Complex composition and genesis of the deposit explain a special interest to the formation conditions of its mineralisation. Whereas ore mineralogy is considerably investigated, data on physical-chemical parameters of the ore formation processes are rather limited. Examination of datolite samples extracted from the hole N 875 (collection by N.A. Nosenko) drilled to the depth of 859.2 m supplied us with information about composition, concentration, and temperature of formation processes of mineral associations with datolite. Numerous gas-liquid inclusions of 5-45 μm size were discovered in datolite, and gas bubbles occupied 20-50 vol%. Most inclusions were of irregular form, and there were also oval and lenticular ones.

Thermometric examination of fluid inclusions was performed at the Far East Geological Institute (Far Eastern Branch of Russian Academy of Sciences) using polarized light microscope NIKON E 600 POL equipped with thermo- and cryo-tables THMS600 (-190 +600°C) in real time regime. Salt concentration was estimated by the temperature of ice melting for H_2O-NaCl system. Fluid pressure was calculated using FLINCOR program [3]. Results of examination of individual inclusions showed presence of Na, Ca, Mg, K, Fe, Cl, and water in phase composition of the salt system (Table 1).

Table 1. Results of examination of fluid inclusions in datolite from the Dal'negorsk borosilicte deposit.

№	Depth, m	Temperature, °C			C_{salt}, mass% eq NaCl	d, g/cm^3
		homogenisation	eutectic	ice melting		
1	from cavities	130-170	-59 ÷ -55	-0.8 ÷ -0.3	1.40-0.53	0.94
2	36,7	300-320	-38 ÷ -33	-12.7 ÷ -6	10.62-9.21	0.81
3	120,8	270-330	-55 ÷ -52	-11.5 ÷ -10.5	15.47-14.46	0.87
4	197,3	290-315	-55 ÷ -49 -35 ÷ -33	-8.2 ÷ -6 -6 ÷ -4.9	11.93-9.21 9.21-7.73	0.82
5	247,8	280-310	-39 ÷ -33	-3.7 ÷ -2.5	6.01-4.18	0.77
6	595	260-300	-56 ÷ -53	-9.7 ÷ -9.1	13.62-12.96	0.88
7	702,5	280-315	-65 ÷ -49	-9.1 ÷ -8.6	12.96-12.39	0.85
8	782,0	270-300	-60 ÷ -52	-10.4 ÷ -6.5	14.36-9.86	0.82
9	859,2	260-310	-52 ÷ -42	-1.9 ÷ -1.6	2.74-3.23	0.74

The concentration varied insignificantly with depth, reaching its maximum of 15.5 eq mass% NaCl. Average fluid density was 0.82 g/cm^3. These inclusions were homogenized in liquid at 260-340°C and the ore deposition pressure of 60-82 bar. Datolite-hosted inclusions from the open cavities were also homogenized in liquid phase, but at lower temperatures of 130-170°C and concentration decreasing to 0.53 eq mass% NaCl. Gas phase showed no presence of free carbon dioxide both at above-zero and below zero temperatures that indicated relatively low CO_2 concentration.

REFERENCES

Kurshakova L.D. Physical-Chemical Conditions of Formation of Skarn Borosilicate Deposits. Moscow: Nauka, 1976. 276 p.

Ushmanov Yu.P., Petrishchevsky A.M. Tectonics, deep structure ad metallogeny of the Coastal Zone of the Southern Sikhote-Alin. Vladivostok: Dalnauka, 2004. 112 p.

Brown P.E. (1989) FLINCOR: A microcomputer program for the reduction and investigation of fluid-inclusion data. Am. Mineralogist 74, 1390-1393.

Raman imaging of fluid and "melt" inclusions in K-bearing clinopyroxene: Second critical end point for UHPM garnet-clinopyroxene rocks (Kokchetav massif, Kazakhstan)

A.V. Korsakov[1], *A.O. Mikhno*[1], *and U. Schmidt*[2]
[1] *V.S. Sobolev Institute of Geology and Mineralogy SB RAS, 630090, Koptyug avenue 3, Novosibirsk, Russia*
[2] *WITec GmbH, Lise-Meitner-STrasse 6, 89081 Ulm, Germany*

INTRODUCTION

The study of deep fluid or melt inclusions in minerals, formed at ultra-high pressure (UHP) conditions, remains one of the most interesting topics in geosciences. Previous studies of fluid inclusions in minerals from UHP metamorphic rocks mainly focused on inclusions in quartz. Recently melt inclusions (Korsakov and Hermann, 2006) and fluid inclusions (Korsakov et al., 2011) were identified in garnet and clinopyroxene from the UHPM metamorphic rocks from the Kokchetav massif. In this paper we present the results of a fluid and "melt" inclusion study in garnet and clinopyroxene from diamond-grade, but diamond-free rocks from the Kokchetav massif.

SAMPLES AND METHODS

The geological setting of the Kokchetav massif (Northern Kazakhstan) has been summarized elsewhere (e.g. Dobretsov et al. 1995; Theunissen et al. 2000). In this study, 5 specimens of Grt-Cpx rocks from the Kumdy-Kol deposit and Barchi-Kol area were utilised for detailed fluid-inclusion investigations. The Grt-Cpx rock is composed of clinopyroxene (20-60%), garnet (30-60%), carbonates (e.g. dolomite or calcite 0-30%) and minor biotite, K-feldspar and quartz all together less than 15%. The confocal Raman images for 3 inclusions were collected by acquiring 2D arrays of complete Raman spectra from a defined sample area with a Confocal Raman Microscope alpha 300R (WITec GmbH, Ulm, Germany). The thousands of Raman spectra were evaluated using cluster analysis. In this data evaluation method, the acquired Raman spectra are grouped in to most similar spectra and images are generated, which display the distribution of the selected components, their various phases and/or their strain state.

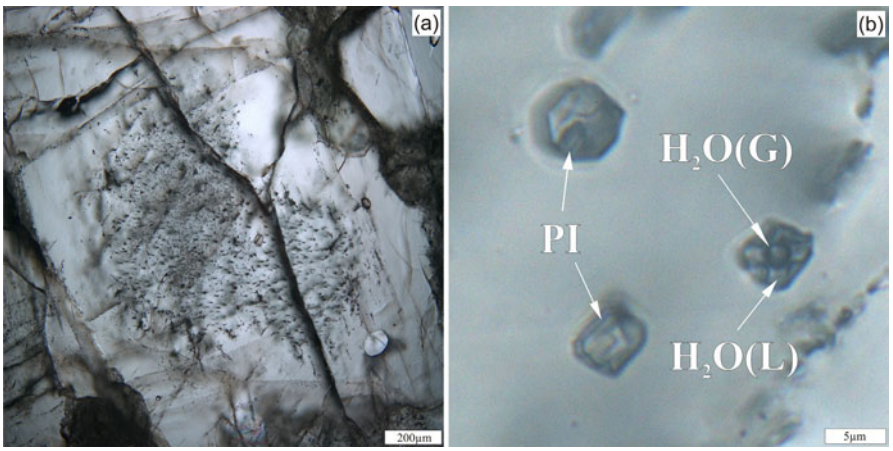

Figure 1: *Fluid (FI) and polyphase(PI) inclusions within the core of K-bearing clinopyroxene.*

Primary fluid and polyphase inclusions (up to 10 µm in size) occur within the same growth zone of K- Cpx (Fig. 1). They have the negative crystal shape of the host-clinopyroxene. On the polished surface of the thin section fluid inclusions appear as holes with small relics of daughter phase, while all minerals in polyphase inclusion are well polished. Raman imaging of fluid inclusions (Fig. 2)

reveals that they consist of H_2O-liquid, H_2O-gas, and daughter phases (e.g. calcite, mica, kokchetavite). No Raman bands of CO_2, CH_4 or N_2 were identified within the analysed fluid inclusions. Polyphase inclusions represent former melt inclusions and consist of mica, kokchetavite, quartz, without traces of H_2O-liquid (Fig. 2).

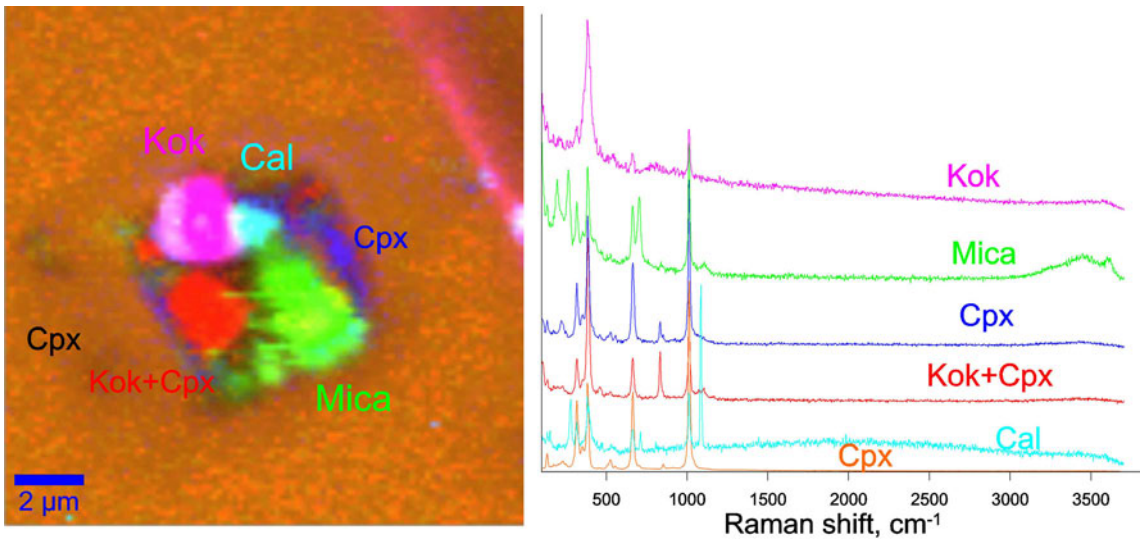

***Figure 2**: Raman image and individual spectra of minerals, identified in the fluid inclusion*

CONCLUSIONS

We believe that polyphase inclusions consisting of mineral assemblages not stable at peak metamorphism conditions have to represent a melt (Korsakov and Hermann, 2006, Hermann et al., 2006). Coexistence of polyphase and fluid inclusions within the same growth zone of K-Cpx may indicate that immiscible fluid and melt were presented prior or even at peak metamorphism (6-7 GPa and 950-1050ºC). Thus, P-T conditions of the second critical end point for garnet-clinopyroxene rocks should be located at higher pressure and temperature. This work was supported by the Russian Foundation for Basic Research (No.10-05-00616-a).

REFERENCES

Dobretsov, N. L., Sobolev, N. V., Shatsky, V. S., Coleman, R. G., Ernst, W. G., 1995. Geotectonic evolution of diamondiferous paragneisses of the Kokchetav complex, Northern Kazakhstan - the geologic enigma of ultrahigh-pressure crustal rocks within Phanerozoic foldbelt. *The Island Arc*, **4**, 267-279.

Hermann J. Spandler C. Hack A. Korsakov A.V., 2006. Aqueous fluids and hydrous melts in high-pressure and ultra-high pressure rocks: Implications for element transfer in subduction zones. *Lithos*, **92**, 399-417

Korsakov A.V., Hermann, J., 2006. Silicate and carbonate melt inclusions associated with diamonds in deeply subducted carbonate rocks. *Earth and Planetary Science Letters*, **241**, 104-118

Korsakov A.V., Golovin A.V., Dieing T., Toporsky J., 2011. Fluid inclusions in rock-forming minerals of ultrahigh-pressure metamorphic rocks (Kokchetav Massif, Northern Kazakhstan). *Doklady Earth Sciences*, **437**, 473-478

Theunissen, K., Dobretsov, N. L., Korsakov, A., et al., 2000. Two contrasting petrotectonic domains in the Kokchetav megamelange (north Kazakhstan): difference in exhumation mechanisms of ultrahigh-pressure crustal rocks, or a result of subsequent deformation? The Island Arc, 9, 284-303.

Na_2CO_3-bearing fluids: Experimental study using synthetic fluid inclusions in quartz

Z. A. Kotel'nikova [1], A. R. Kotel'nikov[2]
[1] Institute of Geology of Ore Deposits, Mineralogy, Petrology and Geochemistry RAS. Moscow, RF
[2] Institute of Experimental Mineralogy RAS, Chernogolovka, Russia

Heterogeneous fluid equilibria in the binary system, H_2O–Na_2CO_3, in the presence of SiO_2 or SiO_2 + $NaAlSi_3O_8$ were studied experimentally. Fluid inclusions in quartz were synthesized by healing of fractures in 1 M Na_2CO_3 solution at 700°C and under 1, 2, and 3 kbar pressure. Some runs were carried out in the presence of albite gel. The microthermomemtric study of the synthesised inclusions showed that under experimental conditions the fluid was heterogeneous and did not remain inert with respect to quartz and albite. Some inclusions contained a glass-like phase, and liquid released from this phase by heating. Having been heated, some inclusions revealed liquid immiscibility. Comparison of the water–silicate–sodium carbonate system with similar systems containing sodium sulfate and fluoride shows that they have much in common. In all cases, the aqueous salt bearing fluid did not remain inert relative to the quartz under relatively low *PT* conditions. The inclusions entrapped in the upper heterogeneous region revealed immiscibility in the presence of vapor within a temperature range of 200 to 400°C. The solutions of various concentrations, including oversaturated solutions in the presence of a solid phase, underwent recurrent heterogenisation. Near 400°C, vapour is either dissolved in one of immiscible liquids or absorbs this liquid. When heating progresses to higher temperature, the inclusions commonly decrepitate.

The experimental data showt that the equilibria of silicate and aqueous salt-bearing fluid are rather complex. During the postmagmatic stage, at 700°C and 1–3 kbar of pressure, the fluid phase is inhomogeneous. This is valid with respect to all P–Q-type salt–water systems studied in experiments (sodium fluoride, complex sulfates, etc.). the critical point Q (minimal temperature of the upper two-phase region) in boundary binary salt– water systems is commonly located within a range of 400–700°C. As is known, the water–silicate (aluminosilicate) systems are also described by P–Q-type phase diagrams, and the upper critical point Q is located rather high. The presence of salt as a third component substantially widens the possibility of recurrent heterogenisation of the fluid at lower temperature and pressure. Moreover, multistage heterogenization is possible. In addition, equilibria of two liquids or rather of liquid and gas are characteristic of the upper segment of critical curve in all known systems, both salt – water and (alumino)silicate – water. Therefore, the equilibrium of two or more liquid phases should be expected in the upper heterogeneous region of the P–Q-type multicomponent silicate–salt– water systems.

Heterogenisation of fluids is the most important mechanism of matter redistribution. Separation of the heavy fluid phase enriched in silicates, salts, and ore components can lead to the development of various superimposed processes with changeable external conditions.

Origin and migration of organic fluids at the Dabashan tectonic belt, central China

Li Rongxi[1,2] *Dong Shuwen*[3] *Zhang Shaoni*[1,2] *Zhu Ruijing*[1,2] *Xia Bin*[1,2]
[1] *Key Laboratory of West Mineral Resource & Geology Engineering, Education Ministry of China, Chang'an University, Xian, 710054, China*
[2] *School of Earth Science and Resource, Chang'an University, Xian, 710054, China*
3. Chinese Academy of Geological Sciences, Beijing, 100037

INTRODUCTION

The Dabashan Tectonic Belt (DTB) in central China, located between the southern Qinling Orogenic Belt and the Yangtze Block, is an arcuate fold and thrust belt. The DTB was divided into three tectonic subunits by big faults, which are the Dabashan Thrust Nappe Belt (DTNB) in the northeast bounded with southern Qinling Orogenic Belt along Hongchunba fault, the Dabashan Foreland Belt (DFB) between the Chengkou-Fangxiang and Wuxi-Tiexi faults, and the Dabashan Foreland Depression (DFD, the Sichuan Basin) southwest of the and Wuxi-Tiexi Fault. The DFB is bounded by the DTNB to the north and by the DFD (Sichuan Basin) to the south. The DFB has been interpreted to be a Late Jurassic-Early Cretaceous foreland structure which is superimposed on the basement of a Triassic orogenic belt (Dong et al., 2006; Shi et al., 2012; Zhang et al., 2009). As an intracontinental foreland fold and thrust belt of Late Jurassic-Early Cretaceous age, the DFB is one of the important oil and gas provinces in the northeastern Sichuan Basin (Dong et al., 2006). Field geology investigation indicated that stratum, deformation and metamorphism as well as characteristics of geo-fluid were obvious difference between different tectonic units in DTB.

FEATURES OF ORGANIC FLUID INCLUSIONS

Microscopic observation shows that characteristics of fluid inclusions are distinct in different tectonic units of DTB. Organic inclusions in the DTNB were found mainly distributed in the calcareous cement of fault breccia and fractures of mineral veins. Organic inclusions in calcareous cement of fault breccia are featured with planar shape and composed mainly by gas-liquid phase dominated with organic composition and a small amount of brine, in which the gaseous phase was grayish black bubble with no fluorescence while the organic liquid phase was gray with tint yellow fluorescence under reflected blue light. Composition analysis show that the gaseous phase composed mainly of methane. Many quartz veins and calcite veins were found widely distributed in the DTNB. This kind of veins contained with plentiful organic fluid inclusions. The organic fluid inclusions are featured with different phases, such as two-phase of gas-liquid, one phase of pure gaseous hydrocarbon and solid phase of bitumen. The pure gaseous hydrocarbon inclusion and the solid bitumen inclusion are the most. The two-phase fluid inclusions were composed of gaseous hydrocarbon and brine with the ratio of gas/liquid about 20%. The pure gaseous hydrocarbon inclusions were dark gray and big without fluorescence. The black solid bitumen inclusions filled mainly in dissolved pores of minerals with shape of tiny dot or in fractures as thin vein with flow structure, which show the feature of migration bitumen. Characteristics of fluid inclusion in the DFB and the DFD are same but they are quite different from that of in the DTNB. Large numbers of organic fluid inclusions developed in both host rocks and mineral veins filled in fractures in the DFB and the DFD. These organic fluid inclusions displayed many types and occurrences, such as liquid hydrocarbon inclusion, pure gaseous hydrocarbon inclusion, oil-bed bitumen and paleo-reservoir bitumen. According to phase and distribution, three stages of organic inclusions were identified by means of microscopic observation. They recorded the history process of oil/gas migration and accumulation during different periods of oil/gas evolution along with the Dabashan orogenesis.

The first stage inclusions had two kinds of occurrences, one of them distributed in dissolved pores of grains with irregular shape, another one was distributed in early fracture of grains without cutting through the whole debris. The first stage inclusion presented with bright yellow fluorescence under reflected blue light. The second stage inclusions were one phase inclusions with pure gaseous hydrocarbon mainly. A little of inclusions were two phases which composed with vapor and brine. The second stage inclusions were generally big with more than 20μm in diameter and mostly distributed in the later fractures or secondary solution pores. They were dark gray observed under polarized light microscopy and no-fluorescence under reflected blue light. The second stage inclusions with pure gaseous hydrocarbon recorded history process of migration and accumulation of the natural gas. The third stage inclusions were the oil-bed bitumen which mainly distributed in inter-granular pore and solution pores as well as fractures. Oil-bed bitumen was the secondary products of the paleo-reservoir which recorded regional destructive event of paleo-reservoir. Paleo-reservoir bitumen was found in several places in the DFB which were the residue of damaged paleo-reservoir.

Petrography features of organic fluid inclusion indicated that not only liquid hydrocarbon reservoir but also gaseous hydrocarbon reservoir was once formed in the area of the DFB and the DFD. But the oil/gas reservoir was damage during the tectonic movement.

THE SOURCE AND FORMATION OF ORGANIC FLUID INCLUSIONS

Analysis to gaseous carbon and hydrogen isotope of organic fluid inclusions in mineral veins show that the $\delta^{13}C_1$ was from -17.036‰ to - 30.39‰ and δD was from -107.712‰ to -156.73‰, which are similar to that of natural gas developed from gas reservoirs in the northeastern Sichuan basin (Ma et al., 2005; Chen et al., 2008). Study to the $\delta^{13}C_1$ and δD of gaseous hydrocarbon within organic fluid inclusions reveals that the gas sourced from marine organic matters with high to over mature degree and captured by mineral veins during migration along faults.

Characteristics of biamarkers of bitumen show that the lower Cambrian black shale and the lower Permian carbonate in the DFB were the main source rocks of the organic fluid.

REFERENCES

Chen Jianfa, Tang Youjun, Xu Liheng, 2008. Comparison of Geochemical Characteristics of Carboniferous and Permian-Triassic Natural Gas in Northeast Sichuan. Natural Gas *Geoscience*, **1 9(6)**, 741-747.

Dong Shuwen, Hu Jianmin, Shi Wei, Zhang Yueqiao and Guang Liu, 2006. Jurassic superposed folding and Jurassic foreland in the Daba Mountain, Central China. *Acta Geoscientica Sinica*, **27(5)**, 403-410.

Ma Yongsheng, Cai Xunyu, Li Guoxiong, 2005. Basic characteristics and concentration of the Puguang gas field in the Sichuan basin. *Acta Geoscientica Sinica*,**79 (6)**, 858-865.

Shi W., Zhang, Y., Dong, S., Hu J., Weisinger, M., Ratschbacher, L., Jonckneere, R., Li, J., Tian, M., Chen, H., Wu, G., Ma, L., Li, H., 2012. Intra-continental Dabashan Orocline, southwestern Qinling, central China: *Journal of Asian Earth Sciences*, **46**, 20-38.

Zhang Zhongyi, Dong Shuwen, Zhang Yueqiao, Hu Jianming, Shi Wei and Liu Guang, 2009. NW Folding distinguished in the Northwestern Daba Mountains, central China, and it's tectonic significances. *Geological Review*, **55(1),** 10-24.

Implications of high temperature opal inversion to quartz

Mavrogenes J.A.[1], *Tanner, D.*[1], *and Henley, R.W.*[1]
[1] *Research School of Earth Sciences, Australian National University, Canberra ACT 0200 Australia*

In high temperature environments such as high sulphidation, epithermal gold deposit feeder zones, silica appears to have ben deposited as opal, which subsequently inverted to quartz (Tanner et al, this volume). The implications of this inversion are profound in hydrothermal ore deposit studies, for which we present the following caveats: (1) growth textures interpreted as 'primary' may have formed during opal inversion, making then *'pseudo-primary'*, dramatically affecting paragenetic interpretations; (2) the geochemistry of quartz and included fluids record the conditions attendant during inversion rather than primary deposition; (3) dehydration during opal inversion causes extreme $\delta^{18}O$ fractionation, yielding isotopically heavy quartz that was never in equilibrium with the depositional fluid; and (4) diffusive re-equilibration of trace elements would have occurred more rapidly through opal than quartz. These implications affect the interpretation of textures, trace elements, stable isotopes and fluid inclusions in quartz from high-temperature hydrothermal systems. The cryptic presence of inverted opal has caused geoscientists to systematically underestimate the temperature of sub-volcanic ore deposits by up to hundreds of degrees (using fluid inclusion entrapment temperatures and geothermometers), and bias fluid provenance calculated from stable-isotope analysis (e.g. the δD-$\delta^{18}O$ plot). The bias in fluid provenance is two-fold. Firstly, the dehydration experienced by inverted opal will cause geoscientists to underestimate the meteoric component of a fluid, but most importantly, underestimating the fluid temperature will overestimate the degree of isotopic fractionation, drastically underestimating the magmatic component of a fluid. These biases do not cancel each other out. Another important factor to consider is that if the precursor opal was deposited from a silica super-saturated fluid, isotopic fractionation may not occur, as opal is a non-equilibrium phase.

Our findings show that quartz is not a robust proxy for primary crustal fluids, particularly in mesothermal veins and sub-volcanic settings. Care should be taken when analysing quartz from any hydrothermal environment where super-saturation could have occurred. However, inverted opal will be difficult to identify, as residual opalline phases will not survive long in high-temperature settings. We suggest that cryptic inverted opal may be recognized by *any* of the following characteristics: (1) morphology (doubly terminated crystals and quartz aggregates with cryptocrystalline cores); (2) intricate euhedral growth bands visible in cathodoluminescence or trace element concentration; (3) geochemical disequilibrium with co-existing phases; or (4) extreme isotopic zonation within individual crystals.

REFERENCES

Tanner, D., Henley, R.W., Mavrogenes, J.A., Mernagh, T.P. and Holden P., 2012. High temperature opal inversion: Evidence from the El Indio Cu-Au deposit, Chile. ACROFI IV Conference Abstracts, Brisbane, Australia, 81-83.

Coral skeleton biomineralisation and seawater chemistry change: implications from fluid inclusions in halite

F. W. Meng[1,2], *P. Ni*[2※], *and X.L. Yuan*[1], *C.M. Zhou*[1], *W. H. Liao*[1]

[1] *State Key Laboratory of Palaeobiology and Stratigraphy, Nanjing Institute of Geology and Paleontology, CAS, Nanjing 210008, China*

[2] *State Key Laboratory for Mineral Deposit Research, Institute of Geo-Fluids, School of Earth Science and Engineering, Nanjing University, Nanjing, 210093, China*

※*corresponding author: peini@nju.edu.cn*

ABSTRACT

The seawater change between the "calcite sea" and "aragonite sea" (Sandberg, 1983), and fluid inclusions in halite can provide the direct evidences of seawater chemistry changes (Kovalevich et al., 1998; Lowenstein et al., 2001). Coral skeletons can also change between calcite and aragonite (Scrutton, 1997; Liao, 2002), and the close correspondence between coral skeletons biomineralisation and seawater chemistry changes suggest that seawater composition affects the biomineralisation of coral skeletons. When an organism's skeleton is first formed, natural selection will choose at first the mineral easiest to precipitate (Knoll, 2003). So when organism's skeleton formed in the "calcite sea", they will favour calcite as the skeletal material; however when an organism's skeleton formed in the "aragonite sea", they will favour aragonite as the skeletal material. Once selected, however, skeleton mineralisation cannot switch mineralogy even though the seawater changes from the "calcite sea" to the "aragonite sea" (Stanley and Hardie, 1998). So the biomineralisation of coral skeletons occurs in the "calcite sea". They will choose calcite as the skeletal material and always keep it; however if biomineralisation of the coral skeletons occurs in the "aragonite sea", they will choose aragonite as the skeletal material and always keep it. Rugosa and Tabulata occur in the Ordovician and have a calcite skeleton ("calcite sea") (Kovalevich et al., 1998; Kovalevich et al., 2006) and disappear after Permian-Triassic extinction, however, Scleractinia occur in the middle Triassic ("aragonite sea"), and have an aragonite skeleton and still have them to today. According to skeletal mineralogy, Scleractinia do not evolve from Rugosa and Tabulata, but a kind of anemone which obtain aragonite skeleton from the "aragonite sea". Until now, no Rugosa and Scleractinia have been found in the early Triassic, and there is an time gap between them.

ACKNOWLEDGMENTS

This research was supported by Major State Basic Research Development Program (973 Program, no. 2011CB403007); National Natural Science Foundation of China (No: 40703018; 41173051; 41172131; J0930006).

REFERENCES

Knoll, A. H., 2003. Biomineralization and evolutionary history. *Reviews in Mineralogy and Geochemistry*, **54**: 329-356.

Kovalevich, V. M., Peryt, T. M. and Petrichenko, O. I., 1998. Secular variation in seawater chemistry during the Phanerozoic as indicated by brine inclusions in halite. *The Journal of Geology*, **106**: 695-712

Kovalevych, V. M., Peryt, T. M., Zang, W. L., Vovnyuk. S. V. 2006. Composition of brines in halite-hosted fluid inclusions in the Upper Ordovician, Canning Basin, Western Australia: new data on seawater chemistry. *Terra Nova*, **18**(2): 95-103

Liao, W. H., 2002. Advance in study of the taxonomy of cnidaria and the origins and relationships of palaeozoic corals. *Acta Palaeontologica Sinica*, **41**(3): 464 468

Lowenstein, T. K, Timofeeff M N, Brennan, S. T., Hardie, L. A., Demicco, R. V., 2001. Oscillations in Phanerozoic Seawater Chemistry: Evidence from Fluid Inclusions. *Science*, **294**: 1086-1088

Sandberg, P.A., 1983. An oscillating trend in Phanerozoic non-skeletal carbonate mineralogy. *Nature*, 305: 19–22.

Scrutton, C.T., 1997. The Palaeozoic corals, I: origins and relationships. *Proceedings of the Yorkshire Geological Society* **51**: 177–208

Stanley, S.M., Hardie, L.A., 1998. Secular oscillations in the carbonate mineralogy of reef-building and sediment-producing organisms driven by tectonically forced shifts in seawater chemistry. *Palaeogeography, Palaeoclimatology, Palaeoecology*, **144** (1-2): 3–19

A Raman microprobe determination of hydrogen sulphide in orogenic gold fluids

Terrence P. Mernagh[1]
[1] *Geoscience Australia, GPO Box 378 Canberra ACT 2601 Australia*

The concentration of reduced sulphur species in ore fluids is still the subject of considerable debate. It is of importance not only because of the presence of sulphur itself but also because sulphur species have the potential to form stable complexes with metals in solution and thus facilitate the transport of metals to the site of deposition. This is particularly true for gold which may be transported as $Au(HS)^{2-}$, $Au(HS)^{0}$ and a range of other hydrosulphide and sulphide complexes (Seward, 1991; Shenberger and Barnes, 1989). In this study Raman spectroscopy has been used to obtain the concentration of H_2S and the fO_2 in individual fluid inclusions from the Archean, sub-amphibolite facies Missouri gold deposit in Western Australia.

In a previous fluid inclusion study of the Missouri gold deposit, Mernagh and Witt (1994) identified six types of fluid inclusions. Type I inclusions contained pure or nearly pure CH_4 in the vapour phase and had an average homogenisation temperature of 338°C. Rare Type II multiphase inclusions contained liquid and vapour and up to four solid phases. Partial homogenisation (S+L+V→S+V) occurred over the range from 287 - 335°C. Type III inclusions were one or two phase inclusions with highly variable ratios of CO_2/CH_4 in the vapour phase. These inclusions homogenised between 220 and 338°C. Type IV inclusions were two phase inclusions with only CO_2 in the vapour phase and they had an average homogenisation temperature of 289°C. Type V inclusion were secondary, low-salinity aqueous inclusion with up to 5 vol.% vapour. These inclusions had an average homogenisation temperature of 190°C. Type VI were high-salinity inclusions with some also containing a halite crystal. They had homogenisation temperatures between 76 and 139°C. Although CH_4 and CO_2 were detected by Raman microprobe in inclusion Types I – IV, H_2S was only previously detected in Type II inclusions (Mernagh and Witt, 1994).

This study focused on Type III H_2O-CO_2-CH_4(+H_2S) inclusions which occur as secondary trails within the relict quartz grains. They have a relatively dark vapour phase, are rounded to irregular in shape and are up to 20 μm in diameter. The vapour content of these inclusions varies from 70 – 100 vol.%. As mentioned above, H_2S was also detected in Type II multiphase inclusions but these were not considered in this study due to the difficulty of accurately estimating the volume of each phase within these inclusions. A representative Raman spectrum obtained from the vapour phase is shown in Figure 1. A band due to the host quartz is observed at 1230 cm^{-1}. The presence of CO_2 is shown by the Fermi diad at 1285 and 1388 cm^{-1} and by additional weak hot bands at 1251, 1267, 1410 and 1425 cm^{-1}. The intense band at ~2917 cm^{-1} corresponds to the ν_1 symmetric stretching mode of CH_4 which also has a very weak antisymmetric ν_2 stretching mode at 3006 cm^{-1} and weak overtones at ~2578 cm^{-1} ($2\nu_4$) and ~3070 cm^{-1} ($2\nu_2$). A weak band at 2609 cm^{-1} (shown in the inserts in Figure 1) indicates the presence of a small amount of H_2S.

Analysis of the Raman spectra show that Type III inclusions contain highly variable CO_2/CH_4 ratios and H_2S fugacities of up to 1.70 MPa. The calculated $m_{\Sigma S}$ values lie within the general pyrite stability field but are also confined to the chalcopyrite stability field. This is in accord with the quartz(-plagioclase)-biotite-carbonate-pyrite alteration assemblage that occurs adjacent to the quartz veins at the Missouri deposit. Geochemical modelling of an aqueous CO_2-bearing fluid in equilibrium with iron oxides and sulphides indicates that the concentration of H_2S is ~60 mM for a fluid governed by the CO_2 – CH_4 buffer. This is in good agreement with the Raman analyses and

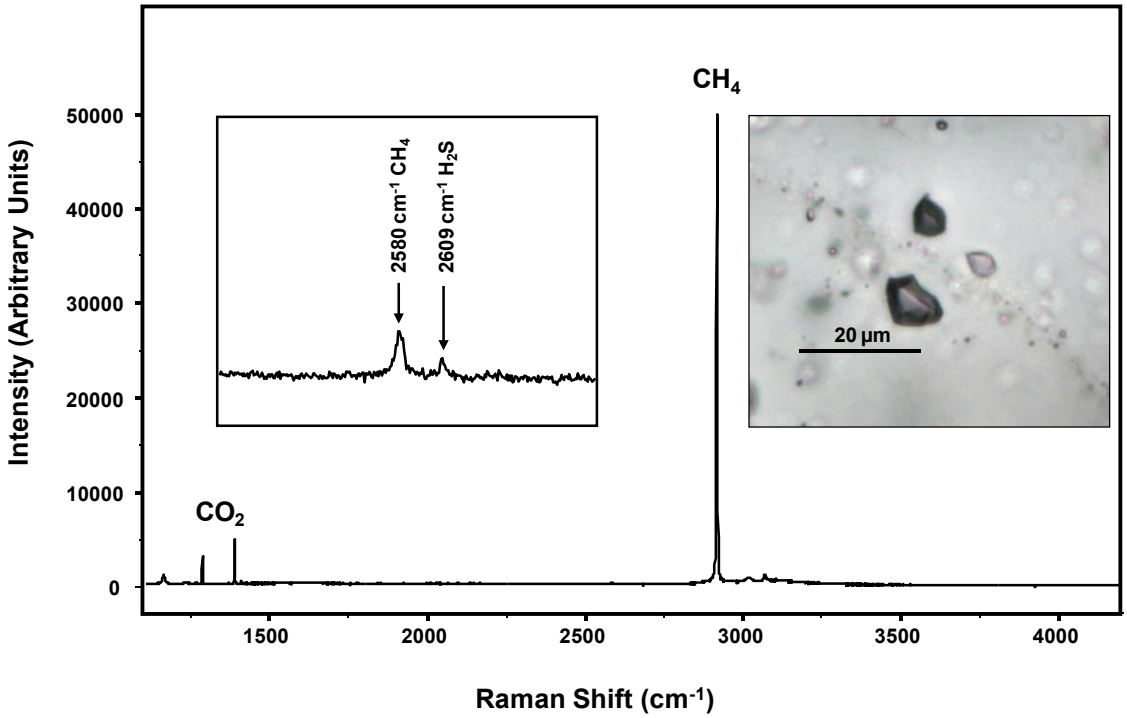

Figure 1: *Raman microprobe spectra of the vapour phase in a 100 vol. % vapour inclusion. The insets show a photomicrograph of the fluid inclusion and an expansion of the Raman spectrum over the region 2450 – 2700 cm^{-1}*

shows that Raman analysis provides both a reliable and simultaneous estimate of the mole fraction of H_2S and the fO_2 of the fluid at the time of trapping of the fluid inclusions.

These results compare favourably with previous solid probe mass spectrometric analysis of fluid inclusions from the Sigma, Norbeau and Tadd gold mines in the Archean Abitibi greenstone belt (Guha et al., 1991). Higher values reported by other bulk sampling techniques must be viewed with caution as they may sample multiple populations of inclusions and they are also prone to contamination from other sources of sulphur.

REFERENCES

Guha, J., Lu, H.Z., Dube, B., Robert, F. and Gagnon, M., 1991. Fluid characteristics of vein and altered wall rock in Archean mesothermal gold deposits. *Economic Geology*, **86**, 667-684.

Mernagh, T.P. and Witt, W.K., 1994. Early, methane-rich fluids and their role in Archaean gold mineralisation at the Sand King and Missouri deposits, Eastern Goldfields Province, Western Australia. *AGSO Journal of Australian Geology and Geophysics*, **15**, 297-312.

Seward, T.M., 1991. The hydrothermal geochemistry of gold, in: *Gold Metallogeny and Exploration*. Foster R.P. (Editor), Glasgow, Blackie, 37-62.

Shenberger, D.M. and Barnes, H.L., 1989. Solubility of gold in aqueous sulfide solutions from 150 to 350ºC, *Geochimica et Cosmochimica Acta*, **53**, 269-278.

Fluid inclusion studies on coexisting wolframite and quartz from tungsten-bearing quartz vein type deposits, Southern Jiangxi, China

P. Ni, X. D. Wang, J.B. Huang, T. G. Wang and G. G. Wang*
Institute of Geo-fluids, State Key Laboratory for Mineral Deposits Research, School of Earth Sciences and Engineering, Nanjing University, China
**Corresponding author: peini@nju.edu.cn*

INTRODUCTION

China ranks number one in the world in terms of tungsten resources and production. The Southern Jiangxi tungsten metallogenic belt hosts a lot of world-class wolframite-quartz vein type tungsten deposits. These tungsten deposits occurred as wolframite-quartz veins in Mesozoic granite or adjacent Cambrian to Devonian strata. Most of previous research work has been done on the features and evolution of Mesozoic granite and its relation to tungsten mineralisation (Le Bel et al., 1984; Xie et al., 2006). However, few investigations involved the study of fluid inclusions. The use of infrared microscopes has made it possible to study fluid inclusions in opaque ore minerals, such as wolframite, cassiterite, and rutile (Campbell et al., 1984; Ni et al., 2008). In this paper, fluid inclusions in both quartz and coexisting wolframite from Southern Jiangxi area were studied, in order to constrain features and evolution process of tungsten-forming fluids.

FLUID INCLUSION STUDIES

Two types fluid inclusions can be recognised in quartz: liquid-rich, two phase aqueous inclusions (type I) and two/three phase CO_2–bearing inclusions (type II). But only one type fluid inclusion can be identified in wolframite coexisting with quartz veins, which are liquid-rich, two phase aqueous inclusions (type I)

Detailed fluid inclusion microthermometry has been conducted in seven tungsten deposits, which include the Xihuashan, Dangping, Piaotang, Muziyuan, Dajishan, Pangushan and Huangsha tungsten deposits.

CONCLUSIONS

1. Fluid inclusions in quartz suggest different fluid-forming processes during the wolframite – quartz vein formation, including fluid mixing and fluid immiscible processes.

2. Fluid inclusions in wolframite coexisting with quartz show decreasing temperatures, but constant salinity, which indicates that a temperature decrease rather than fluid mixing or fluid immiscibility control ore deposition.

3. In the same deposit, there are obvious differences between wolframite and coexisting quartz in fluid inclusion homogenisation temperature, salinity, density and pressure etc. Usually wolframite has higher temperatures and pressures than quartz etc.

4. Wolframite and coexisting quartz may have experienced a different fluid evolution process during the formation of wolframite-quartz veins.

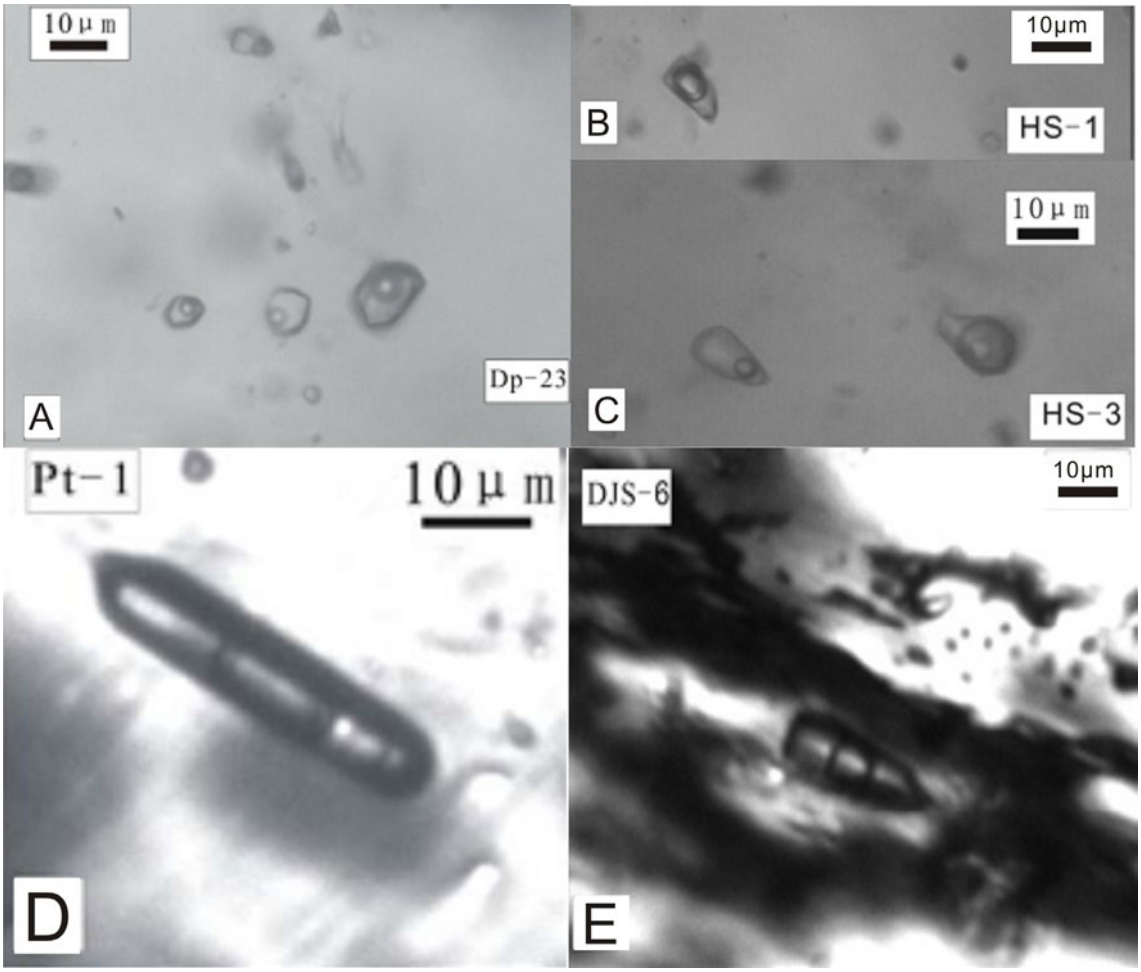

***Figure 1**: Fluid inclusions from tungsten deposits in the Southern Jiangxi tungsten metallogenic belt. (A) type I inclusions from quartz in the Dangping tungsten deposit, (B-C) type I and type II inclusions from quartz in the Huangsha tungsten deposit, (D-E) type I inclusions from wolframite in the Piaotang and Dajishan tungsten deposits.*

REFERENCES

Campbell, A.R., Hackbarth, C.J., Plumlee, G.S., and Petersen, U., 1984, Internal features of ore minerals seen with the infrared microscope. *Economic Geology and the Bulletin of the Society of Economic Geologists*, **79**, 1387–1392.

Le Bel, L., Yi-dou, L., Ji-fou, S., 1984. Granitic evolution of the Xihuashan-Dangping (Jiangxi, China) Tungsten-Bearing system. *Mineralogy and Petrology*, **33**, 149-167.

Ni, P., Zhu, X., Wang, R., Shen, K., Zhang, Z., Qiu, J., and Huang, J., 2008. Constraining ultrahigh-pressure (UHP) metamorphism and titanium ore formation from an infrared microthermometric study of fluid inclusions in rutile from Donghai UHP eclogites, eastern China. *Geological Society of America Bulletin*, **120**, 1296-1304.

Xie, G., Hu, R., Mao, J., Pirajno, F., Li, R., Cao, J., Jiang, G., Zhao, J., 2006. K-Ar Dating, Geochemical, and Sr-Nd-Pb Isotopic Systematics of Late Mesozoic Mafic Dikes, Southern Jiangxi Province, Southeast China: Petrogenesis and Tectonic Implications. *International Geology Review*, **48**, 1023-1051.

Physico-chemical crystallisation conditions of kalsilite-bearing melilitite from Cupaello volcano, Central Italy

A.T. Nikolaeva
V.S. Sobolev Institute of Geology and Mineralogy, Siberian Branch Russian Academy of Sience, Novosibirsk State University, Novosibirsk, Russia

INTRODUCTION

The Cupaello volcano is part of the Intra-mountain Ultra-alkaline Province (IUP) of Central Italy characterized by kamafugitic and carbonatitic magmatism. This district consists of diatremes, maars and tuff rings (Stoppa, Lavecchia, 1992). IUP magmatic centers, such as the San-Venanzo (SV) volcano, the Colle Fabbri (CF) stock, and the Cupaello volcano are found in the Pleistocene/Quaternary continental tectonic depressions which cross cut the Pliocene Apennine thrust-fold system. The Cupaello volcano is mainly represented by lava flow about 700 m long, 60-200 m wide, and up to 6 m thick (Gallo et al., 1984; Stoppa, Cundari, 1995; Cundari, Ferguson, 1991).

PETROGRAPHY

The lava flow is composed of kalsilite melilitite (local name - cupaellite). The studied rock consists of phenocrysts of clinopyroxene and phlogopite and microphenocrysts of melilite. Groundmass of the rock is represented by clinopyroxene, melilite, kalsilite, olivine, monticellite, perovskite, opaque minerals, and glass. Kalsilite melilitite (cupaellite) is undersaturated in SiO_2 (~ 43,8 wt.%), has a low content of Al_2O_3 (~ 7.4 wt.%) and alkalis (4.4 wt.% K_2O and 0.3 wt. % Na_2O), and a high content of MgO (~ 11.3 wt.%), FeO (~ 6.7 wt.%), and CaO (~ 15.4 wt.%).

Clinopyroxene phenocrysts in this rock have a short-columnar and prismatic habit. Their composition is diopside (Mg # 95) and similar to that of the SV clinopyroxene, and has more FeO and Al_2O_3 compared to the CF clinopyroxene (Stoppa, Sharygin, 2009). Phlogopite phenocrysts are corroded in the rock and characterized by high TiO_2 (up to 2.3 wt.%) and Mg/(Mg+F)e values (86-94). Euhedral melilite grains contain about 86% okermanite, up to 2% gehlenite, and about 12% Na-melilite components. This is similar to the SV melilite composition and very different to the CF melilite composition. Kalsilite from the groundmass differ from the SV kalsilite (Cundari, Ferguson, 1990) in a high Fe_2O_3.

MELT INCLUSIONS

Primary silicate-carbonate-salt inclusions were found in the clinopyroxene phenocryst from kalsilite melilitite. They have rounded, irregular and close to prismatic shapes. Their size varies from 10-15 to 50 μm. The content of inclusions is represented by fine-grained aggregates of colorless, light green, brownish phases and gas phase (Fig.1). The scanning electron microscope and Raman spectroscopy identified the following crystalline daughter/trapped phases in the inclusions: calcite - $Ca[CO_3]$, Ba-Sr carbonates, baryte - $Ba[SO_4]$, alkali sulfates, mica, kalsilite - $KAl[SiO_4]$, pectolite - $Ca_2NaH[Si_3O_9]$, combeite - $Na_2Ca_2[Si_3O_9]$, and apatite.

Heating experiment

During heating of inclusions at 350-450 °C carbonate-salt phases, located near gas, begin to melt. At 740-790 °C silicate phases melt, the carbonate-salt melt is transformed into a globule, and the gas bubble is present in a silicate melt. Then, when the temperature rises to 970 °C, gas bubble coalesces with the carbonate-salt globule. The homogenisation of the gas bubble in the carbonate-salt globule is observed at 1025-1050 °C, and carbonate-salt bleb disappears into the silicate melt at 1150-1180 °C.

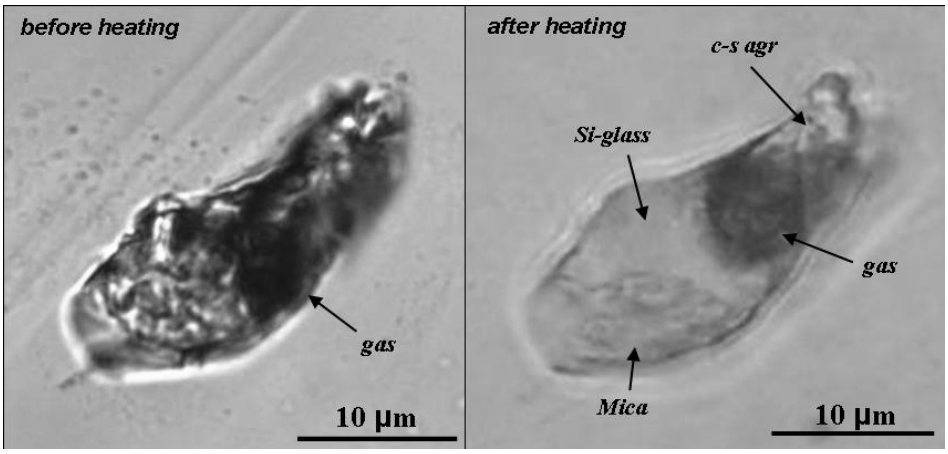

Figure 1: Melt Inclusion in clinopyroxene. Before heating: fine-grained silicate-carbonate inclusion with gas phase; after heating up to 1000 °C: c-s agr – fine-grained carbonate-salt aggregate.

Composition of inclusions

Heated to 1100-1200 °C and then quenched inclusions consist of silicate and carbonate-salt parts. The silicate part is melilitite in composition and characterized (wt%) 35.4-45.4 SiO_2, 0.8-2 TiO_2, 4.5-9.7 Al_2O_3, 4.3-6.9 FeO, 2.3-12.2 MgO, 7.6-16.8 CaO, 0.7-5.2 Na_2O, 5.9-11.3 K_2O, 0.2-1.7 BaO, 0.1-0.7 SrO, 0.6-1.9 P_2O_5, 0.05-0.3 Cl, 0.2-1.9 SO_3. Carbonate-salt part contains (wt%) 1.7-4.81 SiO_2, 0.1-0.2 TiO_2, 0.7-1.1 FeO, 0.6-1.9 MgO, 24.9-40.9 CaO, 1.4-4.5 Na_2O, 8.9-17 K_2O, 3.8-5.1 BaO, 2.4-3.1 SrO, 0.3-0.5 P_2O_5, 0.06-0.24 Cl, 0.2-0.4 SO_3.

CONCLUSIONS

Thermometric data suggest that the crystallisation of clinopyroxene in the Cupaello kalsilite-bearing melilitite occurred at 1150-1180 °C from melilititic melt, enriched in carbonates, sulfates, and alkalies. Silicate-carbonate immiscibility occurred in 1025-1050 °C temperature range. The same phenomenon was previously described in SV melilitolites (Stoppa et al., 1997).

REFERENCES

Cundari A., Ferguson A.K., 1991. Petrogenetic relationships between melilitite and lamproite in Roman Comagmatic Region: the lavas of S. Venanzo and Cupaello. *Contributions to Mineralogy and Petrology*, **107**, 343-357

Gallo F., Giammetti F., Venturelli G., Vernia L., 1984. The kamafugitic rocks of S. Venanzo and Cupaello, Central Italy. *Neues Jahrbuch für Mineralogie-Monatshefte*, **5**, 198-210

Stoppa F., Cundari A., 1995. A new Italian carbonanite occurrence at Cupaello (Rieti) and its genetic significance. *Contributions to Mineralogy and Petrology*, **122**, 275-288

Stoppa F., Lavecchia G., 1992. Late Pleistocene ultra-alkaline magmatic activity in the Umbria – Latium region (Italy): An overview. *Journal of Volcanology and Geothermal Research*, **52**, 277-293

Stoppa F., Sharygin V.V., Cundari A., 1997. New mineral data from the kamafugite-carbonatite association: the melilitolite from Pian di Celle, Italy. *Mineralogy and Petrology*, **61**, 27-45

Stoppa F., Sharygin V.V., 2009. Melilitolite intrusion and pelite digestion by high temperature kamafugitic magma at Colle Fabbri, Spoleto, Italy. *Lithos*, **112**, 306-320

Sulphide – silicate melt immiscibility evidenced through inclusion petrographic study on impactites from Lonar Crater, Maharashtra, India

Prof. R. R. Patil[1] *& Abhijeet Surve*[2]

1. *Director School of Earth Sciences Solapur University, Solapur, India.*
2. *Research Student, Earth Sciences Solapur University, Solapur, India.*

The impactite samples collected during the field work carried out around Lonar Crater, Buldhana Dist. of Maharashtra (19058'N, 76031'E) permitted observation of fluid, melt and glass inclusions in the host quartz, feldspar and vitrified glasses. Doubly polished plates prepared from the sample from the centre and brim of the ejectas showed various types of inclusions entrapment. Seven types of inclusion assemblages are noteworthy during the petrographic study.

1. Silicate melt + glass + gas
2. Silicate melt + gas
3. silicate glass + gas
4. melt + glass + metallic sulphide spherule
5. glass + super saline brine + vapour
6. melt + super saline brine (daughter crystals) + gas
7. glass + gas + brine
8. glass + gas + L1 + L2

The photographic immiscibility evidences are used to explain the nature of fluid media existed during crystallisation of the meteorite magma which cooled in situ and was then expelled out with force on the surface forming the brim of the impact crater inclusion petrographic study of which show quenching due to faster cooling in contact with relatively cooler surface rocks. This study helped in fingerprinting the environment of formation of ejectas surroundings brim, magma behavior during cooling, mixing and boiling at the impact crater. The metallic core samples indicated their richness in chalcophile auriferous and PGE elements which were studied in detail for their ore petrographic evidences. The inclusion thermometry, cryometry, characteristic ore mineral assemblages associated with various processes viz. boiling, cooling, lateral movement associated with alteration, metamorphism etc. are used to derive their respective characteristic environment through the study of inclusions trapped during respective process and the data generated through their study thus the deposition/ trappment and environment of impact crater, ejectas and rim formation is brought out. The photographic evidences and the data acquired during various studies will be presented.

The impactite samples collected during the field work carried out around Lonar Crater, Buldhana Dist. of Maharashtra ($19^0$58'N, $76^0$31'E) permitted observation of fluid, melt and glass inclusions in the host quartz, feldspar and vitrified glasses. Doubly polished plates prepared from the sample from the centre and brim of the ejectas showed various types of inclusions entrapment. Seven types of inclusion assemblages are noteworthy during the petrographic study

Triassic age colloid solutions in fluid inclusions in chalcedony

V. Yu. Prokofiev[1], *S. L. Selector*[2], *V. S. Kamenetsky*[3], *and T. Rodemann*[3]
[1] *IGEM RAS, per. Staromonetny 35, Moscow, 109017 Russia, vpr@igem.ru*
[2] *Frumkin Institute of Physical Chemistry and Electrochemystry RAS, Leninsky pr., 31-4, 119071, Moscow, Russia*
[3] *University of Tasmania, Hobart, Tasmania, 7001 Australia*

INTRODUCTION

Many researchers (Boydell, 1925; Lindgren, 1933, et al.) have discussed the role of colloidal solutions in hydrothermal ore-forming processes. They have presented ideas about transfer of ore material in a colloidal form for the wide range of physicochemical conditions, at which colloidal solutions exist in nature. It is believed that colloidal solutions are not preserved long enough in nature because they are nonequilibrium and energy unstable. Sulfur-bearing compounds, chlorides of alkaline metals, some amphiphilic organic compounds were considered as stability factors prolonging "lifetime" of such systems. It is generally accpted that the time of colloidal solution existence is very small compared to the time scale of geological processes, so researches usually observe results of former colloid presence. For this reason in fluid inclusions scientists search for signs of bygone existence of such solutions and products of their disintegration. However, there are no reliable data about "lifetimes" of colloidal solutions in fluid inclusions. But there is the notion about "stabilizations of" colloidal particles in solution upon the effect of different factors (for instance, surfactants or electrolyte solutions) in modern colloidal chemistry. Consequently colloidal systems are able to survive without coagulation for very long time. The collaurin, prepared by M. Faradey, is kept up to date. However, time expressed by hundreds of years and hundred millions of years differ by six orders of magnitute orders, so any estimate of lifetime of colloidal solutions is important for understanding their role in natural mineral- and rock-forming process.

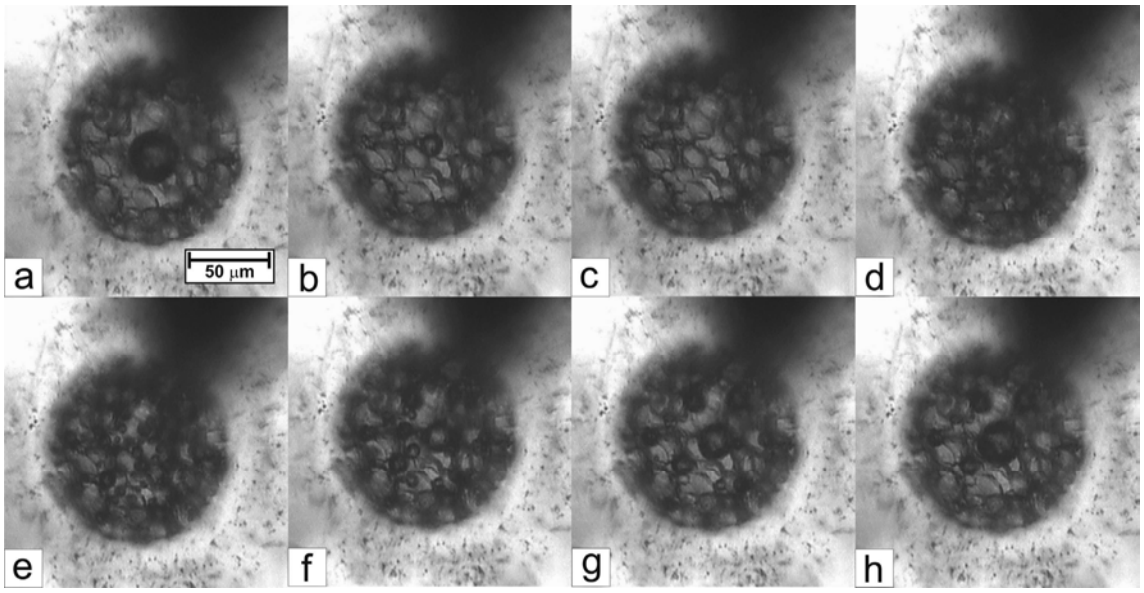

Figure 1: *Fluid inclusion in chalcedony at different temperatures.*
a – +22 ℃, b – +100 ℃, c – +120 ℃, d –+70 ℃, e – +65 ℃, f – +60 ℃, g – +50 ℃, h – +35 ℃.

FLUID INCLUSIONS (FI) STUDY

This report presents the results of the study of FI in chalcedony from amygdules in Triassic basalts at the optical-quality Icelandic-spar deposit of Gonchak, Siberia. The FI are between 30 and 100 μm in diameter. Each of them contains a liquid phase and a gas bubble. There is border, differing on structure from chalcedony and obviously connected with FI formation around all cavities. Analysis of the walls of the FI by scanning electronic microscopy and content of the unopened inclusions by LA-ICPMS has shown, that they consist of amorphous silica occasionally with traces (a few wt. %) of Cl, Na, Ca, Sr, Ba, K, Br and S. The cathodoluminescence image showed that FI are surrounded by chalcedony of specific structure and composition.

The behavior of solutions in FI during microthermometrical measurements was studied using Linkam THMSG-600 stage. Under cooling the solution in FI freezes and becomes opaque at temperatures from -60 to -80 ºC. During consecutive heating a liquid appears within the temperature interval of -35…-60 ºC. This interval may correspond to eutectic temperatures of NaCl and $CaCl_2$ solutions. The ice melts at temperatures from -10.1 to -19.7ºC, corresponding to salt concentrations of 15.0–22.2 wt % eq. NaCl. Most of FI become homogeneous as liquids at temperatures of 70–160 ºC. After cooling the gas phase appears numerous small vapour bubbles that gradually coalesce (first minutes to hours) into one original bubble, but not necessarily in the same place, where it was prior to heating. Such behavior has been never observed for true solutions, and is characteristic of viscous colloidal systems (Fig. 1). Apparently, silica sol is present in a FI solution. Homogenizing of some FI takes place at higher temperatures (up to 380 ºC). In such FI the only one big gas bubble appears immediately on cooling. The destruction at high temperatures (more than 200 ºC) can be the reason of this effect.

The study by a Renishaw micro-Raman spectroscopy system with XYZ stage has found the resemblance of the spectrum of FI solution and chalcedony. The spectra of the contents of the fluid inclusions differ from ones of the host by presence of structurally bound water that also indicates the colloidal state of silica in FI. The mapping has shown presence of water in the contents of the fluid inclusion only.

The colloidal nature of the solution in fluid inclusions was confirmed in the experiment with the side illumination of the fluid inclusion by the laser beam under a microscope. Scattering of the laser beam by the whole volume of the fluid inclusion solution was noted. Here is a gas bubble, interacting with a laser beam, casts shadow with the sharp edge. Such effect has been known as a Tindal-effect, and is used to discriminate the colloidal solutions from the true ones. We thus consider studied fluid inclusions to contain the sol of the silicon acid.

CONCLUSIONS

Formation of chalcedony from a colloidal solution is advocated here based on the study of chalcedony-hosted FI. The main result of this study is preservation of the colloidal solution in the fluid inclusion vacuoles for ca. 250 Ma years without coagulation. The comprehension of this phenomenon is of great importance for understanding the role and behavior of colloidal solutions in geological processes. Understanding chemical composition, physical properties and stability of silicon acid particles in the fluid inclusion solution appears to be very important in further studies.

ACKNOWLEDGEMENTS

This work was carried out within the framework of the Russian Foundation for Basic Research (projects 12-05-01083-a and 11-05-1207ofi-m).

REFERENCES

1. Boydell H. C., 1925. The role of colloidal solutions in the formations of mineral deposit, *Institutions of Mining and Metallurgy Transactions*, **34**, 145-337.
2. Lindgren W., 1933. Mineral deposits. *McGraw-Hill*, New York, 930p.

LA-ICP-MS investigations of ore-forming fluids of Fe-F-REE carbonatite deposits of Central Tuva region, Russia

I.R. Prokopyev, A.S. Borisenko, A.A. Borovikov
Institute of Geology and Mineralogy SB RAS, Koptyug Av. 3 Novosibirsk 630090 Russia

Carbonatites of Tuva are the part of Late Mesozoic Central Asian carbonatite province. They are located in the southern part of Central Siberia (Russia). The Ar-Ar age of the carbonatites is 117.2 ± 1.3 Ma (Prokopyev, unpubl. data), which coincides with the Rb-Sr age of 118 ± 9 Ma (Sugorakova et al., 2004). Carbonatite deposits are localised along the N-S striking REE-belt, and in general can be divided into three ore groups: Chailyukhem, Karasug, and Ulatay-Chezsk. Fluid inclusions in quartz and fluorite found in ankerite-calcite and siderite carbonate matrix were investigated. Inclusions are mainly represented by three types: highly concentrated multiphase crystal-fluid inclusions, gas-liquid ± NaCl inclusions and essentially gaseous inclusions.

FLUID INCLUSION STUDY

The fluid inclusion study of carbonatites from the Central Tuva region (Bredikhina and Mel'gunov, 1989; Prokopiev et al., 2010, Borisenko et al., 2011) showed that they were formed at the fluorite-barite-celestite-bastnaesite stage from the highly concentrated (70 - 85 wt%) melts-brine at temperatures between 700 to 400 °C and pressures of 2.5 - 3.5 kbars. During the later stages of the hydrothermal processes salinity dropped to 40 - 50 wt% NaCl eq., temperature decreased to 480 - 300 °C and pressure was about 1.5 - 2 kbars. At the late hydrothermal stage (calcite–fluorite–celestite), these parameters were as low as 40-25 wt% NaCl eq. and 290 – 140 °C. The main salt components of early multiphase fluid inclusions are halite and/or sylvite, and the secondary ones are carbonates and sulphates of Fe, Ca, Na, and REE: calcite, Ce-ancylite, anhydrite, thenardite, Fe-copiapite, and gaylussite. Liquid CO_2 prevails in the gas phase of early multiphase fluid inclusions, whereas the inclusions in quartz of the late generations are characterised by CO_2–N_2 composition.

LA-ICP-MS RESULTS

The chemical composition of the REE-carbonatite fluid was determined by LA-ICP-MS analysis of the multiphase fluid inclusions in quartz and fluorite from the Karasug and Ulatay deposits (fig.1).

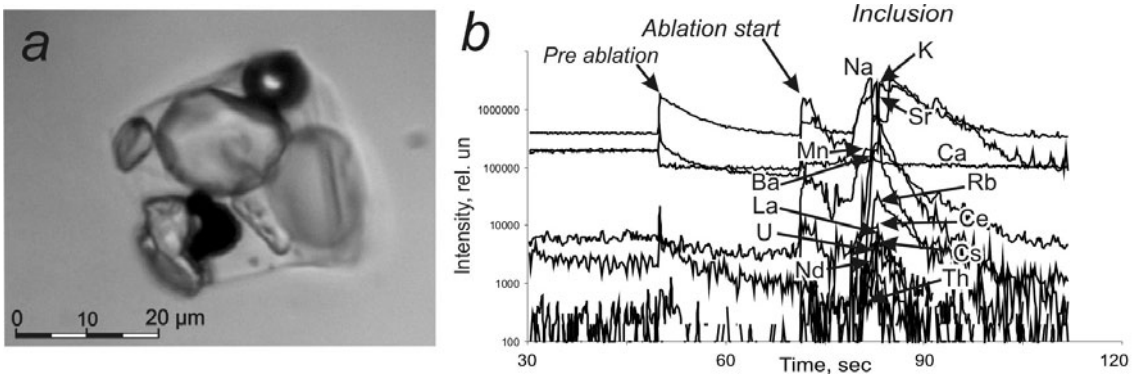

Figure 1 *Multiphase fluid inclusion in quartz of Karasug deposit (a) and LA-ICP-MS record (b).*

Results of the LA-ICP-MS analysis revealed high concentrations (0.1 to 1 wt%) of Fe, Sr, Ba, Mn, and Zn and concentrations (1 to 100 ppm) of Cu, Co, Mo, W, As, Sb, Bi, Pb, and rare-earth elements Y, La, Ce, Nd, Th and U (Table 1).

Table 1: Concentration of elements determined by LA-ICP-MS (ppm)

Element	Karasug Quartz	Ulatay Fluorite	Element	Karasug Quartz	Ulatay Fluorite
Na	181000 - 188700*	137600 - 142500*	**Au**	0.3 - 15	0 - 0.7
K	156000 - 140000*	235570 - 289300*	**Ag**	0.2 - 1.5	0.3 - 4
Ca	3200 - 140	10 - 255	**As**	53 - 4103	1200 - 4500
Mn	11000 - 6500	4000 - 16400	**Sb**	11.8 - 150	70 - 188
Rb	600 - 10	500 - 2100	**Mo**	0.3-34	6
Cs	10-130	160 - 250	**W**	1.8 - 0.3	21 - 35
Sr	6970 - 2800	7000 - 17000	**Pb**	760 - 200	500 - 930
Ba	8000 - 2000	7220 - 14000	**Bi**	15 - 0.5	43040
Y	3 - 40500	2600 - 5500	**La**	60-30	1800 - 5500
Fe	63600 - 48600	10300 - 61500	**Ce**	15 - 70	5000 - 7500
Co	3.3 - 95	25 - 130	**Nd**	1.7 - 11	1580 - 2950
Cu	840 - 40750	110 - 520	**Th**	30 - 3000	0.18 - 2
Zn	2300 - 1200	1500 - 11500	**U**	2.6 - 34.5	2.7 - 5

*- according to the thermometric data

According to the LA-ICP-MS results ore-forming fluids of fluorite-barite-siderite carbonatites contain higher concentrations of potassium and LREE (La, Ce, Nd) than highly concentrated multiphase fluid inclusions in quartz of the ankerite carbonatites. Statistical processing of geochemical data showed that there are two groups of elements with a high correlation (correlation coefficient more than 0.7) between their concentrations (within the group): (1) As, Sb, Bi, Zn, Pb, Fe, Mn, Cs, K, and (2) Ce, Y, Sr, Ba, Rb, U. Data obtained suggests the generally known trend of the evolution of ore-forming REE fluid from ankerite to fluorite-barite-siderite carbonatites (Bailey, 1995). However, the chemical composition and concentration of REE-carbonatite fluid of Central Tuva deposits differ significantly from magmatic fluids of mafic-alkaline complexes of the Altai Mountains, Aldan complex and other regions of Russia and the Maoniuping REE deposit in China (Xie et al., 2009).

REFERENCES

Bailey, D.K, 1995. Carbonate magmas. *Geological Society, London, Memoirs*, **16**, p. 249-263

Borisenko, A.S., Borovikov, A.A., Vasyukova, E.A., Pavlova, G.G., Ragozin, A.L., Prokop`ev, I.R., Vladykin, N.V., 2011. Oxidized magmatogene fluids: metal-bearing capacity and role in ore formation. *Russian Geology and Geophysics*, **52**, 144–164.

Bredikhina, S.A., Mel'gunov, S.V., 1989. Physicochemical parameters of formation of fluorite from fluorite-barite-iron-ore mineralization in the Tuva ASSR. *Russian Geology and Geophysics*, **30 (10)**, 61–68 (56–62).

Prokopiev, I.R., Borovikov, A.A., Borisenko, A.S., Ragozin, A.L., 2010. Composition of ore-forming fluids of Fe-F-REE carbonatite deposits of the Karasug and Ulatai-Chezsk group (Tuva), 2010. *Abstract of ACROFI III and TBG XIV: SB RAS, Novosibirsk*, 184–185.

Sugorakova, A.M., Lebedev, V.I., Yarmolyuk, V.V., Nikiforov, A.V., 2004. Geochronology of Intraplate Magmatism in Tuva. *State and Development of Natural Resources of Tuva and Adjecent Regions of Central Asia: Kyzyl: TuvIKOPR SB RAS,* 50-53.

Xie, Y., Hou, Z., Yin, S., Dominy, S.C., Xu, J., Tian, S., Xu, W., 2009. Continuous carbonatitic melt–fluid evolution of a REE mineralization system: Evidence from inclusions in the Maoniuping REE Deposit, Western Sichuan, China. *Ore Geology Reviews*, **36**, 90–105.

Fluid associated with graphite assemblage from the Almora Crystalline, Kumaun Himalaya, India

Rakhi Rawat[1] *and Rajesh Sharma*[2]
Wadia Institute of Himalayan Geology
33 General Mahadeo Singh Road, Dehra Dun-248 001 (India)
[1] *rakhi84@rediffmail.com*, [2] *rajesh_fluid@rediffmail.com*

The carbonaceous material is widely scattered in the metapelite rocks of the Lesser Himalaya (Valdiya, 1980). Abundant carbonaceous material is found in the Almora Group of rocks mostly within its Gumalikhet formation. The Almora Group comprises garnetiferous mica schist, mica schist, micaceous flaggy quartzite and the black carbonaceous phyllite alternating with black fine grained biotite-rich quartzite. The carbonaceous material occurs in the form of lenses, pods, nodules, layers and pockets, and the associated minerals are quartz, biotite, muscovite, feldspar, garnet, occasional pyrite and rare chalcopyrite forming impurities at the graphite deposits. The XRD analyses of these carbonaceous materials suggest that it is graphitic in nature. The SEM-EDX work reveals flaky and semi-hexagonal graphite crystal of 10-12 microns in size, and features attributing graphite formation through metamorphism of the carbonaceous material together with the host rocks (Rawat and Sharma, 2011), an inference confirmed through carbon isotope signatures of the graphite.

The fluid inclusion studies have been performed on quartz intimately associated with the graphite. The graphite flakes are observed to penetrate the quartz pods and quartz veins and vice-versa. Studied samples represent both the graphite schist and graphitic quartzite. An ubiquitous presence of monophase and bi-phase carbonic inclusions is observed, but the bi-phase aqueous inclusion and monophase aqueous inclusion are also not uncommon in the studied samples. The distributions of fluid inclusions include random occurrences, as well as their presence in the transgranular and intragranular trails. At times they also occur in small groups. The fluid inclusions observed in the graphite bearing assemblage also show some typical shapes like annular rings and 'C' shape of inclusions indicating that the internal pressure exceeded the external pressure, consistent with the Himalayan isothermal uplift. Although, the phase ratio in aqueous carbonic inclusions varies widely, it is constant in the aqueous bi-phase inclusions. We observed the coexistence of different types of inclusions within single grains and even within the same trails. The microthermometry and Raman spectroscopy confirmed that carbonic inclusions consist of CO_2-CH_4-N_2 fluids. The homogenisation of CO_2 occurred between 3 and 26°C. The complete homogenisation of aqueous carbonic inclusions occurred in a temperature range of 205 to 340°C. The monophase carbonic inclusions in the graphitic schist show the enrichment of the methane, with homogenisation varying from -149 to -109°C. The fluid inclusion study reveal that the fluid associated with graphite formation in the metapelites is enriched in methane, and the evolution of nitrogen is also evident. The aqueous inclusions together with the CO_2 fluid inclusions is consistent with the metamorphic conditions, but the large scale flux of methane and nitrogen is related to the conversion of carbonaceous material to graphite.

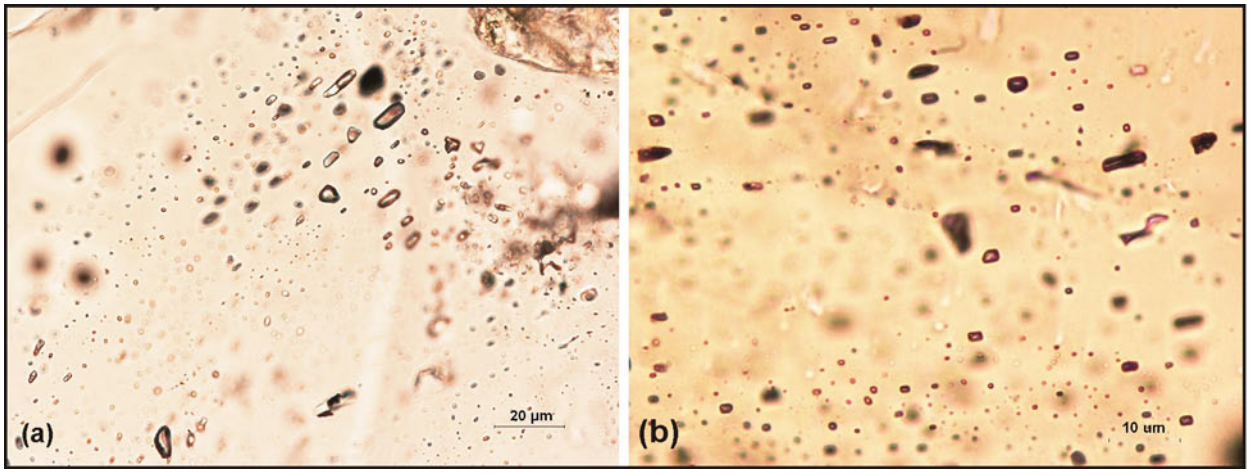

***Figure 1**: (a) CO_2-CH_4 monophase and Biphase aqueous carbonic inclusions, and (b) monophase carbonic inclusions.*

REFERENCES:

Rawat, R. and Sharma, R., 2011. Features and characterization of graphite in Almora crystallines and their implication for the graphite formation in Lesser Himalaya*, India. J. Asian Earth Sci*., **42**, 51- 64.

Valdiya, K.S., 1980. Geology of Kumaun Lesser Himalaya. *Wadia Institute of Himalayan Geology Publication, Dehradun*, p. 291.

Silicate-carbonate-salt immiscibility on crystallisation of peridotites from the Inagli massif (Aldan Shield, Russia)

E. Yu. Rokosova and Yu. R.. Vasil'ev
Novosibirsk State University, V.S.Sobolev Institute of Geology and Mineralogy SB RAS, Novosibirsk, Russia

INTRODUCTION

The Inagli massif belongs to the alkaline ultramafic complexes of potassic series. The massif is situated in the northwestern margin of the Aldan Shield (Yakutia, Russia). It is about 20 km^2 in area and is topographically manifested as a cupola structure with a central caldera. It is nearly isometric in shape and has a concentrically zoned structure. The central part of the massif is a stock, 16 km^2 in area, made up of dunite. The stock is surrounded by alkali gabbroids (shonkinites), melanocratic alkali syenites and pulaskites. A narrow (50 m) zone of peridotites is situated between the dunites and alkali gabbroids. Sills of syenite porphyry occur at the periphery of the massif within the Cambrian carbonate sequence. The central dunite is threaded by numerous pegmatitic veins and veinlets of diverse mineral assemblages which include phlogopite, potassium feldspar, chrome-diopside, richterite and arfvedsonite [Korchagin, 1996; Kostyuk et al., 1990]. We have studied peridotite samples, which are most magnesian Si-undersaturated rocks of the massif. They contain (vol.%) 50 clinopyroxene, 20 olivine, 15 serpentine, 5 biotite, 7 magnetite, 3 apatite.

PETROGRAPHY OF MELT INCLUSIONS

Greenish-yellow euhedral clinopyroxene is often cracked and contains chadacrysts of olivine, titanomagnetite, apatite, potassium feldspar and phlogopite. Clinopyroxene is represented by diopside (wt.%: 49.7-55.2 SiO_2, 0.3-1.6 TiO_2, 1.5-3.1 Al_2O_3, 4.7-6.5 FeO, 0.14-0.26 MnO, 13.6-15.9 MgO, 21-21.98 CaO, 0.6-0.9 Na_2O, 0.03-0.2 Cr_2O_3; Mg# = 0.8-0.86). Primary completely crystallized melt inclusions are found in clinopyroxenes of peridotites of Inagli massif. Inclusions are irregular or rounded in shape and vary from 7 to 30 μm in size. The composition of daughter phases in inclusion was determined by the scanning electron microscope. Daughter phases of inclusions are represented by pale brown phlogopite (wt.%: 40 SiO_2, 13.72 Al_2O_3, 19.45 MgO, 9.3 FeO, 10.2 K_2O, 2.8 TiO_2, 2.1 F), colorless potassium feldspar (wt.%: 60.5 SiO_2, 18.6 Al_2O_3, 15.9 K_2O, 0.9 Na_2O) and/or albite (63.8 SiO_2, 19.4 Al_2O_3, 2.67 CaO, 11.2 Na_2O), apatite, magnetite (wt.%: 86.1-88.9 FeO, 1.4-1.7 TiO_2, 1.7-5.1 Cr_2O_3, 1.3-1.95 Al_2O_3), and fine-grained aggregate of carbonate and salt phases. The latter are observed in the interstices between other daughter phases (Fig. 1a). Calcite is dominant phases in fine-grained aggregate.

HEATING EXPERIMENTS

The carbonate-salt part of the inclusions started to melt at 800°C and one or two gas bubbles appeared between the daughter phases. Gas bubbles disappeared in carbonate-salt melt at 1000-1100°C. Melting of silicate glass occurred at the same temperature range. At 1230°C the carbonate-salt melt was transformed in a globule, which then gradually decreased in size. The homogenisation of carbonate-salt melt globule in a silicate melt occurred at 1280-1300°C. The decrease of temperature to 1270-1280°C resulted in that the carbonate-salt globule appeared again and gradually increased in size during cooling. After heating the inclusions consist of silicate glass, carbonate-salt globule and gas bubble at room temperature. The latter occupies up to 1/5 of the volume of the inclusion (Fig. 1b).

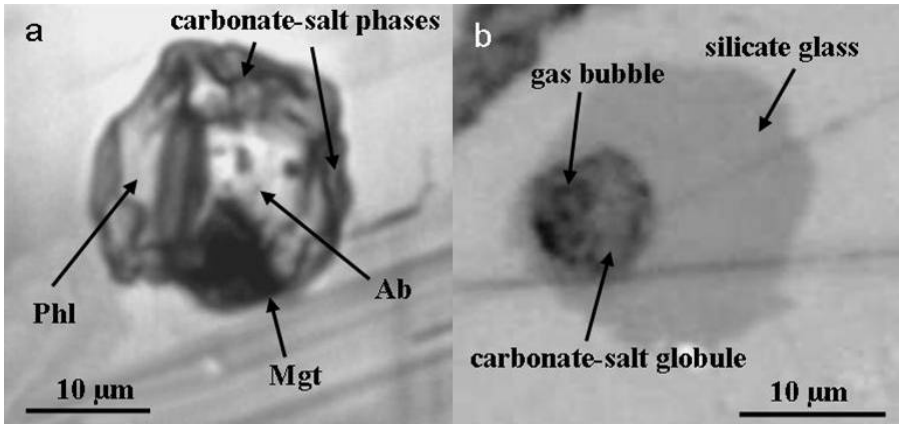

Figure 1: *Silicate-carbonate-salt inclusion in clinopyroxene of peridotites. a) Inclusion before heating. b) Inclusion after heating up to 1300°C.*

The composition of homogenized silicate glasse of inclusions corresponds to trachyandesitobasalts (wt.%): 51-55.5 SiO_2, 0.6-0.8 TiO_2, 13.4-14.8 Al_2O_3, 4.3-6.7 FeO, 0.1-0.25 MnO, 12.5-6 MgO, 9.2-4.5 CaO, 2.2-2.8 Na_2O, 4.2-6.9 K_2O, 0.5-1 P_2O_5, 0-0.1 BaO, 0.4-0.5 Cl, 0.02-0.1 SO_3). The composition of carbonate-salt globules of inclusion is as follows (wt.%): 17.2-23.2 SiO_2, 0.4-1 TiO_2, 1.7-6.1 Al_2O_3, 2.6-4.9 FeO, 0.1-0.13 MnO, 3.1-5.1 MgO, 13.3-22.8 CaO, 1.8-4 Na_2O, 1.9-3 K_2O, 0.9-1.7 P_2O_5, 0-0.14 BaO, 0.06-0.5 SrO, 0.3-1.3 Cl, 0.2-1.3 SO_3. The composition of carbonate-salt globules is close to the carbonatite lavas of Fort Portal (Uganda) [Belousov et al., 1974].

CONCLUSIONS

Clinopyroxene of the peridotite crystallized from homogeneous silicate carbonate-salt melt at 1280-1300°C. The initial melt separated into the silicate and carbonate-salt components with temperature decreasing. It was shown in a review article about liquid immiscibility in deep-seated magmas [Panina, Motorina, 2008] that the carbonate-salt melts spatially separated from silicate parental magma are enriched in Ca, alkalis, CO_2, S, F, Cl, P, H_2O and represent the original Ca-carbonatite melts. The further separation of carbonatite melt into immiscible fractions of carbonate, alkaline-chloride, alkaline-sulfate, and alkaline-phosphate compositions under decreasing temperature and pressure and disequilibrium conditions. The previous study of the Inagly chrome-diopside-hosted inclusions [Naumov et al., 2008] has shown that chrome-diopside crystallized from a silicate melt, which contained the emulsion of salt globules with sulfate-dominated compositions.

REFERENCES

Belousov, V.V., Gerasimovsky, V.I., Goryachev, A.V., Dobrovolsky, V.V., Kapitsa, A.P., Logatchev, N.A., Milanovsky, E.E., Polyakov, A.I., Rykunov, L.N. and Sedov, V.V., 1974. East - African rift system. Moscow, Nauka, *Geochemistry, seismology: main results*, **3**, 287p.

Korchagin, A.M., 1996. Inagli pluton and its natural resources. Moscow, Nedra, 156p.

Kostyuk, V.P., Panina, L.I., Zhidkov, A.Ya., Orlova, M.P. and Bazarova, T.Yu., 1990. Potassium alkaline magmatism of Baikal-Stanovoy rifting system. Novosibirsk, Nauka, Siberian Branch, 239p.

Naumov, V.B., Kamenetsky, V.S., Thomas, R., Kononkova, N.N. and Ryzhenko, B.N., 2008. Inclusions of silicate and sulfate melts in chrome-diopside from the Inagli deposit, Yakutia, Russia. *Geochemistry International*, **46(6)**, 554-564.

Panina, L. I., Motorina, I.V., 2008. Liquid immiscibility in deep-seated magmas and the origin of carbonatite melts. *Geochemistry International*, **46(5)**, 448-464.

Preliminary results from fluid inclusion petrography and microthermometry on quartz and calcite from different types of orebodies at the Telfer Au-Cu deposit, Paterson Orogen, Western Australia

C. Schindler[1], S.G. Hagemann[1], and J. Maxlow[2]
[1] *Centre for Exploration Targeting, University of Western Australia, 35 Stirling Hwy, 6009 Crawley, WA, Australia*
[2]*Newcrest Mining Limited, Brisbane, QLD, Australia*

INTRODUCTION

The Telfer Au-Cu deposit, situated in the Paterson Orogen, Western Australia, is one of Australia's largest Au-Cu deposits (resources of 18.3 Moz Au and 850 kt Cu, Newcrest, 2011). The mineralisation style at Telfer is unique compared to other large orogenic/intrusion related gold deposits worldwide. Several different types of orebodies are observed at Telfer: (1) early Au-Cu mineralisation in reefs (bedding sub-parallel, concordant with lithological boundaries, and forming laterally extensive quartz-sulphide-gold or carbonate-sulphide-gold orebodies), (2) later crosscutting, grid east-west striking and grid north dipping, carbonate-quartz-sulphide-gold veins, and (3) late-stage stockwork type gold orebodies. All of these orebody types are hosted by Neoproterozoic metasedimentary rocks. The early reef mineralisation consists of dolomite, calcite, quartz, pyrite, chalcopyrite, minor bornite and chalcocite, and traces of scheelite. Later stage crosscutting and stockwork veins consist of dolomite, calcite, quartz, muscovite, pyrite, chalcopyrite and traces of scheelite. Several granitic intrusions are located around the Telfer deposit at distances between 10 and 30 km.

There has been limited research conducted on fluid inclusions from the Telfer Au-Cu deposit (Goellnicht et al., 1989) and also nondestructive proton-induced X-ray emission (PIXE) on one of the satellite prospects in the Telfer area (Rowins et al., 2002). However, there is no detailed information on the P-T-X conditions of the ore forming fluids available on the different orebody types at Telfer and the surrounding satellite prospects (e.g. Camp Dome Cu, Minyari Au-Cu, Trotmans Stockwork W-Cu and O'Callaghans W-Cu prospects). This study will also help to understand the possible fluid and metal source (s) (e.g. surrounding granites or black sulphidic shales in the vicinity of Telfer) for the Au-Cu mineralisation at Telfer.

RESULTS

In a preliminary investigation, several ore samples were taken from the three major orebody types at Telfer to investigate the physico-chemical properties of the different fluid pulses.

Based on observations at room temperature (21°C) and low-temperature freezing runs, samples from the Telfer M50 reef show three phase aqueous (L+V+S), liquid- and vapour-rich fluid inclusions in quartz and calcite and two phase aqueous (L+V), liquid-rich inclusions in quartz. These inclusion types are trapped in three specific fluid inclusion assemblages (FIAs) using the criteria from Goldstein and Reynolds (1994): (1) three phase aqueous (L+V+S), liquid- and vapour-rich inclusions in quartz, (2) two phase aqueous (L+V), liquid- and vapour-rich inclusions in quartz and calcite, and (3) two phase aqueous (L+V), liquid-rich only inclusions in quartz.

Samples from the Telfer I30 reef show two phase aqueous (L+V), liquid-rich inclusions in calcite. In quartz these samples show, in addition to the same type of inclusions, several other inclusions types: (1) aqueous two phase (L+V), vapour-rich inclusions, (2) three phase (L_{aq}+$L_{carbonic}$+$V_{carbonic}$) aqueous-carbonic inclusions, and (3) three phase aqueous (L+V+S) inclusions with one or two daughter crystals. These inclusion types are trapped in four different FIAs: (1) two phase aqueous (L+V), liquid-rich inclusions in calcite and quartz, (2) two phase aqueous (L+V), vapour-rich inclusions in quartz, (3) three phase aqueous-carbonic inclusions (L_{aq}+$L_{carbonic}$+$V_{carbonic}$), and (4) three phase aqueous (L+V+S) inclusions with one or two daughter crystals.

Samples from the crosscutting veins show two phase (L+V), liquid-rich inclusions in calcite and four different FIAs in quartz: (1) two phase (L+V), liquid-rich inclusions, (2) two phase (L+V), vapour-rich inclusions, (3) three phase (L+V+S) inclusions with one or two daughter crystals, and (4) three phase aqueous-carbonic inclusions (L_{aq}+$L_{carbonic}$+$V_{carbonic}$).

Preliminary microthermometry results from M50 and I30 reef samples show complex salt compositions for three phase (L+V+S) fluid inclusion types based on first melting of ice (average T_e = -53°C, n=11). Temperature of first melting of ice from two phase (L+V) inclusions (average T_e = -25°C, n=5) point towards a more simple salt composition (e.g., NaCl-KCl) in these inclusions.

CONCLUSIONS

First results from petrography and microthermometry on quartz-calcite samples reveal similar fluid inclusion types and FIAs for all different orebody types at Telfer. Three phase aqueous (L+V+S) inclusions, three phase aqueous-carbonic (L_{aq}+$L_{carbonic}$+$V_{carbonic}$) and two phase aqueous (L+V) inclusions are observed in both early reef and later vein orebodies. These observations are consistent with data presented in Goellnicht (1989). Further investigations on the observed fluid inclusion assemblage (e.g. laser Raman, laser ablation ICP-MS and ion chromatography) will constrain the exact nature of ore forming fluids at Telfer with respect to different deposit types.

ACKNOWLEDGEMENT

This abstract is part of a PhD project of CS, funded by a scholarship for international research fees, a university international stipend, and Newcrest Mining Ltd. CS and SGH thank Newcrest Mining Ltd. for access to the areas described in this abstract and for financial support of this project.

REFERENCES

Goellnicht, N.M., Groves, D.I., McNaughton, N.J., and Dimo, G., 1989. An epigenetic origin for the Telfer gold deposit, Western Australia. in Keays, R. R., Ramsay, W. R. H., and Groves, D. I., eds., *Economic Geology Monograph*, **6**, 151 - 167.

Goldstein, R. H., and Reynolds, T. J., 1994. Systematics of fluid inclusions in diagenetic minerals: *SEPM Short Course*, **31**, 199.

Rowins, S.M., Yeats, C.J., and Ryan, C. G., 2002. New PIXE Evidence for Magmatic Vapor Phase Transport of Copper in Reduced Porphyry Copper-Gold Deposits. *Eighth Biennial Pan-American Conference on Research on Fluid Inclusions*, Halifax, Canada, 2002.

The fluid system associated with the volcano sedimentary sulphide mineralisation in the Himalayan tectonic domain

Rajesh Sharma
Wadia Institute of Himalayan Geology, Dehra Dun 248 001 India
email: sharmarajesh@wihg.res.in

The present study focuses on the sulphide ores of the Lesser Indian Himalaya, which are found in a Proterozoic rock suit consisting entirely or partly of quartzites, interlayered basic metavolcanic rocks, chlorite schist, sericite-quartz schist and dolomitic limestone. Representative occurrences include chalcopyrite, pyrite, galena at Dhanpur (Nair and Singh, 1982) and chalcopyrite, pyrite at Galpakot. The main sulphide minerals are pyrite, chalcopyrite, galena, rare sphalerite and pyrrohotite, which are observed in veins, pockets and stringers in the host rocks, together with the secondary minerals covelite, chalcocite and malachite. Polycrystalline masses of pyrite are found in matrix carbonates at Dhanpur, and the chalcopyrite is mutually replaced with pyrite. In addition to coexisting spahlerite and chalcopyrite, spahlerite also occurs as globular grains within chalcopyrite. Fracture fillings are also rare. The EPMA work shows that chalcopyrite is enriched in Mo, and Co is always higher than Ni, and the average Co/Ni ratio is about 18 favouring a submarine synsedimentary deposition environment for these sulphides. The carbon and oxygen isotope signatures collectively suggest that the dolomites are marine carbonate, with contributions of hydrothermal fluids.

Broadly, the fluid inclusions observed in mineralised quartz and calcite gangue are filled with two types of fluids: early carbonic-aqueous and late saline-aqueous fluids. The Raman spectroscopy further points to methane enriched and methane poor carbonic fluids. CO_2 rich fluid inclusions are common, both in trails and in small clusters, whereas methane rich fluid inclusions are rare. Some deformed cavities also reveal the presence of a H_2O+CH_4+CO_2 fluid (Figure 1a). Figure 1b shows a spread of Th CO_2 from 2.1 to 20.5 ^oC without any well-defined trend, however a higher CO_2 density is noticed with CH_4. The CH_4 rich fluid homogenised between -88 and -103 ^oC.

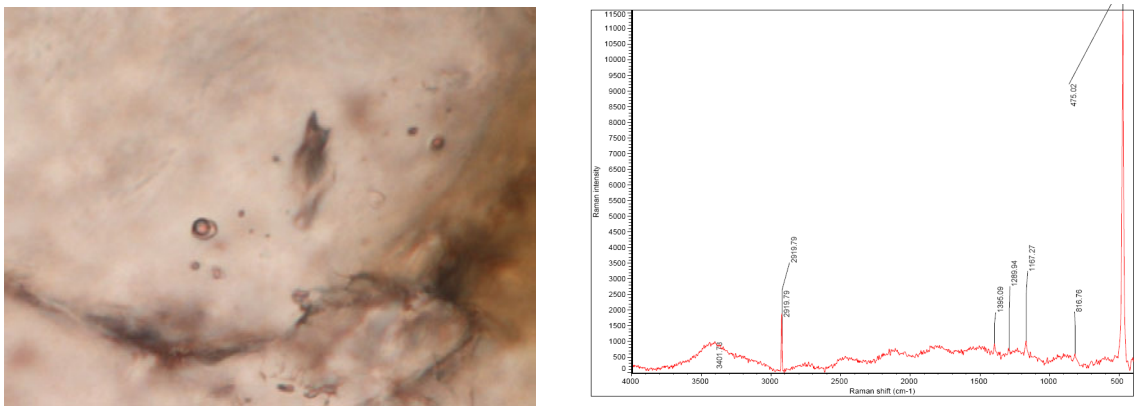

Figure 1: (a) Typical *H_2O+CH_4+CO_2 bearing fluid inclusion, and (b) Raman Spectra of this inclusion.*

Microthermometry data also suggests the presence of minor Mg in addition to Na+K in the saline aqueous fluid inclusions. The fluid inclusions in quartzite are very small and their composition is often difficult to identify. However, in unmineralised quartzites from the Lesser Himalaya dominately aqueous fluids have been observed elsewhere (Sharma and Misra, 1998, Verma and

Sharma 2007). The fluid inclusions in dolomite are low salinity locally with minor CH_4 and sporadic CO_2. The coeval carbonic and aqueous fluids exhibit variation in their proportions and some decrepitate before total homogenisation indicating that carbonic-aqueous immiscibility evolved before fluid entrapment.

On the bases of studies carried out on these ores, it is interpreted that initially sulphides were deposited in a submarine volcano sedimentary environment with exhalative fluxes. The rapid precipitation of ores occurred as a result of the interaction between subsea floor exhalations with the submarine sediments (Symonds et al., 2003) in a free space environment. The $H_2O+CH_4+CO_2$ fluid participated in the primary deposition of these ores, and immiscibility of aqueous and carbonic phases might be an effective cause of their deposition. However, significant H_2O-CO_2 in trails is representative of the syntectonic Himalayan event which mobilised these sulphides to the fractures.

REFERENCES

Nair, N.G.K. and Singh, R.P., 1982. Geology and Sulphide mineralization of the area around Dhanpur, Chamoli District (U.P.), Garhwal Himalaya. *In* A.K. Sinha ed., *Contemporary Geoscientific Researches in Himalaya*, **2**, 145-148.

Sharma, R. and Misra, D.K., 1998. Evolution and resetting of the fluids in Manikaran Quartzite, Himachal Pradesh: Application to Burial and Recrystallization. *Journal of the Geological Society India*, **51**, 785- 792.

Verma P. and Sharma R., 2007. Primary to re-equilibrated fluids and geochemical signatures for the evolution of Nagthat Siliciclastics in Tons valley, Lesser Himalaya, India. *Journal of Asian Earth Sciences,* **29**, 440-454.

Symonds, Robert B., Poreda Robert J., Evans, William C., Janik, Cathy J. and Ritchie, Beatrice E. 2003. Mantle and crustal sources of carbon, nitrogen, and noble gases in Cascade-Range and Aleutian-Arc volcanic gases. *USGS Open-File Report* 403-436.

PVT compositional history of Kuh-I-Mond Field, Zagros Basin

Zeinab Shariatinia[1], Sadat Feiznia[2], Manouchehr Haghighir[3], and Ali Mousavi Dehghani[4]
[1] *Dept. of Geosciences, University of Tehran, Tehran 141556455 Iran*
[2] *College of Natural Resources, University of Tehran Iran*
[3] *Australian Schools of Petroleum, University of Adelaide, Adelaide SA 5005 Australia*
[4] *RIPI-NIOC- Tehran Iran*

This research investigated the compositional history and saturation pressure of oil inclusions during the accumulation of oil into the reservoir at the Kuh-I-Mond Field, which is a conventional heavy oil resource east of the Zagros Basin. PVT thermodynamic modules of the Eclipse software calculated post entrapment changes of petroleum using oil inclusions along with reservoir fluid data, for this purpose. This method was used previously by some researchers to study the compositional history of oil that migrated to petroleum reservoirs in the North Sea (Aplin et al. 1999). Pristine hydrocarbon inclusions preserved within fractured Tertiary carbonates of Asmari Formation. Oil inclusions were observed in the rims and in fracture filling of carbonate-evaporite cements. Their saturation (homogenisation; Th) temperature was measured by microthermometry (Bodnar 1993). The maximum distribution temperature is about 54°C. With only the data from the oil inclusion homogenisation temperature (Th), the saturation pressure and molar composition of hydrocarbon inclusions were calculated. Based on these results, the early reservoir filling occurred as undersaturated oil with around 21 % methane migrated to the reservoir. Later, a more saturated oil containing approx. 40% methane migrated to the reservoir. The saturation pressure of fluids changed from 100 to 110 bars.

REFERENCES

Aplin, A.C., Macleod, G., Larter, S.R., Pedersen, K.S., Sørensen H, Booth, T., 1999. Combined use of confocal laser scanning microscopy and PVT simulation for estimating the composition and physical properties of petroleum in fluid inclusions. *Marine and Petroleum Geology*, **16**, 97–110.

Bodnar, R.J., 2003. Introduction to fluid inclusions. *In* Samson, I., Anderson, A. and. Marshall, D., eds., Fluid Inclusions: Analysis and Interpretation. Mineralogical Association of Canada, Vancouver, Canada, *Short Course Series,* **32**, 1-8.

Melt and fluid inclusion constraints on the late-magmatic crystallisation of Pia Oak tin-bearing leucogranites (Northern Vietnam)

S.Z. Smirnov[1,2], *A.G. Vladimirov*[1,2], *N.N. Kruk*[1], *E.I. Astrelina*[2], *E.N. Sokolova1*[2], *I.Yu. Annikova*[1]

[1] *VS Sobolev Institute of Geology and Mineralogy, SB RAS, pr. ac. Koptyuga, 3, Novosibirsk 630090, Russia*

[2] *Geology and Geophysics department, Novosibirsk State University, Novosibirsk, Russia*

GEOLOGICAL BACKGROUND

Pia Oak granite-leucogranite massif in the Kao Bang province of Vietnam is a plate body confined to deep-seated fault dividing Devonian sedimentary carbonates and Triassic black shales. Rare aplite dykes and pegmatitic veins occur within the massif, but no dykes or pegmatites were found in wall rocks outside the massif borders. Such geological relations suggest closed system evolution of the single magma chamber. Small scale Sn-W-sulfide mineralisation is confined to greisens and quartz stockworks at western and eastern flanks of the massif. Greisen mineralisation, developed around the Pia Oak massif is believed to be a precursor for a large scale Tin Tuk cassiterite placer deposit.

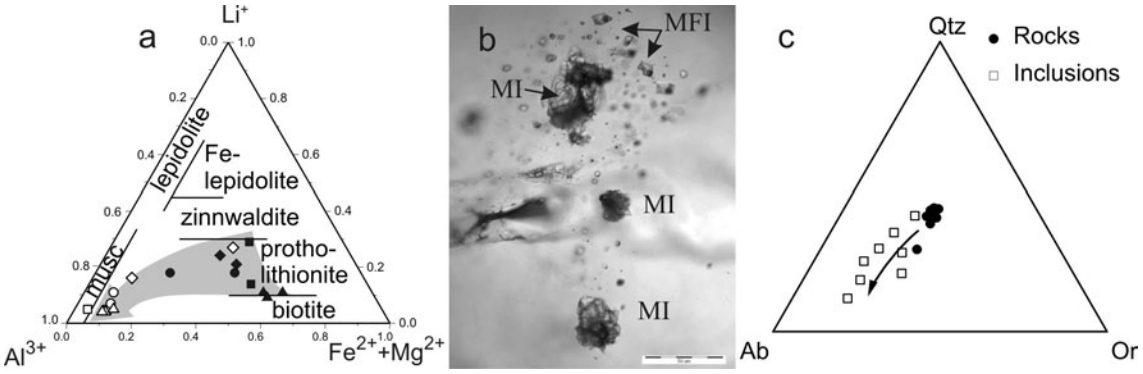

Figure 1: *a – compositional evolution of mica in the Pia Oak leucogranites (filled signs – cores, open signs – rims); b – primary melt inclusions (MI) associated with inclusions of magmatic fluid (FMI); c – melt inclusion and bulk rock compositions.*

GEOCHEMISTRY AND MINERALOGY OF THE PIA OAK LEUCOGRANITES

Leucogranites of the major intrusive phase are peraluminous (A/CNK ~ 1.2) with normal alkalinity and K predominating over Na. They are enriched in rare litophile elements (Li, Rb, Cs, Be, Sn, W) and F (average 0.3 wt %). The later phases of intrusion are somewhat more enriched in fluorine (0.4 wt %). However, they do not show significant enrichment in Li, Rb, Cs and Be compared to the earlier phases. Greisens, which replace major phase leucogranites, are strongly enriched in K, F, Li, Be, Sn and W compared to unaltered granites.

Compositions of leucogranitic mica evidence for abrupt change of the geochemistry of magma at the late stages of crystallisation. Early mica of the major and additional phases of the Pia Oak massif have protolithionite compositions, while the later generations belong to Li-rich and Li-poor muscovite (Fig. 1a). Frequently Li-rich muscovite replaces protolithionite and forms zoned mica crystals.

The aim of this study was to determine P-T-X conditions of the final stages of magmatic evolution of the Pia Oak tin-bearing granite intrusion.

FLUID AND MELT INCLUSIONS

Quartz in leucogranites of the major and additional intrusive phases contains abundant silicate-melt and fluid inclusions. Primary melt inclusions at room temperature contain crystalline aggregates and fluid segregations. Fluid segregations consist of aqueous solution and vapor bubble. Some melt inclusions are surrounded by haloes of tiny fractures healed with small fluid inclusions. In order to re-melt crystalline phases and homogenize inclusions their heating was conducted in the autoclave under external water pressure of 1 and 2 kbar. First homogeneous melt inclusions appear after experiments quenched at 600 and 635°C. These inclusions are typically small <10 mm. Larger inclusions become homogeneous after heating at 650°C. After the heating inclusions composed of the glass and fluid bubble coexist with homogeneous vitreous inclusions.

Both primary and secondary fluid inclusions were found in the quartz of the studied leucogranites. The major attention was paid to those primary fluid inclusions, which accompany the silicate-melt ones in the same assemblages (Fig. 1b). They were interpreted as magmatic fluid inclusions. At room temperature these inclusions contain two phases – aqueous solution and gas bubble. Microthermometry revealed that inclusions of magmatic fluid have eutectic temperatures between -12 and -20°C. Elevated ice melting temperatures (-1…-5°C) show their low salinity. Inclusions homogenize into liquid within broad temperature range 115-280°C. No correlations were recorded between homogenisation and ice-melting temperatures. It indicates that variation in the homogenisation temperature may evidence for variations of fluid pressure in the course of the quartz growth.

Quench glasses of re-melted and homogenized silicate melt inclusions from both major and additional intrusive phases showed unusual compositions. In comparison to bulk rock compositions they are depleted in SiO_2 (61-67 wt %), domination of Na over K, high total amount of alkalis (Na_2O+K_2O average 8.4 wt %) and have low totals which are attributed to high H_2O content. The glass compositions projected to the Qtz-Ab-Or diagram show that they are shifted toward the Ab corner of the diagram compared to bulk rock compositions (Fig. 1c). Similarly to bulk rocks inclusion glasses are peraluminous (A/CNK ~ 1.2) and rich in F (0.12-0.86 wt %). SIMS analyses showed enrichment in Rb (up to 800 ppm), Cs (up to 3000 ppm), Nb (up to 65 ppm).

DISCUSSION

The studied fluid and melt inclusion assemblages indicate that its crystallisation proceeded in the heterogeneous medium composed of silicate melt and aqueous fluid. The strong compositional difference between the melt inclusions and bulk rocks suggest that the melt inclusions are not representative of the initial magma composition. The shift of composition to Ab corner of the Qtz-Ab-Or diagram, enrichment in alkali, supposed high concentrations of H_2O are interpreted as an evidence of the latest portions of the crystallizing magma. These portions are characterised by strong enrichment in volatiles and rare lithophile elements indicating high ore potential of the residual leucogranitic melts. However, depletion of leucogranitic mica in Li and F and similarity in concentrations of Li, Rb, Cs, Be and Sn between major phase leucogranites and late applites suggest that these elements were lost from the magmatic source. Fluid inclusions revealed significant variation in fluid pressure at the latest stages of crystallisation. The cause of this change should be a contraction fracturing of the solidified part of the magma chamber or small scale tectonic fracturing. The fracturing occurs when residual portions of the melt cannot leave the chamber, while magmatic fluids were able to move along these fractures toward the upper parts of the chamber and surrounding wall rocks. On the basis of mineral and rock geochemistry we conclude that the magmatic fluids were enriched in Li and F, and, probably, in Sn, W and Be.

Fluid regime of crystallisation and ore potential of rare-metal felsic dyke rocks in Kalba-Narym complex (Eastern Kazakhstan)

Sokolova E.N.[1,2], Smirnov S.Z. [1,2], Khromykh S.V. [1,2]
[1] Novosibirsk State University, Pirogova str., 2, Novosibirsk 630090, Russia
[2] V.S. Sobolev Institute of Geology and Mineralogy SB RAS, Novosibirsk, Russia

INTRODUCTION AND GEOLOGICAL SETTING

Kalba-Narym complex consists of large granite Kalba batolith, extending to several hundreds of kilometers, smaller intrusions varying in composition from gabbroids to felsic rocks, rare-metal pegmatites, W- and Sn-bearing ore veins. The complex intrudes Variscan structures of Irtysh folded zone. Radiogenic ages (Maslov et al., 1994) and geological position show that the youngest magmatic formations in the folded zone belong to the system of dyke belts. Two belts of this system - Chechek and Akhmirovka, which are composed of rare-metal (RM) felsic dykes - occur near Ust-Kamenogorsk city in the Eastern Kazakhstan. Notably, dykes of these belts differ from earlier granitoids by increased Sn, Nb and rare lithophile element content. However, in spite of high rare-metal concentrations none of the belts is associated with hydrothermal ore mineralisation.

GEOLOGY, MINERALOGY AND GEOCHEMISTRY OF THE DYKES

The studied belts are several kilometers long. Single dyke thicknesses are about 1-2 m. Chechek belt is composed of series of parallel dykes striking to north-east. Akhmirovka belt contains several dykes oriented similarly. The dykes are composed of microgranites, granite-porphyry and felsite-porphyry. Major phenocrystic minerals are quartz, albite, K-feldspar and muscovite. Accessory apatite, fluorite, tanatalite-columbite, cassiterite, zircon, xenotime and monazite occur in groundmass and as crystalline inclusions in phenocrysts. On the basis of detailed geochemical study the rocks of Chechek belt are divided into two groups. The first one is featured by highest concentrations of F (up to 1.4 wt %) and P_2O_5 (up to 0.35 wt %), high concentrations of rare metals (Li+Rb+Cs up to 2500 ppm) and low total REE (3-15 ppm). The second group is composed of rocks with lower rare metal (up to 1000 ppm), F (up to 0.45 wt %), and higher total REE (40-100 ppm) contents. The rocks of these two types differ in La_N/Yb_N: 3-5 for the first group and 0.7-3 for the second group. The rocks of Akhmirovka belt differ from those of Chechek one by higher rare metal (up to 4000 ppm) and total REE (110-180 ppm) contents with positive REE slopes (La_N/Yb_N 0.3-0.4).

MELT AND FLUID INCLUSION STUDY

Quartz phenocrysts of the dyke rocks from Chechek and Akhmirovka belts contain similar melt (MI) and fluid inclusion (FI) assemblages. MIs are completely crystallized and often contain fluid segregation (Fig.1a). Large and medium size MIs (20-50 μm) are surrounded by decrepitation haloes of tiny fissures and FIs. Primary FIs contain low-salinity (1,5-8 wt% NaCleq) aqueous solution and gas bubble.

MI heating

The majority of MIs decrepitate on heating under atmospheric pressure due to a high internal fluid pressure. Homogenisation experiments were conducted in autoclave under external water pressure 2 kbar by a stepwise quenching method. MIs homogenize into silicate melt at temperature $\leq 625^0$C. Low crystallisation temperature results from high concentrations of fluorine and water which decrease a solidus temperature.

MI composition

Crystalline aggregate of MIs at room temperature is dominated by daughter muscovite, with minor albite and K-feldspar. Many inclusions contain tiny grains of apatite (Fig.1 b). Monazite, cassiterite, barite and calcite were sporadically found in unheated MI. The quenched MI glasses contain moderate silica (68 – 70 wt%) and elevated F (up to 1.5 wt%) and P2O5 (up to 0.4 wt%). The majority of glasses are peraluminious (A/CNK =1,1-1,4) with Na predominating over K. From total analytical deficiency of EMP analyses high water content may be supposed. In general compositions of MIs correspond to the bulk rocks. It is important to note that division of the rocks into three groups is reflected in MI glass compositions. More distinctly this difference can be seen in P and F abundances: high RM rocks of Chechek belt and MIs from their phenocrysts have the highest content of these elements.

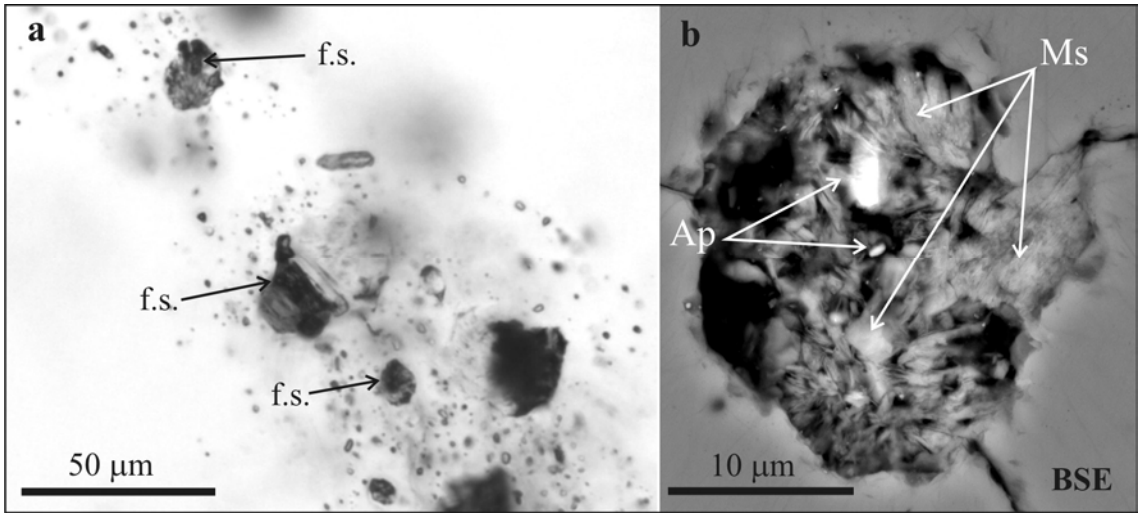

Figure 1: *a – Group of cogenetic silicate melt inclusions and aqueous fluid inclusions. MIs are devitrified and contain fluid segregation (fs). b - Crystalline aggregate in MI before heating, consisting of muscovite (Ms) with apatite grains (Ap).*

DISCUSSION AND CONCLUSION

The obtained geochemical, FI and MI data indicate that Chechek and Akhmirovka dyke belts were formed by three compositionally different types of rare-metal and volatile rich magma. The compositional difference may be related to spatially separated magmatic sources with different differentiation history. The similarity of MI and bulk rock compositions evidences for no significant melt evolution after MI entrapment before the dyke emplacement. The presence of accessory ore minerals in the dyke rocks, high concentration of ore elements in the bulk composition, and crystallisation under water saturated conditions indicate high ore potential of the Chechek and Akhmirovka dykes (Reif, 1990). The absence of hydrothermal mineralisation is explained by short crystallisation history and conservation of magma derived fluid within magmatic bodies.

This work was supported by RF President grant for young scientists MK-1753.2012.5 and RFBR grant 10-05-00913.

REFERENCES

Maslov, V.I., Kozlov, M.S., Dovgal', V.N.,and Distanova ,A.N., 1994. Complex of ongonites and lithium-fluorine granites in south-west Altay. *Petrology*, **2**, № 3, 331-336.

Reif, F.G., 1990. Ore-forming potential of granites and conditions of its realization. Moscow, Russia, 180p.

Fluid inclusion study of the carbonate hosted Pb-Zn mineralisation from Riasi Inlier, Jammu & Kashmir (India)

Pankaj K. Srivastava, Ishya Devi and Surjeet Singh
Department of Geology, University of Jammu, Jammu,180006, India

Himalayan foot hills of the Jammu region are characterised by the presence of four NW-SE trending inliers of Precambrian carbonate sequence, namely Devigarh, Kalakot-Mahogala, Riasi and Lopri inliers within the Tertiary sequence. The Riasi inlier is the largest with about 40 km lateral extension. Thick sequences of carbonates of the Riasi Inlier, known as Sirban Limestones, contain Pb-Zn mineralisation at Khairikot, Sersandu, Chiralakot, Rahotkot, Darabi and Gainta areas. The Pb-Zn mineralisation is mostly in form of lenses, pockets and veins mostly concentrated at the contact of quartzite and dolostone. The variation in the Pb:Zn ratio is observed in the area represented by the higher sphalerite concentration within the dolostones, whereas more galena is observed in the siliceous dolostones or at the contact of dolostone and quartzite.

Fluid inclusion studies of the gangue mineral associated with lead mineralisation in the Kharikot area of Riasi inlier indicate the presence of only two types of fluid inclusions. They are represented by two-phase aqueous inclusions (Type I) and monophase aqueous inclusions (Type II). The monophase aqueous inclusions are very small in size and hence could not be observed during freezing studies. However, when some of the monophase aqueous inclusions were frozen to -160ºC, but no phase change was observed. This may be either due to leakage of fluids or due to the presence of CH_4. The freezing studies of the two-phase inclusions suggest that the aqueous fluid in these inclusions also contain $MgCl_2$. The heating studies of two-phase aqueous inclusions give a wide range of homogenisation temperatures ranging from 146 ºC to 225 ºC with an average 176 ºC. The salinity of fluid inclusions varies from 4 to 15 wt% NaCl eq and density ranges from 0.85 to 1.03 g/cm^3. Fluid mixing is suggested for the lead-zinc deposition in the area.

Magmatic-hydrothermal fluid evolution for tungsten mineralisation in Kalni-Kotariya area, Rajasthan, north-western India: Evidence from fluid inclusion studies

Pankaj K. Srivastava
Department of Geology, University of Jammu, Jammu - 180006, India

INTRODUCTION

The early to middle Proterozoic Aravalli-Delhi orogen in Rajasthan forms an important segment of the Precambrian metallogenic province and includes one of the few known tungsten deposits of India. The Kalni-Kotariya area forms a central link between the Balda – Tosham tungsten belt present on the western margin of the Delhi fold belt. Tungsten mineralisation in the area was first reported by Jain and Bhattacharjee (1992). The mineralisation in the area is mainly concentrated in quartz veins hosted by granite. The fluid inclusion study in the coeval vein quartz is presented here in order to understand the hydrothermal fluid evolution responsible for the tungsten mineralisation in the area.

GEOGICAL SETTING

The Pre-Delhi metamorphic rocks represented by high grade schist and gneiss forms the basement for the unconformably overlying metasedimentary sequence of Meso-Proterozoic Delhi Supergroup. These rocks are intruded by Sewariya granite. Bhattacharjee et al (1993) suggested two phases of the Sewariya granite, represented by biotite granite and leucogranite.

Sporatic and sparse tungsten mineralisation is recorded as disseminated wolframite and also occurs as pockets of wolframite in quartz veins. These structurally controlled, N-S to NNE-SSW trending quartz veins occur in a 14 km long zone between Kalni to Kotariya. Greisenisation and tourmalinisation are the common wall rock alteration styles present in the area.

FLUID INCLUSION STUDIES

Fluid inclusion microthermometric experiments for the vein quartz coeval with wolframite mineralisation, reveal the presence of three distinct types of fluid inclusions. These are represented by two-phase aqueous inclusions, aqueous-carbonic inclusions, and halite bearing multiphase inclusions. The homogenisation temperature of different types of inclusions vary between 230 to 434 °C with varying salinities of up to 43 wt. percent NaCl equivalent.

Three stages of ore fluid evolution have been inferred from the study. It is suggested that initially the high salinity and high temperature hydrothermal fluid, which was rich in volatiles, was formed during the late stage of the cooling granite body. Upwelling of magmatic derived fluid through shear zones and pressure loss is suggested to be responsible for boiling of the hydrothermal fluids. A flux of the carbonic fluid represented by carbonic-aqueous inclusions is the result of unmixing. This hydrothermal fluid later underwent a simple cooling and mixing of the meteoric fluid, which culminated in a lower temperature and fluid dilution. The tungsten mineralisation ceased during this stage.

A shallow environment of vein emplacement and low pressure conditions are inferred for the tungsten mineralisation in the Kalni-Kotariya area. It is inferred that tungsten, which was transported in solution, was mainly in form of chloride complexes.

REFERENCES

Bhattacharjee, J., Fareeduddin, and Jain, S.S. (1993) Tectonic setting, petrochemistry and tungsten metallogeny of Sewariya granite in south Delhi fold belt, Rajasthan. *Journal Geological Society of India*, **42**, 3-16.

Jain, S.S. and Bhattacharjee, J. (1992) A note on wolframite prospects associated with the Sewaria granite pluton, Rajasthan. *Indian Minerals*, **46**, 159-164.

Fluid inclusions in garnet of calcic skarns, the Tazheran massif (western Baikal area, Russia)

A.E. Starikova
Sobolev Institute of Geology and Mineralogy SB RAS, Novosibirsk, Russia

INTRODUCTION

The hypabyssal Tazheran massif of alkaline and nepheline syenites is the part of the Olkhon collision system of the western Baikal area. Metasomatic processes are widespread within the massif. Most abundant metasomatites are magnesian skarns and calciphyres that formed on the contact of nepheline syenites and dolomite marbles at relatively high temperatures (700-850˚C). In places magnesian minerals were replaced by lower temperature calcic skarn assemblage (450-550˚C). Uncommon high-temperature melilite-bearing calcic skarns developed at the central part of the massif. The object of present research is calcite vein containing garnet-pyroxene skarn aggregates and their single grains. This vein is located in the south-western part of the massif and strikes from south to north more than 2 km. It has no apparent connection with magmatic source and physico-chemical parameters of formation are uncertain. Typical mineral assemblage of skarn aggregates consist of grossular-andradite garnet (Grs – 86-65%, Adr – 30-12%), diopside (#Mg>71%), titanite, scapolite and rare apatite. The aim of the study is to determine characteristics of skarn-forming fluids.

Figure 1: *inclusion Changes in inclusion in garnet during freezing: (a) 25˚C; (b) -110˚C; (c) -22˚C; (d) 0˚C (after freezing). H – halite, HH – hydrohalite, SY –sylvite, G – gas bubble, L – liquid phase.*

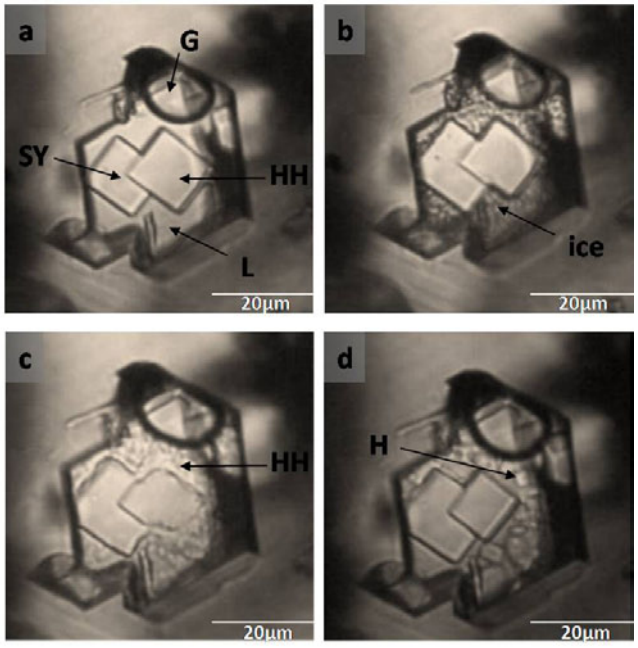

METHODS

Study of fluid inclusions was performed by optic (BX51 Olympus polarizing microscope), microthermometric (THMSG 600 Linkam heating-freezing stage) and Raman spectroscopic (Raman U-1000 Jobin Yvon) methods.

RESULTS

Numerous primary inclusions with high-salinity aqueous fluid were found in garnet crystals (Fig.1). Predominantly they form negative crystals with worm-like or isometric habit and rarely have

irregular shape. Inclusions have size up to 40-50 μm and located randomly or along the growth zones in the host garnet. Almost all of them contain four phases at room temperature: liquid (~55 vol.%), vapor (~15 vol.%) and two daughter crystals: NaCl (~18 vol.%) and KCl (~12 vol.%).

Table 1: **Microthermometric data**

(˚C)	n=10
T_{EU}	-55 - -50
$T_{M(ICE)}$	-30 - -28
$T_{M(HH)}$	0 - 3
$T_{M(SY)}$	125 - 150
$T_{M(H)}$	350 - 380
$T_{H(TOTAL)}$	380 - 410

Besides, a few combined inclusions were found with captured crystals of calcite. Identification and distinction of daughter crystals can be made by their optical characteristic and by hydrohalite appearance on freezing (Fig.1, Tab.1). Raman spectroscopy and deep freezing (-110˚C) do not detected significant amounts of carbon dioxide. Eutectic temperatures of 10 examined inclusions range from -46˚C to -55˚C. Such low temperatures indicate the presence of $CaCl_2$ in solution. Thus composition of skarn-forming fluids can be described by the NaCl-KCl-$CaCl_2$-H_2O system. Almost all studies of such system were made for unsaturated fluids or at room temperature. In this study estimations of concentration of fluids were done assuming 30 wt.% $CaCl_2$, which is maximum for mentioned $CaCl_2$ unsaturated solutions at room temperature (Marcus, Soffer, 1988), and for 0.1 wt.%. The system NaCl-KCl-H_2O was used for the second case. Approximate volume was used for estimations of concentrations NaCl and KCl (Table 2). It can be proposed that the content of main components lies in the range 29.33 – 39.29 wt.%, 20.78 – 24.6 wt.% and 15.78 – 0.05 wt.% for NaCl, KCl and $CaCl_2$ respectively. Thus Ca-bearing fluids with high-salinity played a significant role during formation of the garnet-pyroxene skarns.

ACKNOWLEDGEMENTS

The research was supported by the Russian Foundation for Basic Research (12-05-00229-a) and special grant by OPTEC LLC.

REFERENCES

Marcus Y., Soffer N., 1988. Solubilities and Vapour Pressures in the Quinquinary System NaCl-KCl-$MgCl_2$-$CaCl_2$-H_2O. Part 1. - Predictions and measurements at 25°C *J. Chem. Soc., Faraday Trans. 1,* **84** (10), 3575-3585.

Homogenisation of ultra-high pressure melt inclusions by high pressure experiments

A.S. Stepanov[1], J. Hermann[1], D. Rubatto[1], and A.V. Korsakov[2]
[1] *The Australian National University, Research School of Earth Sciences, Canberra, Australia*
[2] *Institute of Geology and Mineralogy of Siberian Branch Russian Academy of Sciences, Novosibirsk, Russia*

INTRODUCTION

Experiments on the homogenisation of fluid and melt inclusions are performed routinely with volcanic and hydrothermal samples. For homogenisation of inclusions to be applied to high grade metamorphic rocks, the experiments must be performed at high pressure in order to stabilise the minerals hosting the inclusions (Malaspina et al., 2006; Bartoli et al., 2011). Here we describe a technique, which allowed successful homogenisation of polyphase inclusions in ultrahigh pressure rocks from the Kokchetav complex, Kazakhstan, which reached metamorphic conditions of 45-70 kbar and 950-1000°C. This method makes it possible to investigate major and trace element compositions of melts formed at such extreme conditions.

SAMPLE DESCRIPTION AND EXPERIMENTAL CONCEPT

Abundant polyphase inclusions were observed in garnet from UHP garnet-biotite gneiss consisting of Grt, Bt, Phe, Fsp, Qtz, Rt and Zrn. The layered gneiss is composed of a melanosome with the assemblage biotite, feldspars and ≈30 % of high-Ca (Grt-M) garnet and a leucosome, which contains quartz, feldspars and ≈10 % of low-Ca (Grt-L) garnet. Most polyphase inclusions have polygonal negative crystal shapes, and dimensions varying from less than 1 μm to 1 mm. Large polyphase inclusions have outgoing cracks filled by chlorite. Polyphase inclusions are composed of Qtz, Bt, Phe, Chl and feldspars, and occasionally contain accessory minerals such as Rt, Ilm, Ap, Zrn, Bdl, Mnz and Aln. The bulk rock composition of the sample is strongly depleted in LREE, Th and U, in contrast polyphase inclusions contain high-REE minerals Mnz and Aln.

Mineral associations and minerals compositions in inclusions are very variable and often are not in equilibrium, presumably due to crystallisation associated with decrepitation during exhumation. This precludes the calculation of the bulk compositions of inclusion from the minerals. Laser ablation of polyphase inclusions resulted in abundances and ratios of trace elements varying by orders of magnitude between different inclusions. These variations are attributed to presence of accessory minerals in the inclusions.

The main purpose of the experiments in this study is to transform heterogeneous associations into glass suited for analysis by micro beam methods and to demonstrate that inclusions indeed represent trapped melts. Homogenisation experiments were performed in a piston-cylinder press at the Research School of Earth Sciences, the Australian National University. In such experiments there are several important variables: temperature, pressure, duration, composition of matrix material and how the inclusion bearing material is prepared. Experiments should be performed at conditions where garnet is stable, the hydrous granitic melt is above the solidus and temperature is high enough for complete dissolution of secondary accessory minerals. The experiments were performed at high temperature (900-1000°C) in order to homogenise inclusions and to dissolve completely the accessory minerals. Duration of experiments was relatively short (0.5-1 h) in order to reduce decomposition of garnet. High pressure (10-20 kbar) is necessary for the stabilisation of garnet. Garnet for experiments was prepared by two different methods: firstly garnet grains 0.4-0.6 mm in size were separated from crushed rock, and secondly a large grain of garnet (5x2.4x2 mm) was cut from a sample, fitted into the capsule and immersed into the matrix powder. The experiments were performed with a powdered matrix of SiO_2-$Al(OH)_3$ mix in order to cushion garnet grains from the strain occurring in the press assembly. In order to prevent fluid leakage from the inclusions, most of the experiments were performed with an addition of $Al(OH)_3$, which releases water on heating.

Glass inclusions were analysed by SEM and laser ablation ICPMS. Absolute concentrations of trace elements were obtained using the method proposed by Halter et al. (2002).

RESULTS

Several experiments were performed with garnets separated from the crushed sample. The capsule was filled with layers of garnet grains separated by layers of matrix powder. In this experiment 90 % of garnet recrystallised and obtained spongy textures. The spongy garnet had lower Ca content and higher Mg# than the original garnet. Approximately 10% of garnet after the experiment was represented by homogeneous grains with small glass inclusions and had Grt-L composition. In an optical microscope, inclusions appear transparent and isotropic without bubbles or crystalline phases. Melt inclusions have low LREE and Th content and are interpreted to represent low temperature melts formed on exhumation. In these experiments Grt-M was completely decomposed, whereas Grt-L survived and presented homogeneous inclusions.

In the experiment performed with a large garnet grain cut from the sample melanosome, a large fraction of garnet survived the experiment and contained glassy inclusions, though most of the inclusions have thin cracks. In this experiment garnet preserved its initial Grt-M composition. Melt inclusions in this experiment have high LREE and Th abundances. These melts were formed at peak UHP conditions when monazite was completely dissolved in the melt and these are melts responsible for depletion of the rock in REE, Th and U. .

DISCUSSION AND CONCLUSIONS

- High temperature melt inclusions in crustal rocks are likely to have high concentrations of trace elements and thus contain accessory minerals. This makes such inclusions unsuitable for bulk ablation and homogenisation by high pressure experiments is necessary for reliable determination of melt composition.
- Metamorphic rocks can contain several generations of minerals with inclusions of different compositions. Different mineral compositions can behave in a very different ways even during short re-homogenisation experiments and these experiments can induce a bias in the selection of inclusions. A thorough examination of pre-experimental and post-experimental minerals is necessary and detailed petrographic description and mapping is absolutely essential. Details of experimental set up, such as method of preparation of experimental material or percentage of matrix material, can affect experimental results.
- High pressure experiments result in melting of the matrix material and generation of new (secondary) melt inclusions. These inclusions can be distinguished from the original melt inclusions by their composition. Whereas experimental melts are formed at the expense of matrix material and garnet, metamorphic inclusions derive from genuine granitic melts with high concentrations of elements such as LREE, Th and U.

REFERENCES

Halter, W., Pettke, T., Heinrich, C. & Rothen-Rutishauser, B., 2002. Chemical Geology 183, 63-86.

Bartoli, O., Cesare, B., Poli, S., Bodnar, R., Frezzotti, M., Acosta-Vigil, A. & Meli, S., 2011. *Mineralogical Magazine* **75/3**, 495

Malaspina, N., Hermann, J., Scambelluri, M. & Compagnoni, R., 2006. *Earth and Planetary Science Letters* **249**, 173-187.

Pegmatites of the Shibanovsky Ore Field (Russian Far East): Physical-chemical parameters

Y.A. Stepnova and V.A. Pakhomova
Far East Geological Institute, Far Eastern Branch of Russian Academy of Sciences, Vladivostok, Russia

The Shibanovsky Ore Field is located in the eastern part of the Khanka superterrain on the southeastern slope of the Siniy Ridge, in the basin of the Shibanovsky Creek, a left tributary of the Arsenyevka River (the Spassky District of the Primorsky Region). The Shibanovsky ore field is composed of rocks of the Matveevka-Nakhimovka Terrain: Middle Paleozoic, Late Permian, and Palaeogenic (Late Cretaceous) granites, Upper Permian volcanogenic-sedimentary and sedimentary rocks, as well as pegmatites, greisens, and hydrotermalites.

Uncovered by quarrying pegmatites in the Shibanovsky granites occur rather frequently as lenses and small veins 0.2-0.8 m in length and 0.1-0.7 m in thickness. The structure of the pegmatites is zoned. An external zone is composed of fine-grained biotite granites. Next is the zone of fine-grained graphic pegmatite which is followed by the internal zone of coarse-crystalline block pegmatite mainly consisting of quartz (60-80%) and feldspar (20-40%). `The internal zone is often accomplished by euhedral hexagonal-shaped crystals of morion. Quartz forms hexahedral pyramidal black or dark grey crystals, sometimes white and transparent ones having transverse shading. Crystals have length of 0.2-30 cm, width of 0.1-20 cm, common dimensions of 5x2cm.

We have investigated the parts of quartz crystals that had single inclusions of pegmatite and were confined to the central (axial) zones of the crystals. In examination of zonal crystals, preference was given to fluid inclusions uniformly distributed in the scope of one of the zones of quartz crystals and having consistent phase ratio. We regarded them as primary inclusions. We measured phase transitions while freezing and heating up to the temperature of homogenisation of gas-liquid inclusions. Eutectic temperatures were used to estimate possible salt composition in solutions preserved in fluid inclusions and to calculate pressure (P) characteristic for mineral forming episodes occurring at different times.

Optical examination of pegmatite plates let us classify the inclusions in quartz and reveal time sequence of their formation. According to phase composition and formation time, the inclusions were subdivided into 4 groups: a) primary multiple-phase gas-liquid inclusions having solid phases; b) primary-secondary gas-liquid inclusions having solid phases; c) late secondary essentially gas inclusions; d) secondary gas-liquid two-phase inclusions. The earliest primary inclusions are often multiple-phase ones. They contain two solid cubic phases which total volume makes from 35 to 60 % and a gas phase occupying 20-25 % of a vacuole volume. Size of the primary inclusions is tens-first hundreds microns, though smaller ones occur as well.

The authentically primary multiple-phase inclusions have up to 5-6 crystalline phases. Cubic isotopic crystals which occupy a significant part of the vacuole volume are regarded as halite and sylvite, rarer as carrobiite (KF), by their optical properties and behavior during heating. Therefore, sodium and potassium chlorides play a determinant role in the composition of the preserved solutions. Among other trapped minerals there are shapeless crystals with high refraction index.
Homogenisation of the gas-liquid inclusions with solid phases proceeds, in most cases, into a liquid phase at about 400°C. Dissolution temperature of sylvite is 118-120°C, and of halite is about 400°C. The inclusions sometimes contain a mineral phase showing no reaction to heating up to homogenisation temperature of the neighboring inclusions free from this phase. The examination has shown that the discussed phase corresponded to albite. This component of vacuoles is regarded as an

"accompanying" phase due to its origin, and the albite-containing inclusions are regarded as composite ones. By the temperatures of halite and sylvite dissolution and in accordance with the diagrams of their solubility in H_2O-NaCl and H_2O-NaCl-KCl systems [5], the saltiness of the mineral-forming fluids is greater than 36.6%.

Results of cryometric studies show that thawing of eutectic occurs at about -78°C, and the most low temperature solid phase starts to thaw at -75°C that corresponds to joint presence of lithium and calcium chlorides in the solution (Borisenko, 1982). Additional gas phases immiscible with carbon dioxide are formed in the bubble's rim at deep freezing of the inclusions that admits presence of an admixture of other gases. IR-spectroscopy revealed the presence of CH_2, CO, CO_2, and NO_2 admixtures in quartz samples with different amount of the gas phase in the inclusions studied in a range of 4000 – 2000 cm^{-1}. Liquid phase of the solution contains compounds of H_3BO_3, HBO_3, and H_2S.

Later inclusions in quartz phenocrysts belong to essentially gas ones by their phase composition, because they contain a gas bubble occupying 80-902% of vacuole volume, a thin rim of solution, and sometimes a solid phase. Presence of daughter phases insoluble at heating, lack of signs of disclosure of essentially gas fluid inclusions when heated up to extremely high temperatures indicate that the solutions in the inclusions are most likely belong to P-Q type (Peretyazhko and Savina, 2010; Peretyazhko and Tsaryova, 2007; Ravich, 1974; Sourirajan and Kennedy, 1962; Valyashko, 1990).

REFERENCES

Borisenko A.S., 1982. Analysis of the salt composition of gas-liquid inclusions with the help of criometrical method. // Using of thermobarogeochemical methods during search and studies of the ore deposits. / Edited by N.P. Laverov, *Nedra*, Moscow, p. 37-41.

Peretyazhko I.S. and Savina E.A., 2010. Fluid and magmatic processes in the formation of the Ary-Bulak ongonite massif (Eastern Transbaikalia) // *Geology and Geophysics,* **51(10),** 1423-1442.

Peretyazhko I.S. and Tsaryova E.A. 2007. Magmatic fluids of P-Q type in processes of crystallisation of ongonite melt (massif Ary-Bulak, Eastern Transbaikalia). // Geochemical Problems of Endogenous Processes and the Environment.. Irkutsk. p. 190-194.

Ravich M.I., 1974. Water-salt systems at Elevated Temperatures and Pressures. *Nauka*, Moscow, p. 151.

Sourirajan S. and Kennedy G.C. 1962. The system H_2O-NaCl at elevated temperatures and pressures // *American Journal of Science***, 260**, 115-141.

Valyashko M.V., 1990. Phase Equilibria and Properties of Hydrothermal Systems. *Nauka*, Moscow, 270 p.

High-temperature opal inversion: Evidence from the El Indio Cu-Au deposit, Chile

D. Tanner[1], R.W. Henley[1], John A. Mavrogenes[1], Terrence P. Mernagh[2] and Peter Holden[1]
[1]*Research School of Earth Sciences, Australian National University, Canberra, ACT 0200, Australia*
[2]*Geoscience Australia, GPO Box 378, Canberra, ACT 2600, Australia*

QUARTZ IN THE EL INDIO CU-AU DEPOSIT

The El Indio Cu-Au deposit is a high-sulphidation deposit located in Chile. The El Indio Cu-Au deposit formed in feeder zones ~1000 m beneath a 7 Ma fossil fumarole field (Henley and Berger, 2011). The high-grade Cu-Au ore is hosted in sulphosalt veins containing enargite-tennantite assemblages. The sulphosalt veins contain symplectic textures and crystal lined vugs, indicative of high-temperature deposition (Mavrogenes et al., 2010). Sulphosalt phase relations reveal that sulphide ore was condensed as melt from rapidly ascending magmatic vapour at ~680°C, which subsequently fractionated and crystallised down to 550°C (Henley et al., *in press*).

But most strikingly, we have discovered euhedral quartz microcrystals 'floating' within the sulphosalt ore (Figure 1). This is the first time such crystals have been studied, however we have documented similar quartz microcrystals in at least twelve other high-sulphidation deposits, as well as Cordilleran polymetallic deposits and a porphyry Cu deposit. The El Indio quartz microcrystals are contemporaneous with Cu-Au mineralisation, as they contain sulphosalt melt inclusions. We have undertaken a detailed geochemical and petrological study, to reveal a complex history recorded by fine oscillatory zoning, distinct morphology, residual opal and an unusual isotopic signature.

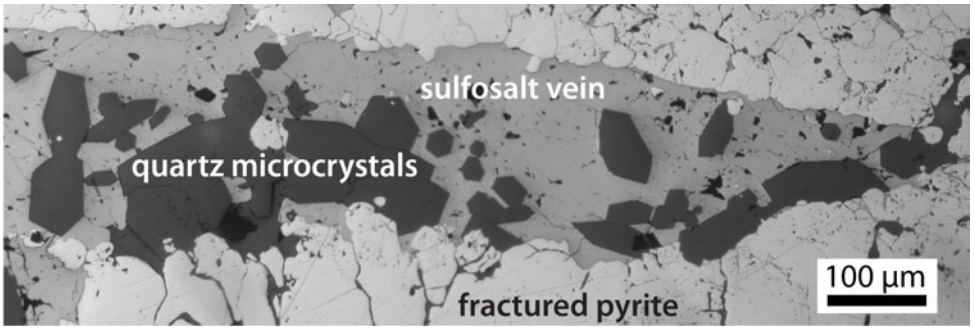

Figure 1*: Euhedral quartz in enargite-tennantite ore hosted within fractured pyrite, El Indio.*

EVIDENCE OF INVERTED QUARTZ

Several lines of evidence suggest that the El Indio quartz microcrystals did not grow directly from magmatic gas responsible for Cu-Au mineralisation. The quartz morphology, Raman spectroscopy, and *in-situ* oxygen isotope analyses all suggest that the magmatic gas initially deposited hydrous amorphous silica (i.e. opal), which then recrystallised to anhydrous, euhedral quartz microcrystals – *'inverted quartz'*. These results are discussed in further detail below:

Texture and Morphology

The texture and morphology of El Indio quartz crystals was investigated using secondary electron (SE) imaging, optical microscopy and cathodoluminescence (CL) imaging. SE imaging of crushed quartz separates revealed α-quartz morphology. SELFRAG was then used to crush the sulphosalt ore, to preserve the delicate morphology of El Indio quartz, including clusters of quartz microcrystals as well as doubly-terminated microcrystals. CL imagery revealed complex internal

textures, including euhedral quartz nucleating from regions of cryptocrystalline silica and doubly-terminated quartz crystals with cores of cryptocrystalline silica.
These textures are analogous to textures observed in "diagenetic" quartz matured from amorphous silica from sandstones and silica sinters (e.g. Lynne et al., 2007). Such studies have shown that at low-temperatures, opal progressively matures to quartz. This stepwise metamorphosis occurs in the following order, with increasing crystallinity:

opal-A (amorphous)➔opal-CT (bladed lepispheres)➔
opal-C±moganite (paracrystalline)➔quartz microcrystals (doubly-terminated)

Thus, the morphology of the El Indio quartz crystals suggests they may have also matured from amorphous silica. In order to investigate the mineralogy of the cryptocrystalline silica at the roots of quartz clusters, we used Raman spectroscopy.

Raman Spectroscopy

Raman spectroscopy of El Indio quartz microcrystals revealed two features in the cryptocrystalline silica: discrete regions of quartz containing crystalline water (i.e. opal) and discrete regions of moganite, a metastable silica polymorph. We suggest that the residual opal and moganite phases within cryptocrystalline silica represent residual metastable silica phases left over from the transition of quartz to opal.

In-situ Oxygen Isotope Analysis (SHRIMP II)

In-situ oxygen isotope analysis of El Indio quartz microcrystals was conducted using the sensitive high-resolution ion microprobe (SHRIMP) II, located at the Australian National University. *In-situ* analyses revealed *extreme* isotopic fractionation in quartz microcrystals ($\delta^{18}O$ up to 16.2 ‰). The heavy oxygen isotope signature suggests that dehydration occurred during opal inversion to quartz: the released water was enriched in ^{16}O, thus residual quartz became enriched with respect to $\delta^{18}O$.

HOW AND WHY DOES 'INVERTED QUARTZ' FORM?

We suggest that high-temperature opal can form in any high-temperature hydrothermal system that becomes super-saturated in silica. Silica super-saturated fluids do not deposit silica in its equilibrium form (quartz). Instead, metastable amorphous phases such as opal precipitate. These amorphous phases can contain up to 15.3 wt% water. However, the high-temperatures present in sub-volcanic environments (e.g. >550 °C at El Indio) force the opal to rapidly invert to quartz. This transition has been shown to occur in <26 weeks in environments <100°C (Lynne et al., 2006).

REFERENCES

Day, R. & Jones, B., 2008. Variations in water content of opal-A and opal-CT from geyser discharge aprons. *Journal of Sedimentary Research,* **78**, 301-315.

Henley, R.W., Mavrogenes. J.A., Tanner, D., 2012. Sulfosalt melts and heavy metal (As-Sb-Bi-Te-Sn-Pb-Tl) fractionation during volcanic gas expansion: the El Indio (Chile) paleofumarole. *Geofluids,* in press.

Lynne, B.Y., Campbell, K.A., Perry, R.S., Browne, P.R.L., Moore, J., 2006. Acceleration of sinter diagenesis in an active fumarole, Taupo volcanic zone, New Zealand. *Geology,* **34**, 749-752.

Lynne, B.Y., Campbell, K.A., James, B.J., Browne, P.R.L., Moore, J., 2007. Tracking crystallinity in siliceous hot-spring deposits. *American Journal of Science,* **507**, 612-641.

Mavrogenes, J.A., Henley, R.W., Reyes, A., Berger, B.R., 2010. Sulfosalt melts: evidence of high-temperature transport of metals in the formation of high-sulfidation lode-Au deposits. *Economic Geology*, **105**, 257-262.

Henley, R.W. & Berger, B.R., 2010. Magmatic-vapor expansion and the formation of high-sulfidation gold deposits: Chemical controls on alteration and mineralization. *Ore Geology Reviews*, **39**, 63-74.

The composition of melt inclusions in minerals of pyroxenite xenoliths from Avacha volcano

T.Yu. Timina, S.V. Kovyazin, and A.A. Tomilenko
V.S. Sobolev Institute of Geology and Mineralogy SB RAS, Novosibirsk, Russia

SAMPLE DISCRIPTIONS

Avacha volcano (53°15'N, 158°51'E) is one of the most active stratovolcanoes at the southern Kamchatka. The recent volcanic activity started in the late Pleistocene. Volcanic cone and soma are built up of basalts, andesite-basalts and andesites, containing the ultramafic xenoliths. Spinel harzburgites are dominant among the ultramafic xenoliths of Avacha volcano while lherzolites, verlites, websterites, clinonopyroxenes occur scarcely. The majority of previous publications were dedicated to the study of peridotite xenoliths (Koloskov, 1999; Ishimaru et al., 2009; Ionov, 2010). Our research is based on the study of melt inclusions in minerals of pyroxenite xenoliths from the Avacha volcano.

Pyroxenites consist mainly of clinopyroxene, (Mg# - 0.86-0.89; in wt.%: Cr_2O_3 – 0.1-0.4, Al_2O_3 – 0.8-2.2, TiO_2 – 0.1-0.2, MnO – 0.1-0.22, CaO – 21.7-23, Na_2O – 0.2-0.35), orthopyroxene (Mg# - 0.84-0.87; in wt.%: Cr_2O_3 – 0.0-0.5, Al_2O_3 – 1-2.3, MnO – 0.2-0.35, CaO – 0.82-1.11) and amphibole (Mg# - 0.81-0.86; in wt.%: Cr_2O_3 – 0.15-1.8, Al_2O_3 – 7.2-11.4, TiO_2 – 0.4-1.1, CaO – 10.4-12, Na_2O – 1.6-2.3, K_2O – 0.1-03. Rarely the studied xenoliths contain olivine relics with crystal-fluid inclusions.

PHASE COMPOSITION OF MELT INCLUSIONS

Primary silicate melt inclusions were found in clinopyroxene and amphibole. All melt inclusions in clinopyroxene belong to three types: 1) normal melt inclusions, containing at room temperature fluid, glass and daughter amphibole (Fig.1-a); 2) anomalous melt inclusions, where the main part of the volume is occupied by a fluid phase with small rim of silicate glass around; 3) combined melt inclusions, containing fluid phase, glass and trapped crystals of amphibole, orthopyroxene, spinel (Fig.1-b).

Amphibole contains silicate anomalous and combined melt inclusions. Phase composition of anomalous melt inclusions is glass + single or multiple bubbles (Fig.1-c). Combined melt inclusion: fluid ± glass + xenogeneic clinopyroxene (Fig.1-d).

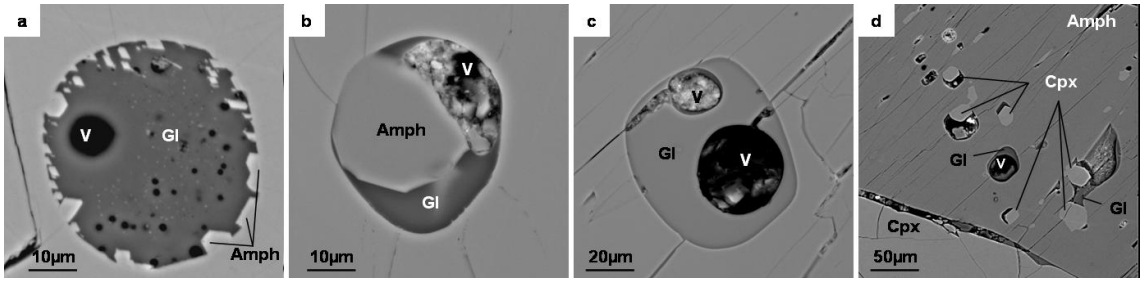

Figure 1:. *SEM BSE images of primary melt inclusions in minerals of pyroxenite xenoliths from Avacha volcano. (a) normal melt inclusion in clinopyroxene, (b) combined melt inclusion in clinopyroxene , (c) an anomalous melt inclusion in amphibole, (d) combined melt inclusions in amphibole. Cpx – clinopyroxene, Amph – amphibole, Gl – glass, V – fluid phase.*

CHEMICAL COMPOSITION OF MELT INCLUSIONS

According to the electron microprobe analysis, the glass compositions of primary melt inclusions are close to the andesitic melts (SiO_2 is 59 – 63.6 wt.%). The glasses of normal melt inclusions in clinopyroxene are characterized by the lower contents of mafic components and alkalies in comparison to the glasses of anomalous and combined melt inclusions (Table 1). The low total of EMP analyses of glasses in normal melt inclusions may suggest significant water contents.

Table 1. Chemical composition of glasses of primary melt inclusions in minerals from the pyroxenite xenoliths of Avacha volcano (wt.%).

type of inclusion	Unheated							homogenized		
	Normal			Anomalous		Combined		Normal		
host mineral	Cpx	Cpx	Cpx	Cpx	Amph	Cpx	Amph	Cpx	Cpx	Cpx
SiO_2	63.63	62.73	60.06	62.61	60.43	61.24	59.90	60.99	63.51	61.13
TiO_2	0.17	0.18	0.17	0.34	0.17	0.32	0.22	0.19	0.17	0.16
Al_2O_3	16.81	16.36	17.34	17.23	18.57	18.63	18.94	17.03	16.97	17.79
Cr_2O_3	0.00	0.03	0.00	0.06	0.04	0.01	0.04	0.01	0.04	0.02
MgO	0.07	0.08	0.05	1.46	1.93	2.17	0.53	0.54	0.58	1.00
FeO	0.52	0.54	0.54	2.84	3.79	2.99	2.32	2.32	1.96	1.47
MnO	0.05	0.02	0.05	0.07	0.11	0.04	0.08	0.07	0.07	0.02
CaO	3.45	3.55	4.25	3.96	5.75	3.69	4.52	4.01	3.80	4.46
Na_2O	1.67	3.10	3.21	5.30	3.36	3.76	2.86	2.33	1.18	1.39
K_2O	0.81	0.98	1.00	1.37	1.28	1.23	0.74	1.14	0.82	0.71
Total	87.18	87.57	86.67	95.25	95.43	94.08	90.14	88.62	89.10	88.15

THERMOMETRY

The thermometric experiments with clinopyroxene-hosted inclusions were performed using the high-temperature heating stage with argon atmosphere. The first evidence of a glass softening was observed at ≈ 900°C; daughter amphibole disappeared at 990-1010°C. Homogenisation temperatures for primary normal melt inclusions in clinopyroxene range from 1040 to 1090°C. Notably, some daughter amphibole reappeared during rapid quenching of inclusions.

DISCUSSION

Melt inclusions in clinopyroxenes from pyroxenite have similar phase and chemical composition to inclusions from clinopyroxenes of recrystallized and metasomatized peridotite xenoliths of Avacha volcano. Similar homogenisation temperatures were measured previously for the primary nomal melt inclusions in clinopyroxene from metasomatized peridotite xenoliths (Tomilenko et al., 2010). The chemical composition of clinopyroxenes from both types of xenoliths (pyroxenites and metasomatized peridotites) is also identical. The data obtained indicate that the pyroxenites should be interpreted as a final product of metasomatic transformation of "primary" mantle peridotites beneath Avacha volcano described earlier (Tomilenko et al., 2010; Timina et al., 2012).

ACKNOWLEDGEMENTS

This work was supported by the Russian Foundation for Basic Research (grant no. 12-05-00888).

REFERENCES

Koloskov A.V., 1999. Ultramaphic inclusions and vulcanite as a self-regulated geological system. World science, 200 p. (in Russian)

Ishimaru S., Arai S., 2009. Highly silicic glasses in peridotite xenoliths from Avacha volcano, Kamchatka arc; implications for melting and metasomatism within the sub-arc mantle. *Lithos*, **107,** 93-106.

Ionov D.A., 2010. Petrology of mantle wedge lithosphere: new data on supra-subduction zone peridotite xenoliths from the andesitic Avacha volcano, Kamchatka. *J. Petrol*.**, 51**, 327-361.

Tomilenko A.A., Kovyazin S.V., Sharapov V.N., et al., 2010. Metasomatic recrystallisation and melting of ultrabasic rocks of mantle wedge beneath Avacha volcano, Kamchatka. *ACROFI III and TBG XIV Abstract Volume*, 248-249.

Timina T.Yu., Kovyazin S.V., Tomilenko A.A., 2012. The composition of melt and fluid inclusions in spinel of peridotite xenoliths from Avacha volcano (Kamchatka). *Doklady RAN*, **442**, 239-243.

Metal transport and deposition vis-à-vis fluid inclusion study: Sona Pahari gold prospect, Sonbhadra District, U.P., India

G. S. Tiwari
Fluid Inclusion Lab, Petrology Division, Geological Survey of India, Lucknow-226024, INDIA
Present Address: Geological Survey of India, North Eastern Region, Shillong-793003, INDIA
email: gstiwarigsi@gmail.com

The Sona Pahari (literal meaning - *mountain of gold*) Gold Prospect, Sonbhadra district, U.P. (India), is situated in the central part of the Mahakoshal Belt representing low-grade metamorphic rocks of the Mahakoshal Group of Proterozoic age. This has been further subdivided into two formations, viz. older, Agori Formation and younger Parsoi Formation along with late intrusives like quartz veins, basic dykes and leucocratic granites. Gold mineralisation occurs in both the Agori and Parsoi Formations and has two modes of occurrences: (1) Disseminated sulphide type (DST), and (2) Quartz vein type (QVT). Gold mineralisation of QVT occurs in two types: (a) mineralisation associated with quartz, carbonate, sulphide and siderite veins developed within the shear zones. Ancient mining activity for gold seems to have been confined to these quartz veins, (gold occurs as "free gold"). (b) mineralisation associated with quartz - carbonate sulphide veins developed along tension fractures in the shear zones. Arsenopyrite, pyrite, pyrrohotite, sphalerite, galena and chalcopyrite arecharacteristically associated with such mineralisation. The quartz-carbonate (rare siderite) veins, in general, show better concentration of gold as compared to quartz / quartz-siderite veins. Wall rock alteration in the form of chloritisation, carbonatisation and clay development is common.

Fluid inclusion microthermometric experiments have been carried out on primary two-phase inclusions in quartz intimately associated with gold mineralisation at Sona Pahari. On the basis of detailed fluid inclusion petrography, three types of fluid inclusion population were identified: Type-I: aqueous-carbonic two-phase inclusion; Type-II: aqueous-two-phase inclusion, and Type-III: monophase inclusion. Opaque mineral grains occur as captive phases in some monophase and two-phase fluid inclusions (Fig.1). The homogenisation temperature for carbonic inclusion varies in the range of 254.7 °C to 371°C (Table 1) and for aqueous inclusions the homogenisation temperature varies from 127°C to 435 °C. The relation of ice/clatherate melting temperatures (interpreted as salinity) with homogenisation temperatures is significant to the fluid processes involved in the genesis and evolution of the ore deposits. To establish the relation between these two parameters a Th vs. salinity plot is shown in Figure 2, which shows an inverse relation indicating a negative correlation trend. It suggests gradual dilution of the parent fluid as it cooled down as a result of mixing with two kinds of fluids. It is possible to assume that mixing of the two fluids (H_2O - CO_2 ± CH_4 and H_2O – NaCl ± $CaCl_2$ ± $MgCl_2$) has played an important role in metal transport and deposition. Furthermore, the frequency plot of the homogenisation temperatures indicates a maxima around 300 °C. However, a similar plot of salinity data shows variable salinity indicating dilution induced by mixing of the fluid. Most of the gold deposits around the world are associated with carbonic fluids i.e., CO_2, CH_4 (Murphy and Roberts, 1997; Klemd and Otto, 1997, 1998; Klemd et al, 1993; Mishra and Panigrahi, 1999). In many mineralisation environments, sulphide complexes are the most effective agent for gold transport. Gold deposition occurred mainly at temperatures between 250 °C and 325 °C, likely due to decrease in sulphur activity accompanying mixing of the two fluids.

Figure 1. *Captive opaque phases in primary two-phase carbonic inclusions*

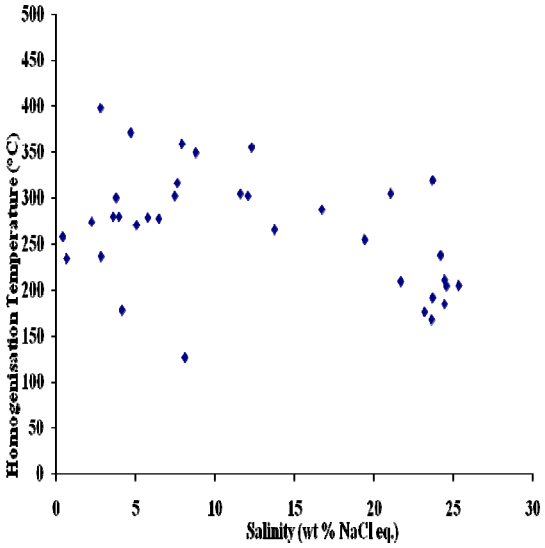

Figure 2*. Plot of the Th vs. Salinity data, Sona Pahari*

Table 1: Microthermometric data of aqueous-carbonic inclusion, Sona Pahari, Sonbhadra district, UP, India

Sample No	TmCO2	Tm (Clath)	Th CO2	XH2O	XCO2	X NaCl	Salinty	Density (Aq)	Density (Carb)	Bulk Density	Th total
SPE-4/Inc.1	-58.5	8.9	11.2	0.8291	0.1651	0.0057	2.196	1.0084	0.8528	0.9525	274
SPE-4/Inc. 3	-57.2	6.1	21.5	0.8846	0.0942	0.0212	7.211	1.046	0.7576	0.9745	273
SPE-4/INC.4	-57.2	8.6	12.7	0.9122	0.0798	0.0087	2.7698	1.01184	0.8411	0.9777	
SPE-4/INC.6	-57	6.5	19	0.9625	0.0167	0.0208	6.5408	1.0414	0.7847	1.0286	257.7
SPP-12/9	-59.1	9.8	26.1	0.9279	0.0708	0.0012	0.4249	0.9933	0.6939	0.9305	300
SPP-12/Inc-10	-57	7.9	23.1	0.9253	0.0626	0.0121	4.0738	1.022	0.7381	0.9710	280
SPP-12/INC.11	-59.8	8.1	15.4	0.9114	0.0778	0.0108	3.706	1.019	0.8185	0.9791	280
SPP-12/INC.12	-60.2	8	27	0.9305	0.0578	0.0116	3.8904	1.019	0.677	0.9577	277.9
SPP-12/INC-13	-58.1	8.2	16.2	0.9255	0.0641	0.0104	3.5207	1.0177	0.8114	0.9827	---
SPP-12/INC.14	-57.2	6.6	22	0.9091	0.0718	0.0191	6.3708	1.0401	0.7518	0.9825	371
SPS-1/INC-36	-58	7.6	24	0.9536	0.0322	0.0142	4.618	1.0263	0.726	0.9963	302
SP-17/52.52M	-62	5.9	8.7	0.9174	0.0595	0.0231	7.5404	1.0493	0.8713	1.0227	270.7
Sp-17-2.52M/INC.19	-60.1	6	8.7	0.8957	0.0823	0.022	7.376	1.048	0.871	1.0128	254.7
SPS-1-52.62m/inc.30	-61.6	7	14.4	0.787	0.1979	0.0146	5.6813	1.034	0.8271	0.9476	304.7
SPS-1/119.60m/inc.49	-57.1	9.8	24,1	0.925	0.0737	0.0012	0.4249	0.9936	0.7246	0.9372	294.7

REFERENCES

Klemd, R. and Ott, S., (1997). Compositional characteristics of fluid inclusions as exploration tool for Au - mineralisation at Larafella, Burkina Faso. *Journal of Geochemical Exploration*, **59**, 251-258

Klemd, R., (1998). High CO_2 of fluid inclusions in gold mineralisation in the Ashanti belt, Ghana: A new category of ore forming fluids ? - a comment: *Mineralium Deposita*, **33,** 317-319.

Klemd, R.., Hirdes W., Olesch M. and Oberthur T., (1993). Fluid inclusion in quartz –pebbles of the gold bearing Tarkwaian conglomerates of Ghana as guides to their provenance area. *Mineralium Deposita,* **28**, 334-343

Mishra, B. and Panigrahi, M.K., (1999). Fluid evolution in the Kolar Gold Field: Evidence from Fluid inclusion studies, *Mineralium Deposita*. **34**, 173-181.

Murphy, P.J. and Roberts, S., 1997. Evolution of a metamorphic fluid and its role in lode gold mineralisation in the central lberian Zone. *Mineralium Deposita,* **32**, 459-474.

Some syngenetic melt and mineral inclusions in the Popigai silica glasses: General features and petrologic significance

S.A. Vishnevsky
Institute of Geology & Mineralogy,3 Koptug prospect, Novosibirsk-90, 630090, Russia

INTRODUCTION

The young, 35.7 Ma-age, well-preserved and good-exposed Popigai 100–km in diameter astrobleme in the Arctic Siberia, Russia, which is one of the most unique terrestrial impact sites, shows a number of various peculiar features, as far as its geology, geochemistry, etc., are concerned (Vishnevsky, Montanari, 1999; Vishnevsky, 2007). Fluid, melt and mineral inclusions in the impact glasses are not the exclusion in this aspect. Earlier, high-pressure water fluid inclusions trapped in mono-mineral glasses at pressures up to 3 GPa in near-surface conditions, were described here (Vishnevsky, Gibsher, 2006; Vishnevsky, 2007; and refs. therein). Below, the melt and mineral (calcite, montmorillonite) inclusions syngenetically trapped in silica glasses are reported.

MIXED IMPACT MELT GLASS INCLUSIONS OF GNEISS-DERIVED COMPOSITION

Immiscible globules of the glasses are very common in lechatelierite and other high-silica glasses from the Popigai impactites. They are present either as jet injections and single inclusions or their groups and even the abundant accumulations in order to form the globular dispersion with the host glass (Fig. 1). Shock experiments show (Vishnevsky, Staver, 1985) that such structures are jet-originated at the boundaries of the various impact melt phases as a result of their dynamic interaction due to high unstable micro flow gradients at shock pressure condition.

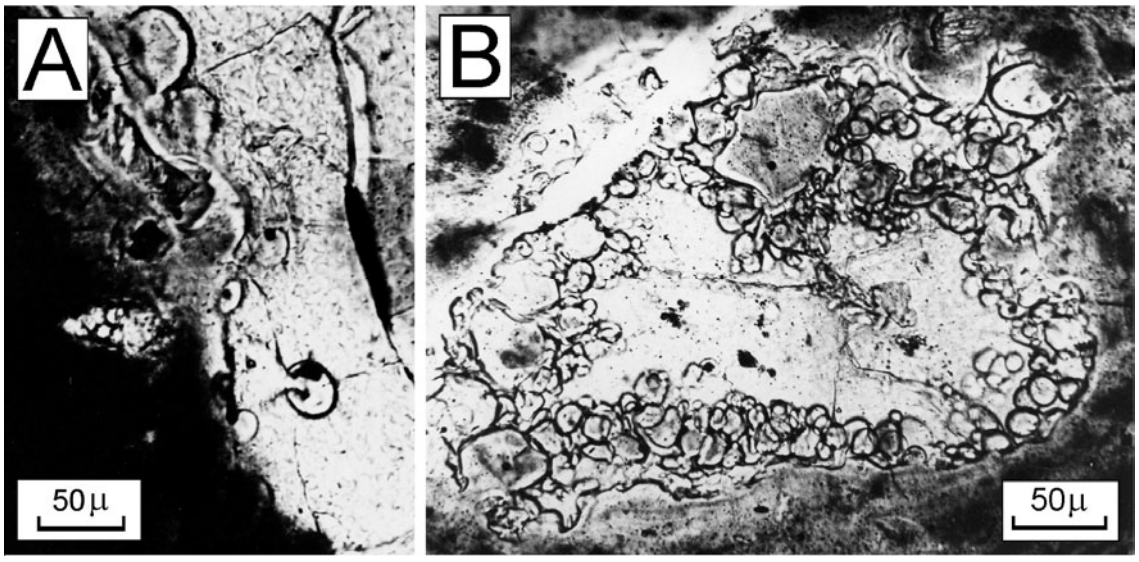

Figure 1. *Mixed impact melt glass inclusions in lechatelierite. A – an initial stage of the jetting into the silica glass; B – more developed stage of the process: mixed glass forms the globular dispersion along the borders of the lechatelierite schlieren. Popigai impact melt rocks. Plane polarized light. Photomicrograph.*

CALCITE INCLUSIONS

Calcite globules are found in lechatelierite (Fig. 2A) as well as in other (high-silica and mixed) glasses. Their shapes show that the carbonate melt was immiscible with the host melts during its ejection from outside at high shock pressures and temperatures (not less that 1700 ^{o}C). The calcite

melt was derived from the Cambrian carbonate member of the Popigai target. The impact melting zones of both the carbonate member and Archean gneiss basement were spatially distant from each other. This fact shows a very mobile state of the interacting components during the impact cratering.

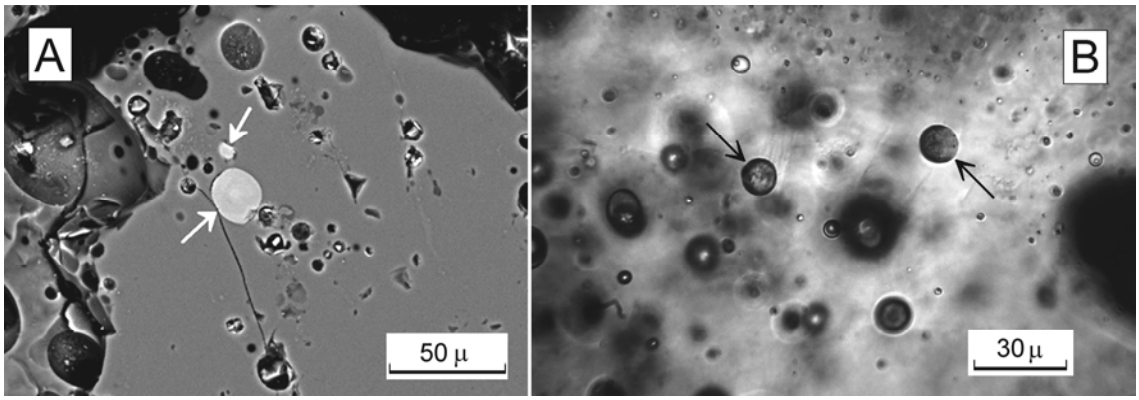

Figure 2. *Arrow-indicated mineral inclusions in lechatelierite from the Popigai impactites. A – globules of calcite, SEM-image. B – montmorillonite globules together with water fluid inclusions of various densities, plane polarized light. Micro photos. After Vishnevsky (2007) and unpublished data.*

MONTMORILLONITE INCLUSIONS

Montmorillonite globules of regular elliptic form are found in the lechateliertes and some other Popigai impact glasses (Vishnevsky, 2007; and refs. therein). The similar ones are also reported for the Ries crater (Osinski, 2003). After (Osinski, 2003) and (Vishnevsky, 2007), these globules are the re-crystallized products of quenched highly hydrous silicate melt, immiscible with the host glass. "Drops" of the melt were ejected from outside, showing a very mobile state of the interacting components during the cratering. Maturated, Na–depleted, and H_2O–saturated sandy-clay Mesozoic-Cenozoic target lithologies could be the potential source for the melts.

CONCLUSION

The data presented (as well as the data on: fluid inclusions in impact glasses; the impact anatexis with the segregation of hydrous Si–Na–K and some other melts; traces of highly-mobile supercritical fluid+melt products with unlimited mixing of the components, etc., earlier reported in papers cited in the reference list below) show that the impact petrology is a very important field of science which is still poorly highlighted in aspect of inclusion studies. In the meantime, the impact processes took an important place in the geologic evolution of the Earth's crust, and origin of its essential components.

ACKNOWLEDGEMENT

This study was supported by RFBG grant #08–05–00408.

REFERENCES

Osinski G.R., 2003. Impact glasses in fallout suevites from the Ries impact structure, Germany: an analytical SEM study. *Meteoritics and Planetary Science,* **38, No.11,** 1641–1667.

Vishnevsky, S.A., 2007. *Astroblemes.* Novosibirsk: "Nonparel Press", 288 pp. (in Russian).

Vishnevsky, S.A., Gibsher N.A., 2006. Water inclusions in lechatelierite from impact fluidizites of the Popigai Astrobleme. *Doklady Earth Sciences,* **409A, No.6,** 802–806.

Vishnevsky, S.A., Montanari A., 1999. Popigai impact structure (Arctic Siberia, Russia): Geology, petrology, geochemistry and geochronology of glass-bearing impactites. *In* Dressler B.O., and Sharpton V.L., eds., *Geological Society of America Special Paper* **339,** 19–59.

Vishnevsky, S.A., Staver A.M., 1985. Some destructive features of deformation and melting in impact metamorphism. *Soviet Geology and Geophysics,* **26, No.2,** 19–27.

Ore-forming property and vertical evolution of the Yinshan Cu-Au-Pb-Zn-Ag deposit, South China and implications for exploration

G. G. Wang[1], P. Ni[1]*, H. Chen[1], Y. T. Cai[1], C. Zhao[1], J. H. Xu[2], and Z. H. Zhang[3]
[1]Institute of Geo-fluids, State Key Laboratory for Mineral Deposits Research, School of Earth Sciences and Engineering, Nanjing University, China
[2]Geological Exploration Company of Jiangxi Copper Corporation, China
[3]Yinshan Lead & Zinc Company of Jiangxi Copper Corporation, China
* Corresponding author: peini@nju.edu.cn

INTRODUCTION

The Yinshan Cu-Au-Pb-Zn-Ag deposit is adjacent to the world-class Dexing porphyry Cu-Au deposits, South China (Fig. 1). This deposit has two types of mineralisation, including the early Pb-Zn-Ag mineralisation controlled by the rhyolitic quartz porphyries, and the late Cu-Au mineralisation associated with the dacitic porphyries. The samples for fluid inclusion studies were collected from +96 m to -1174 m mine levels which give a unique opportunity to obtain the properties and the vertical evolution of ore-forming fluids to constrain the origin of the Yinshan deposit.

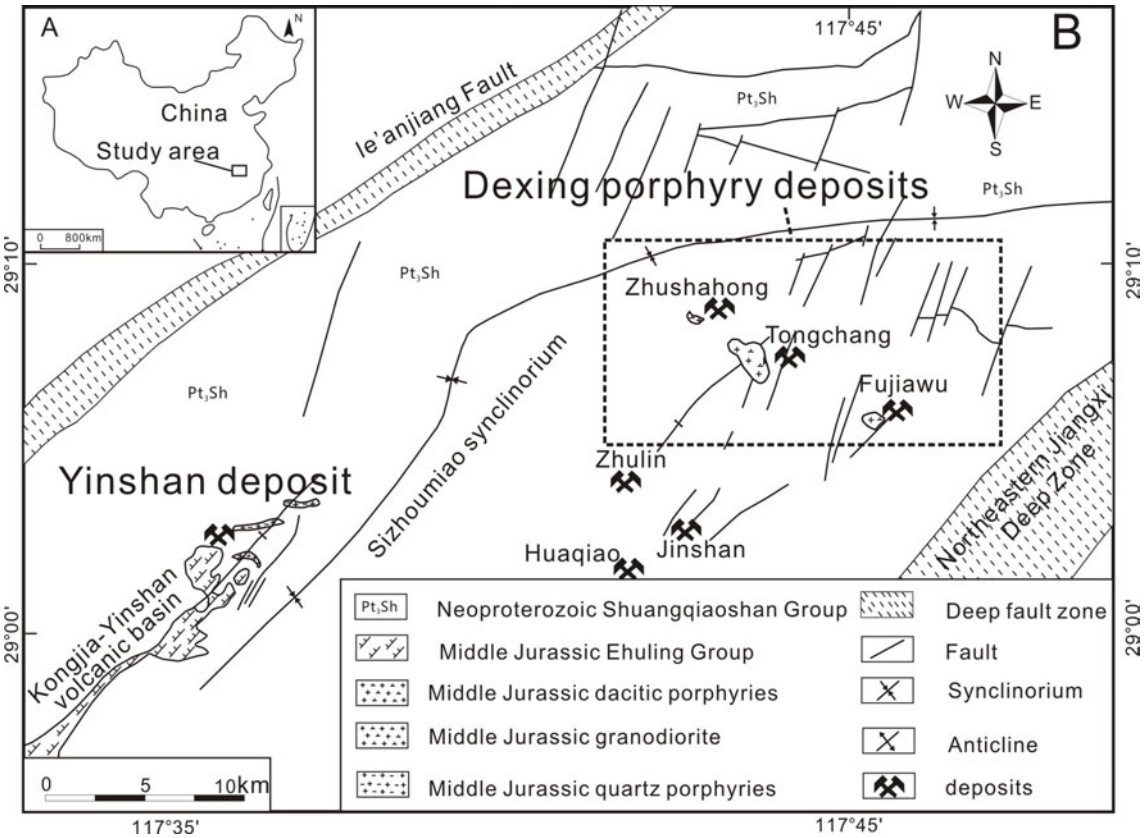

Figure 1: *The location of study area and regional geological map of Dexing region*

PETROLOGY OF FLUID INCLUSIONS

Three types of fluid inclusions can be recognised from samples of sulphide-quartz veins in the Yinshan deposit. Type I liquid-rich, two phase inclusions, and type II vapour-rich, two phase

inclusions are widespread in the two types of mineralized quartz-sulphide veins. Type III halite-bearing inclusions occur locally in the Cu-Au mineralised ore veins from the deep zone and show close association with type II inclusions (Fig. 2).

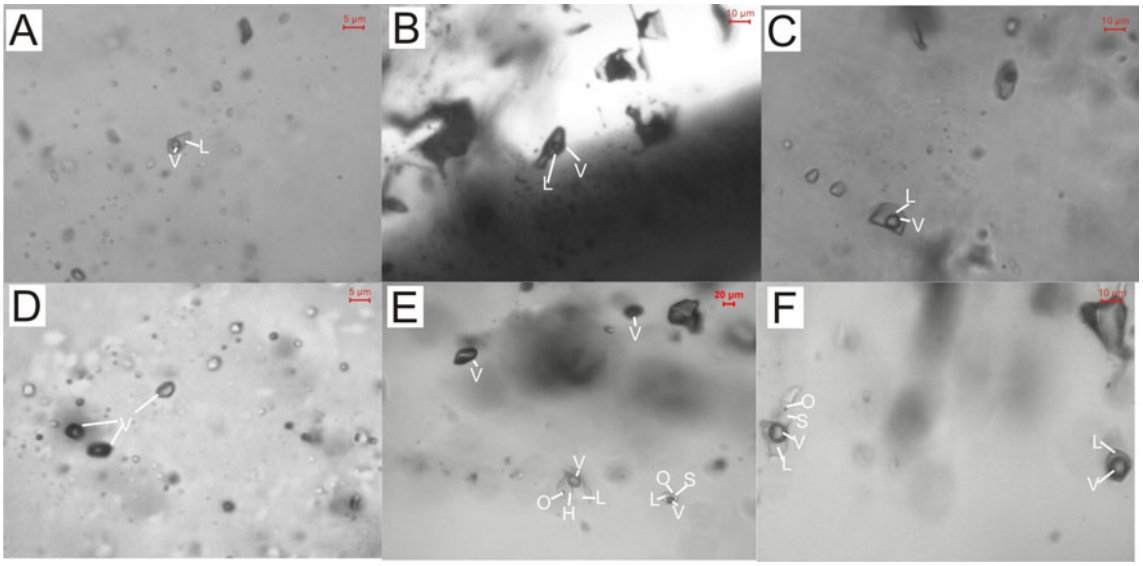

Figure 2: *Photomicrographss of fluid inclusions in the Yinshan deposit. (A) type I inclusions from quartz in Pb-Zn-Ag ore veins; (B) type I inclusions from sphalerite in Pb-Zn-Ag ore veins; (C) type I inclusions from quartz in Cu-Au ore veins; (D) type II inclusions from Cu-Au ore veins: (E-F) type II and type III inclusion assemblage from quartz in Cu-Au ore veins*

RESULTS AND CONCLUSIONS

The type I inclusions in the Pb-Zn-Ag ore body have homogenisation temperatures between 160 to 285 °C and salinities of 3.9 to 9.7 wt. % NaCl equivalent. The type I inclusions in the Cu-Au ore body show homogenisation temperatures between 207 to 351 °C and salinities ranging from 3.6 to 9.6 wt. % NaCl equivalent. The pervasive occurrence of type I fluid inclusions with medium to low homogenisation temperatures (160 to 351 ^{o}C) and medium to low salinities (3.6 to 9.7 wt. % NaCl equivalent) imply that the mineralising fluids formed in an epithermal environment. In addition, the two types of mineralising fluids commonly show a vertical evolution with gradually increase in temperature from the shallow to deep parts, respectively.

The co-existing vapour-rich and halite-bearing inclusions from deep drill hole samples share the similar homogenisation temperature ranging from 289 to 457 ^{o}C, but variable salinities of 0.2 to 4.1 and 30.9 to 36.8 wt. % NaCl equivalent, respectively, which indicates a local boiling event took place at depth in the Cu-Au zones. The local boiling process shows the possibility that porphyry Cu-Au orebodies may exist at even deeper zones.

REFERENCES

JGEB (Jiangxi Geological Exploration Bureau), 1996. Yinshan Cu-Pb-Zn-Au-Ag deposit in Jiangxi Province. Geological Publishing House, Beijing.

Mao, J., Zhang, J., Pirajno, F., Ishiyama, D., Su, H., Guo, C., Chen, Y., 2011. Porphyry Cu–Au–Mo–epithermal Ag–Pb–Zn–distal hydrothermal Au deposits in the Dexing area, Jiangxi province, East China—A linked ore system. Ore Geology Reviews, 43, 203-216.

The study of fluid inclusions of exhalative pipe facies and unstratified ore body in the Xitieshan sedimentary-exhalative lead-zinc deposit

Wang Lijuan[1,2], *Zhu Xinyou*[1], *Wang Jingbin*[1,2] , *Zhu Heping*[2]
[1]*Beijing Institute of Geology for Mineral Resources, Beijing 100012, China;*
Email:wlj@mail.iggcas.ac.cn
[2] *Key Laboratory of Mineral Resources, Institute of Geology and Geophysics, Chinese Academy of Sciences, Beijing 100029, China*

INTRODUCTION

The Xitieshan lead-zinc deposit is located at the northern margin of the Qaidam basin, Qinghai Province and is hosted in intermediate-basic volcanic-sedimentary rocks of an early Paleozoic rift basin. Several origins have been put forward for the deposit, including a hydrothermal type, volcanogenic massive sulphide type and sedimentary-exhalative (SEDEX) type. It is now commonly accepted that the Xitieshan lead-zinc deposit is a SEDEX type deposit, with a complete marine sedimentary-exhalative system, including exhalative pipe facies, vent facies and sedimentary facies. The altered stockwork pipe is long and narrow, >2 km in length and >200 m in width, and consists of mainly quartz and albitite, thus representing the huge exhalative pipe facies. The wall rock marble extends to >3km in length and >1km in width with maximum thickness of >200m and is distributed outside of the altered stockwork rocks, hereby representing exhalative sedimentary rocks. The sulphide ore bodies have two modes of occurrence. One is as unstratified ore body penetrating the thick-bedded marble and is formed as a result of un-erupted ore fluid filling and replacing the marble. It, together with the thick-bedded marble, forms the vent-proximal facies. The other is banded, stratified lead-zinc ore bodies occurring conformably between banded marble and calcareous quartz schist. It is distal from the altered stockwork rocks and forms the sedimentary facies (Zhu et al., 2006 ; 2007). Based on previous studies, in this paper we concentrate on fluid inclusions in carbonates associated with the unstratified ore bodies from both the exhalative pipe facies and vent-proximal facies and then discuss the relationship between fluid evolution and mineralisation.

FLUID INCLUSIONS

1. Results of homogenisation temperature and salinity

The homogenisation temperature (Th), and calculated salinity for inclusions in quartz from altered stockwork rocks and in carbonates from unstratified ore bodies are listed in Table 1

Table 1: Results of Th and Tm measurements and calculations of salinities form the Xitieshan lead-zinc deposit.

Type of samples		The range of Th(℃)	Average Th(℃)	SALINITY RANGE (wt%)	THE AVERAGE OF SALINITY (wt%)
altered stockwork rocks (pipe facies)	stockwork rocks (total)	110-468	284	0-21.7	9.43
	altered breccia	314-468	367	0-18.22	13.31
Carbonate (in unstratified ore bodies)		250-415	322	0-40.61	18.47

2. Laser Raman analysis of individual fluid inclusion

Representative individual fluid inclusions in quartz from altered breccia in the pipe facies were chosen for laser Raman microprobe analysis. They are isolated and regular in shape and have various gas/liquid ratios.

Apart from the peak of the host mineral quartz, only the CO_2 peak is observed in gas inclusions in quartz. Both CO_2 and H_2O peaks can be observed in inclusions with high gas/liquid ratios. No CO_2 peaks and only a H_2O peak is observed in inclusions with intermediate gas/liquid ratios. It is suggested that separation of CO_2 and H_2O may take place due to the opening of the system and decreasing temperature. It is likely that the unmixing results in the deposition of ore minerals.

DISCUSSION

1. Ore fluids of the pipe facies of the sedimentary-exhalative system

Fluid inclusions in quartz from altered stockwork rocks are abundant and have a wide range of homogenisation temperatures and low to moderate salinity. This reflects intense fluid activity and multiple, superimposed fluids. Fluid inclusions in quartz from the altered breccia have moderate to high homogenisation temperatures and moderate salinity and show evidence of boiling at 430 ºC. Because the altered breccia occurs widely in the altered stockwork rocks which are the least affected by later events (Zhu et al., 2007), fluid inclusions from the altered breccia are the most representative of fluids in the sedimentary-exhalative system. They provide the prerequisite for later mineralisation in the unstratified ore bodies.

2. Fluid evolution and mineralisation

Fluid inclusions in quartz from the altered breccia and in carbonates from the unstratified ore bodies are similar. They both belong to the $H_2O-NaCl-CO_2$ system. However, fluid inclusions from the latter have slightly lower homogenisation temperatures, indicating that the fluids migrate from the former to the latter.

Fluid inclusions in quartz from the altered breccia show evidence of boiling at 430 ºC. In combination with the laser Raman microprobe analysis, it is considered that CO_2 in the fluids separates into the vapour phase as boiling continues, resulting in the separation of H_2O and CO_2 phases. With the opening of the system, the high temperature fluids migrate into the neighbouring unconsolidated thick-bedded marble. Accompanied by the escape of CO_2, the temperature and pressure of the fluids decrease. In addition, there is perhaps some involvement of seawater in the ore fluids. All these factors cause the unmixing of fluids with high and low salinity, leading to the deposition of the sulphides that make up the ore bodies. The two unmixed fluids were trapped in unconsolidated carbonates and the ore-forming materials were deposited in the thick-bedded marble to form the sedimentary-exhalative type unstratified ore bodies.

The characteristics of the Xitieshan deposit are similar to those of the Sullivan lead-zinc deposit in Canada in which the ore bodies occur above the breccia pipe and form by hydrothermal mineralisation under the sea floor, accompanied by widespread thermal breccia (Craig et al., 2000).

ACKNOWLEDGEMENTS

This research is supported by the National Natural Science Foundation of China (No. 40672061) and 'National Science Support plan program' (2006BAB01A06) and 'National Basic Research Program of China' (No.2007CB411304).

REFERENCES

Craig, H B., Robert, J W., Katherina, V R., etc., 2000. Wallrock alteration at the Sullivan deposit, British Columbia, Canada. In: The geological environment of the Sullivan Deposit, British Columbia. Edit by: J W Lydon,: *Special Publication* **1**, 633-652.

Zhu Xinyou, Deng Jiniu, Wang Jingbin, Lin Longjun, Fan Junchang, Sun Shuqiu, 2007. Identification and study of stockwork altered pipe of Xitieshan lead-zinc deposit, Qinghai Province. *Geochemistry*, **36(01),** 37-38 (in Chinese with English abstract).

Zhu Xinyou, Deng Jiniu, Wang Jingbin, Lin Longjun and Fan Junchang, 2006. Study of two types of ore bodies in Xitieshan lead-zinc SEDEX deposit , Qinghai Province. *Mineral Deposit*, **25(03),** 0252-0262 (in Chinese with English abstract).

Fluid inclusion study on the Duobaoshan porphyry deposit and Sankuanggou skarn deposit, Heilongjiang, China

Hao Wei[1], Jiuhua Xu[1], Qingdong Zeng[2], Jianming Liu[2] and Shaoxiong Chu[2]
[1] *Resource Engineering Department, University of Science and Technology Beijing, Beijing, China*
[2] *Institute of Geology and Geophysics, Chinese Academy of Sciences, Beijing, China*

GEOLOGICAL SETTING

The NW trending Luohe-Duobaoshan-Sankuanggou metallogenic belt, located in Nengjiang county of Heilongjiang province, China, is the important area for porphyry Cu-(Mo) and skarn Fe-Cu deposit in the Duobaoshan ore field. Frequent tectonic-magmatic events within the Caledonian, Hercynian and Yanshanian have yielded widespread plutonic and volcanic rocks throughout the area. The NW-striking arc tectonic zone, which crops out along a 16 km NW to SE trending area, controls most of the intense hydrothermally altered and mineralised zones. Duobaoshan ore bodies are hosted in a Hercynian granodiorite pluton, which underlies the Ordovician Duobaoshan Formation. East-west striking faults generally formed after mineralisation as a result of later orogenic processes (Wu, 2009). The alteration in the central core of the Duobaoshan porphyry deposit is pervasive and predominantly consist of sericite. The sericite core grades outward into one side of a poorly mineralised potassic halo. The other side grades into a peripherally widespread propylitic alteration. Moreover, the Sankuanggou ore bodies are mainly hosted at the contact zone between the Yanshanian granodiorite and marble, where abundant skarns occur.

FLUID INCLUSION STUDY

Four ore-forming stages are recognised at the Duobaoshan deposit: (I) a potassic and silicic stage; (II) a silicic-molybdenum stage; (III) a phyllic-copper stage; and (IV) a carbonate-quartz stage. Fluid inclusions of stage (I) are characterized by H2O, CO2-H2O and pure CO2, with homogenisation temperatures of 245 - 400 ºC, salinities of 6 - 10 wt% NaCl eq., and those of stage (II) are dominated by H2O, CO2-H2O, daughter mineral-bearing inclusions, with peak homogenisation temperatures of 260 - 300 ºC and salinities of 1.7 to about 39 wt%NaCl eq. Stage (III) is also characterised by H2O and CO2-H2O inclusions, with peak homogenisation temperatures of 200 - 280 ºC, salinities of 0.1-24.8% wt%NaCl eq., whereas stage (IV) inclusions are simply aqueous, with homogenisation temperatures of 125 - 170 ºC, salinities of 0.5 - 12.8 wt% NaCl eq. Respective trapping pressures for stages (I), (II), (III) are 110 - 160 MPa, 58 - 80 MPa, 8 - 17 MPa, and corresponding formation temperatures are 375 - 650 ºC, 310 - 350 ºC, and 210 - 290 ºC respectively. Inclusions within quartz from chalcopyrite-quartz veins at the Sankuangou skarn deposit are characterised by a combination of aqueous, daughter mineral-bearing and vapour-rich inclusions. The homogenisation temperatures of fluid inclusions are 370 ~ 430 ºC, corresponding to salinities of 17.7 ~ 50.85 wt% NaCl eq., which suggests a high temperature and high salinity magmatic hydrothermal fluid; in addition this data suggests a boiling event for the formation of metal sulphides.

ISOTOPE COMPOSITIONS

Hydrogen (δD) and oxygen ($\delta^{18}O$) isotopic compositions for stage (I) fluid at the Duobaoshan deposit range from -87.2 to -95.5 per mil and 7.2 to 8.1 per mil, respectively. In combination this data suggest a magmatic fluid. Stage (III) fluid is characterised by δD values of -82.2 to -104.2 per mil and $\delta^{18}O$ values of 2.0 to 3.4 per mil, which indicates an evolution from magmatic hydrothermal fluid to a mixing magmatic and meteoric fluid. The $\delta^{34}S$ values of sulphides mainly range from -1.6 to -4.6 per mil, suggesting that sulphur predominantly was derived from a deep magma chamber.

CONCLUSION

The Duobaoshan porphyry deposit and Sankuanggou skarn deposit are both associated with magmatic hydrothermal fluids. The immiscibility and boiling of the ore-forming fluids resulted in a

sharp decrease in solubility for metallic sulphides. Besides a magmatic fluid input for the Duobaoshan deposit, distinct mixed fluids, which generally belong to the H_2O-CO_2-NaCl fluid system, were also a dominant factor in the mineralisation. Moreover, the NW trending Luohe-Duobaoshan-Sankuanggou tectonic zone provides access for magmatic hydrothermal fluids which can transfer as well as store minerals. This was a pre-requisite for the formation of super large porphyry Cu-(Mo) deposit during the Hercynian and a skarn Fe-Cu deposit at Yanshanian.

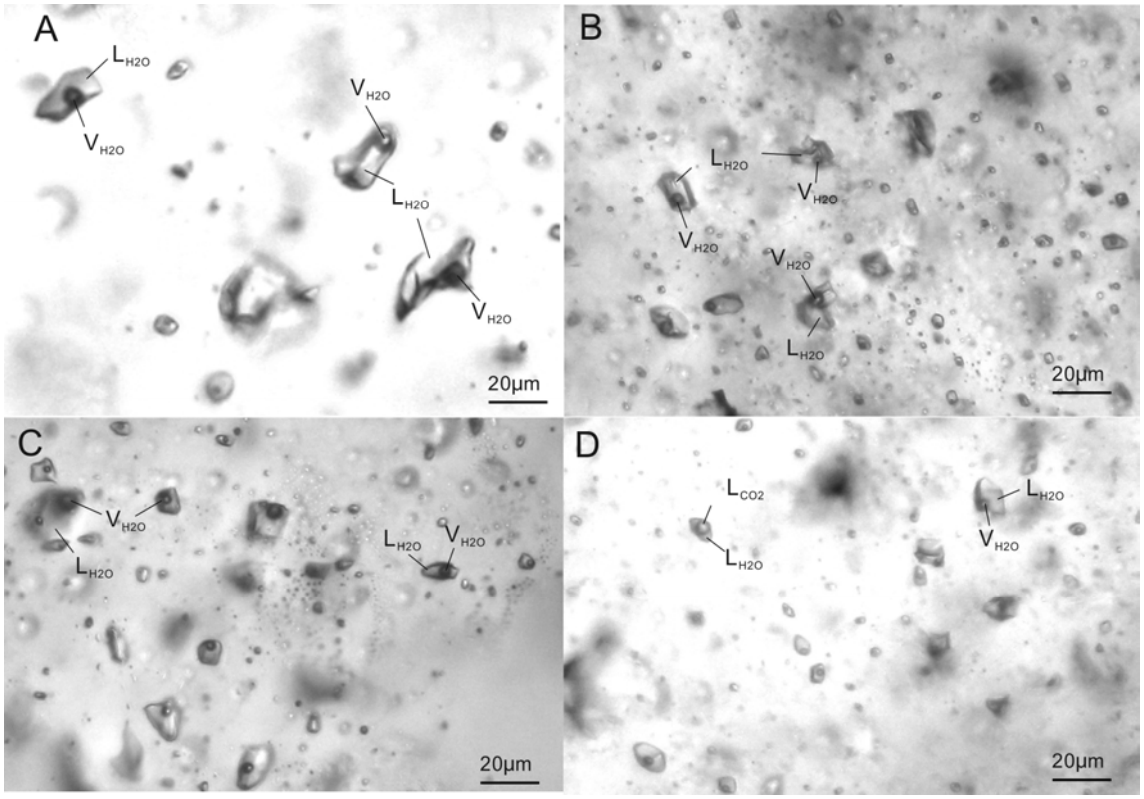

Figure1. *Photomicrographs of fluid inclusions from the Duobaoshan porphyry Cu-(Mo) deposit.*

REFERENCES

Liu, Y., Cheng, X.Z., Wang, X.C., Liu, J.Y., Wang, L. and Wang, X.L., 2008. Cu source and enrichment laws of the Duobaoshan porphyry copper deposit in Heilongjiang province. *Chinese Journal of Geology*, **43(4),** 671-684.

Wu, G., Liu, J., Zhong, W., Zhu, M.T., Mi, M. and Wan, Q., 2009. Fluid inclusion study of the Tongshan porphyry copper deposit, Heilongjiang province, China. *Acta Petrologica Sinica*, **25(11),** 2995-3006.

Fluid inclusion and stable isotope compositions of the Dongchuang-Dongtongyu gold deposits in Xiaoqinling Mt area, China

J.H. Xu[1], L.H. Lin[1], X.G. Wu[1], H. Wei[1], and D.F. Xian [2]
[1] Resource Engineering Department, University of Science and Technology Beijing, Beijing 100083, China
[2] Tongguan Gold Mine, Gold Co., Ltd. of China, Shanxi 714300, China

GEOLOGICAL SETTING

The Xiaoqingling Mt. area, extending from east Shaaxi province to west Henan province, is one of the most productive gold districts in China. The Archean Taihua Group, mainly composed of amphibolite, plagioclase gneiss and migmatites, forms an east-west trending folded structure and is bounded by two regional scale faults—the Taiyao fault on the north side and the Xiaohe fault on the south side (Fig.1). The gold-bearing quartz veins are controlled by a series of east-west shear zones within the Archean Taihua Group, and related to the late Yanshanian (Cretaceous) granite. The principal hydrothermal alteration processes around shear zones are sericitisation, silicification, pyritisation and carbonisation. Four structural stages of mineralisation can be distinguished: (I) a pyrite-quartz stage forming the main bodies of the veins; (II) a quartz-pyrite stage, characterised by abundant pyrite and minor amounts of grey quartz; (III) a carbonate-polymetallic sulphide, including chalcopyrite, galena, sphalerite, pyrrhotite and fine-grained pyrite, associated with siderite, quartz and ankerite; and (IV) a quartz-calcite stage. Stages II and III are the main gold mineralisation stages.

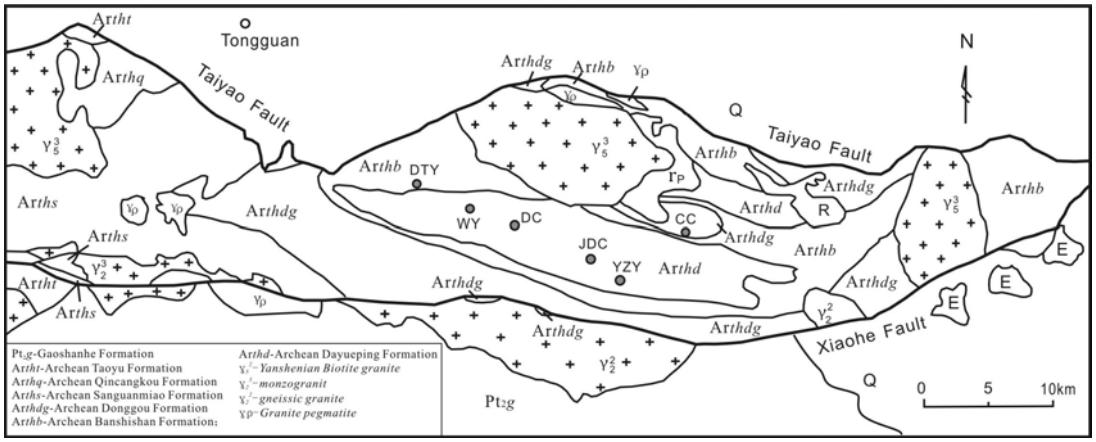

Figure 1. *Regional map of the Xiaoqinling gold province (modified from Jiang et al., 1999).*

FLUID INCLUSION STUDY

Fluid inclusion petrography

Fluid inclusions are abundant in various stages of vein quartz. Three types of primary fluid inclusions can be observed at room temperature. These are: carbonic-aqueous inclusions, carbonic inclusions, and aqueous inclusions. The 5 to 20 μm CO_2-H_2O inclusions are commonly seen in stages I, II, and III. They are two-phase inclusions including an aqueous liquid with 20 to 90 vol. % of CO_2 vapour . The CO_2-H_2O inclusions usually appear as three-phase inclusions with an aqueous liquid phase, CO_2 gas phase (10-40 vol. %), and liquid CO_2 phase (30 to 50 vol.%; Fig.2). Carbonic inclusions are one-phase inclusions with a dense liquid CO_2 phase, which occupies almost 100% of the whole inclusion cavity; they are associated with CO_2-H_2O inclusions. Aqueous inclusions are seen in the late stage mineralisation.

Microthermometry

The homogenisation temperatures (Th) of CO_2-H_2O inclusions range from 221 to 392 ºC , for stage

I, from 205 to 350ºC for stage II, and 224 to 271ºC for stage III, whereas Th of aqueous inclusions for stage IV range from 175 to 185ºC. The salinities of CO_2-H_2O inclusions range from 5.5 to 7.9 wt% NaCl equiv. for stage I, and from 5.1 to 7.1 wt% NaCl equiv. for stages II and III, according to

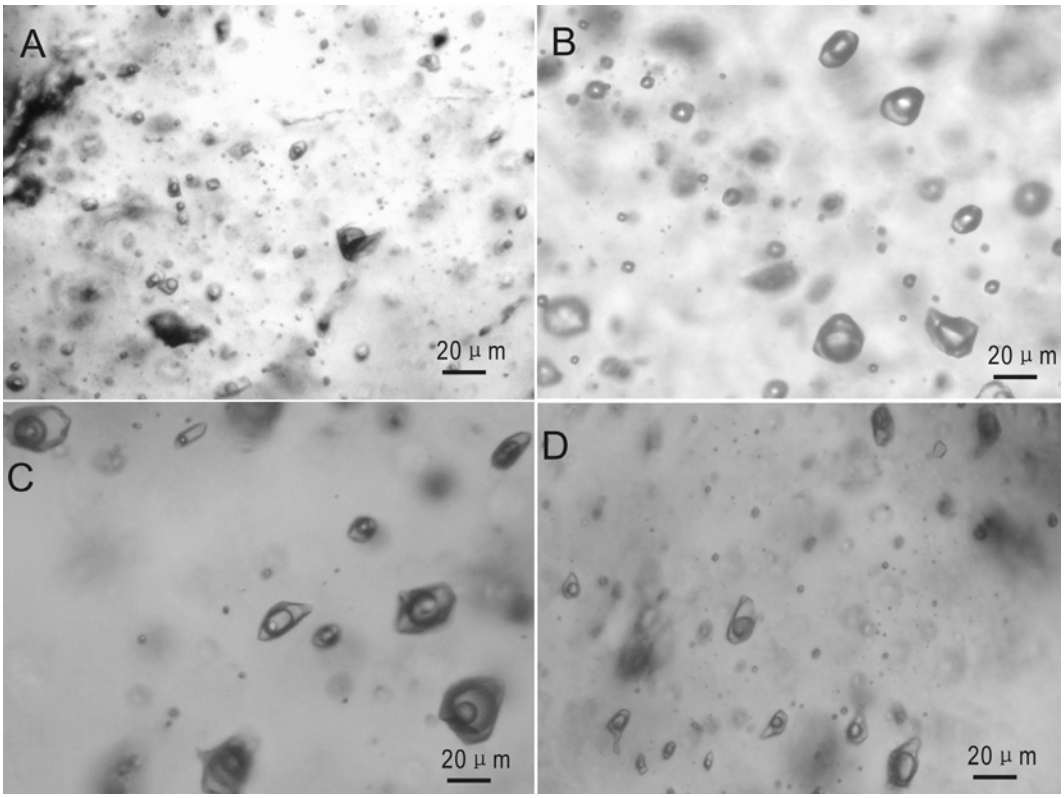

melting temperatures of clathrate. The minimum ore-forming pressures of the gold-rich stage at the Xiaoqinling gold deposits are estimated to be 270 – 290 MPa based on the P-X phase diagram of H_2O-CO_2-NaCl system (Brown and Lamb, 1989).

***Figure 2**. Fluid inclusions in quartz veins of gold deposits in the Xiaoqinling area.*

A.CO_2-H_2O inclusions in pyrite quartz veins, V507, 8-2 (2110m); B. CO_2-H_2O inclusions in white quartz veins (QI), V507, 9-2 (2110m); C. Three-phase CO_2-H_2O inclusions in weakly deformed quartz veins, V531, Ty010 (1300m); D. CO_2-H_2O inclusions in quartz vein (QII+III) near a chalcopyrite grain, Q8, TY028 (550m).

STABLE ISOTOPE GEOCHEMISTRY

The $\delta^{18}O$ values of quartz range from 10.9 to 14.3 ‰ for stage I, and from 7.9 to 9.7 ‰ for stage II. The calculated $\delta^{18}O$-H_2O of fluid inclusions varies from 7.2 to 10.2 ‰ for stage I, and from 4.1 to 5.9 ‰ for stages II and III. The δD of fluid inclusions ranges from –78.1 to -29.5 ‰ for stage I, and from -50.8 to -43.8 ‰ for stages II and III. It is concluded that the water in the hydrothermal fluids, which transports the sulphides and gold could have been mainly derived from a magmatic and/or metamorphic source. The δ34S values for pyrite from the ores range from 2.5 to 8.2 ‰ for stage I, and from 3.7 to 7.1 ‰ for stage II. Those of other sulfides (chalcopyrite, galena and, sphalerite) range from -3.7 to 3.4 ‰.

REFERENCES

Jiang, N., Xu, J.H. and Song, M.X., 1999. Fluid inclusion characteristics of mesothermal gold deposits in the Xiaoqinling district, Shaanxi and Henan Provinces, People's Republic of China. *Mineralium Deposita*, **34**, 150-162.

Brown, P.E. and Lamb, W.M. 1989. P-V-T properties of fluids in the system H2O±CO2±NaCl : New graphical presentations and implications for fluid inclusion studies. *Geochimica et Cosmochimica Acta*, **53**, 1209-1221.

Microthermometric study of melt inclusions in olivine from Barren Island, India

Yadav S.S., Jadhav G.N. and Chandrasekharam D.
Department of Earth Sciences, Indian Institute of Technology,Bombay Powai. Mumbai, India
(sudhanshuyadav@iitb.ac.in,jadhav@iitb.ac.in,dchandra@iitb.ac.in)

INTRODUCTION

The most common mineral hosts being used for the study of melt inclusions in basaltic and related rocks from the study area are olivine, plagioclase and pyroxene. Olivine is often preferred as it is an early formed mineral, together with basaltic magma preserving melt inclusions from the relatively early stages of magmatic evolution and readily trapped melt inclusions in many volcanic rocks (Kent, 2008)

STUDY AREA

Barren Island (India) is an effusive as well as explosive mafic stratovolcano in the Andaman Sea, North-Eastern Indian Ocean. It is the northernmost active volcano of the great Indonesian arc. The volcano is 3 km in diameter, has restricted public access, and no regular monitoring. The volcano is known to have been active from 1787 to 1832 (its "historic" eruptions), when it produced basalt and basaltic andesite tephra and lava flows from a cinder cone located in a 2-km-diameter caldera. The lavas flowed into the sea through a breach in the caldera wall on the western side (Sheth et.al 2011, Luhr and Haldar, 2006).

MATERIAL AND METHODS

The doubly polished wafer thin sections of collected from the study area samples were prepared (thickness of 200-250 μm). The melt inclusions in olivine host mineral were selected for micro-thermometric study. These studies were done on LINKAM-TMS94 heating stage (UK Made) attached with CCD camera. The heating experiment performed under inert argon supply with 5.5-6.5 mbar pressure under vacuum condition. During and after microthermometric study, microphotographs of the melt inclusions were taken using CCD camera and Environmental Scanning electron microscope, respectively.

MICROTHERMOMETRIC STUDY

The microthermometric studies of melt inclusions (Gas bubble+Solid phases) were carried out in olivine host mineral. The heating experiment started at room temperature (25°C) and keeping heating rate of 50°C/min upto 600°C. After 600°C, the heating rate was lowered to 30°C/min till 1300°C. During heating of melt inclusions, we observed the changes after 1100°C-1150°C i.e initiation of melting of gas bubble but could not able to see much changes in the trapped/daughter crystal (solid phase) till 1300°C. Later during cooling of experiment, we kept 50°C/min rate under same inert atmospheric condition for all melt inclusions. During re-crystallisation of melt inclusion, we saw formation of dendritic growth of titanomagnetite(?).

Figure.1 *Microphotograph of Biphase melt inclusion (Gas bubble + Solid) during heating (A) and cooling (B) experiment.*

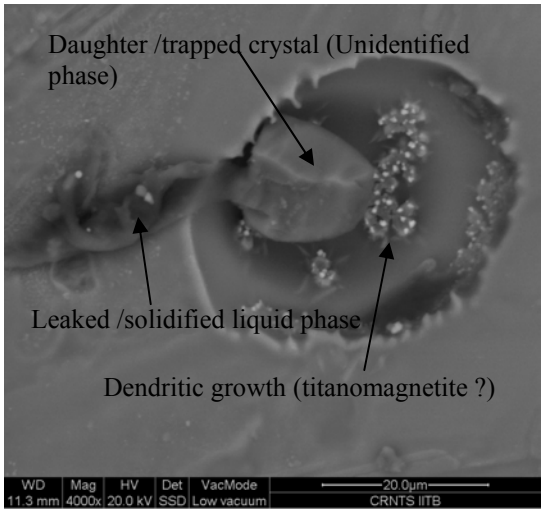

Figure.2 *Backscattered ESEM photograph of melt inclusion (break open cavity)*

RESULTS AND DISCUSSION

We examined several melt inclusions in olivine mineral of andesitic basalt samples and observed trapped/daughter crystal (unidentified crystalline solid) within the cavity and also in break open cavity of the melt inclusions: Fig.1 and Fig.2, respectively. The microthermometric studies indicate homogenisation/melting temperatures of melt inclusions, higher than 1300°C. During heating of melt inclusions, bubble got homogenized at 1250°C but the melting point of trapped solid phase was higher than 1300°C. The re-crystallisation of melt inclusion showed break open cavity containing dendritic growth/skeletal growth of formation and leaked phase (Fig.2). The formation of skeletal growths were started at 1201°C-1210°C and most of the skeletal growth might be titanomagnetite?

CONCLUSION

The microthermometric studies of melt inclusions in olivine host mineral shows homogenisation/melting temperatures higher than 1300°C. The re-crystallisation of a few melt inclusions showed rapid growth of dendritic/skeletal solid phases (titanomagnetite?). During petrographic observation of Barren Island rock samples, we saw the dendritic growth of titanomagnetite inclusions. The formation of dendritic/ skeletal growth could be because of low volume eruption within ocean environment. This study is useful for understanding compositional changes during magma solidification in regards to the study area.

ACKNOWLEDGEMENTS

This work is supported by the Department of Science and Technology, Government of India for research project to Prof.G.N.Jadhav (07DS025). Authors want to thanks, Prof.H.C. Sheth (Department of Earth Sciences, IIT Bombay) and Dr.Jyoti Ray (PRL,Ahemdabad) for providing valuable samples. We also would like to thanks technical staffs of SAIF, IIT-B for ESEM analysis.

REFERENCES

Kent, A J., 2008. Melt inclusions in basalt and related volcanic rocks. Reviews in Mineralogy and Geochemistry, **69**, 273-331.

Luhr, J.F., Haldar,D, 2006. Barren Island volcano (NE Indian Ocean): Island-arc high alumina basalts produced by troctolit contamination of volcanology and geothermal Research, **146**, 177-212.

Sheth, H.C., Ray,J.S., Kumar, A, Bhutani,R.,Awasthi,N., 2011. Tooth paste lava from the Barren Island Volcano (Andaman Sea). Journal of Volcanology and Geothermal Research, **202**, 73-82.

Infrared microthermometric measurement of fluid inclusions from Shalagang antimony deposit in southern Tibet, China

Liang Yeheng[1,2], Mo Ruwei[3],Sun Xiaoming[1,2,3], Zhai Wei[1,2], Wei Huixiao[3], Zhou Feng[3]*
1. School of Marine Sciences, Sun Yat-sen University, Guangzhou 510275, China;
2. Guangdong Provincial Key Laboratory of Marine Resources and Coastal Engineering, Guangzhou 510275, China;
3. Department of Earth Sciences, Sun Yat-sen University, Guangzhou 510275, China

INTRODUCTION

The Himalayan orogenic belt is the youngest and largest collisional orogenic belt worldwide (Yin et al., 2000). During the orogenisis, a series of gold deposits, antimony deposits and gold-antimony deposits, which comprise the south Tibet gold-antimony orogenic belt and lie between the Yarlung Zangbo Suture and the Himalaya north slope. The Shalagang is the most representative antimony deposit of the gold-antimony belt in southern Tibet, but its genesis is still controversial. Some researches think it is an epithermal deposit (Yang et al., 2006), but our study has shown it may be a typical orogenic Sb deposit (Mo et al., 2011). Infrared microthermometry is the direct approach to study the fluid inclusions in opaque minerals. A microthermometric study using infrared microscopy was performed on fluid inclusions hosted in stibnite and symbiotic quartz, in order to directly characterise the physicochemical conditions of ore-forming fluid from the Shalagang antimony deposit.

FLUID INCLUSIONS IN STIBNITE AND QUARTZ

Based on petrographic analysis under the infrared microscope, four types of fluid inclusions have been recognized in stibnite: (I) liquid aqueous inclusions: only one phase of liquid can be seen at room temperature, with no vapor content (Fig.1-A), (II) liquid-rich two-phase fluid inclusions: the liquid and vapour bubble can be seen at room temperature, the vapour phase occupies less than 50% volume (Fig.1-B), (III) gas-rich two-phase inclusions: the liquid and vapour bubble are both visible at room temperature , the gaseous phase occupies more than 50% in volume (Fig.1-C), (IV) pure gaseous inclusions：only vapour phase is present in these fluid inclusions (Fig.1-A). The type II and type III inclusions are the dominant ones. Co-existence of inclusions with variable liquid/vapor ratios manifests that heterogeneous fluids were captured by the inclusions (Fig.1-C). Boiling might

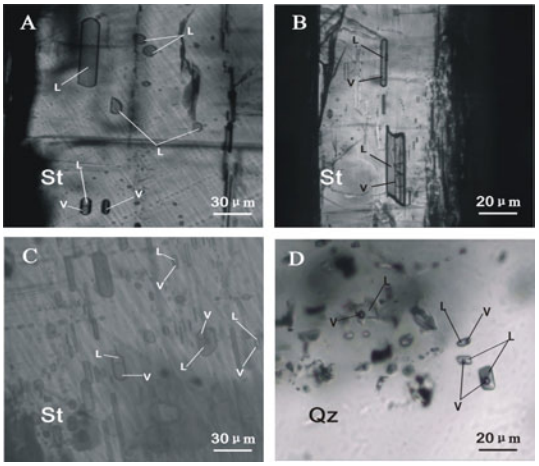

Figure 1 *Fluid inclusions in stibnite (infrared) and symbiotic quartz (normal)*

have occurred when stibnite formed (Roedder, 1984). Results of infrared microthermometry show that fluid inclusions hosted in stibnite have homogenisation temperatures of 134.9～221.9ºC, with a

peak of 160～190ºC, salinity values of 1.65 wt%～7.25 wt% NaCl eqv, with a peak of 5.0 wt%～6.0 wt% NaCl eqv, and density values of 0.879～0.958 g/cm^3,with an average of 0.934 g/cm^3. Fluid inclusions hosted in symbiotic quartz are mostly liquid-rich two-phase inclusions. They have homogenisation temperatures values of 142.5～205.6℃, with a peak of 160～190℃, salinity values of 2.31wt%～6.96wt%NaCleqv, with a peak of 4.0wt%～6.0wt%NaCleqv, and density values of 0.910～0.947g/cm^3,with an average of 0.929g/cm^3. With Laser Raman analysis of fluid inclusions hosted in symbiotic quartz, trace CO_2, N_2, CH_4 gases have been detected (Fig.2). D_{H2O} and $^{18}O_{H2O}$ values of the fluid inclusions in quartz are -162.9~-173.4 (‰) and 7.3~9.3(‰), respectively.

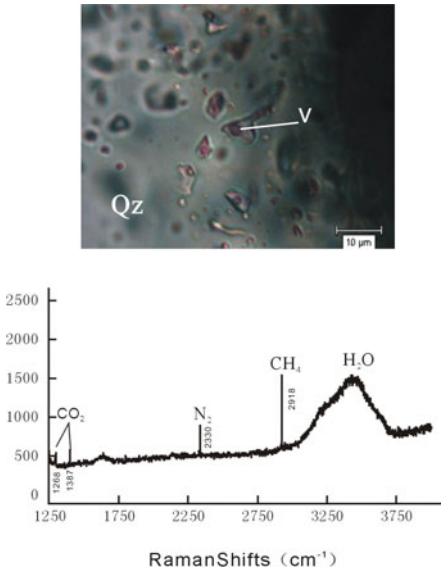

Figure 2 *Laser Raman spectra of fluid inclusions hosted in quartz from Shalagang antimony deposit*

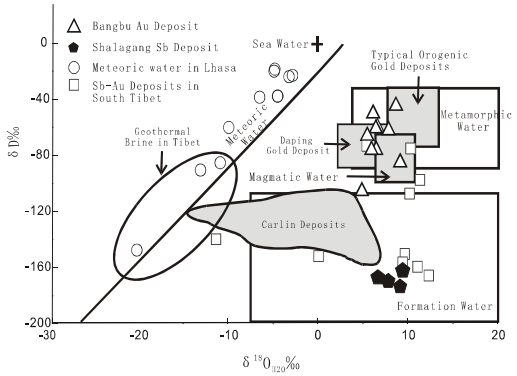

Figure 3 *Plot of δD versus $\delta^{18}O$ for quartz from Shalagang Sb deposit. Magmatic, metamorphic, and formation water after Sheppard (1986); Field for typical orogenic gold deposits after Goldfarb et al. (2004); Field for Nevada Carlin deposits after Field et al. (1985); Field for Daping gold deposit in Ailaoshan gold belt after Sun et al. (2009); Values for antinony and gold deposits in South Tibet after Yang et al. (2006)*

DISCUSSION

A comparative study of fluid inclusions in stibnite and symbiotic quartz from Shalagang indicated that stibnite and quartz formed in the same physicochemical conditions and captured the same ore-forming fluids. Laser Raman analysis of fluid inclusions hosted in symbiotic quartz shows that the ore-forming fluids of the Shalagang antimony deposit belong to the NaCl-H_2O fluid system which is characterised by low homogenisation temperatures, low salinity, low density and trace CO_2, N_2, CH_4 gases, which is similar to ore-forming fluids in orogenic gold deposits. The boiling of ore-forming fluid is the dominant factor for stibnite deposition. D_{H2O} and $^{18}O_{H2O}$ values of quartz plot within the area of formation water (Fig.3), suggesting that ore-forming fluids are formed by circulation of atmospheric water and the formation water in the stratum.

ACKNOWLEDGEMENTS

This study was financially supported jointly by the National Natural Science Foundation of China (No. 40830425, 40673045, 40373027), the National Key Basic Research Program (No.2009CB421006, 2002CB412610) from the Ministry of Science and Technology, China, Higher school specialized research fund for the doctoral program funding issue (No. 200805580031), (No. 20100171120009), Young teachers started funding scheme of SYSU (No. 42000-3181401)and the

Project Supported by Guangdong Province Universities and Colleges Pearl River Scholar Funded Scheme (2011).

REFERENCES

Field C W and Fifarek R H. 1985, Light stable-isotopic systematics in the epithermal environment. *Reviews in Economic Geology*, **2**:,99-128.

Goldfarb R J, Ayuso R, Miller M L et al. 2004,The Late Cretaceous Donlin Creek gold deposit, Southwestern Alaska: Controls on epizonal ore formation. *Economic Geology*, **99(4)**, 643-671.

Roedder, E., 1984. Fluid Inclusions. Mineralogical Society of America, Michigan, USA*, Reviews in Mineralogy*, **12**, 644p.

Sheppard SMF. 1986, Characterization and isotopic variations in natural waters. *Reviews in Mineralogy*, **16**, 165-183.

Sun X M , Zhang Y, Xiong D X, et al. 2009. Crust and mantle contributions to gold-forming process at the Daping deposit, Ailaoshan gold belt, Yunnan, China. *Ore Geology Reviews*, **36(1-3)**, 235–249.

Mo RW, Sun XM, Zhai W,. et al. 2011. Infrared fluid inclusion microthemometry from Shalagang antimony ore in southern Tibet, China. *Acta Petrologica Sinica* (in press)

Yang ZS, Hou ZQ, Gao W et al. 2006. Metallogenic characteristics and genetic model of antimony and gold deposits in south Tibetan detachment system. *Acta Geological Sinica*, **80(9)**, 1377-1391 (in Chinese with English abstract).

Yin A and Harrison TM. 2000. Geologic evolution of the Himalaya-Tibetan orogen. *J. Ann. Rev. Earth Planet. Sci*., **28**, 211-280.

Fluid inclusion characteristics and genetic model of the Neoproterozoic Jinshan gold deposit, Jiangxi province, South China

Chao Zhao, Pei Ni, Junying Ding, Guoguang Wang, and Yingfeng Xu*
Institute of Geo-fluids, State Key Laboratory for Mineral Deposits Research, School of Earth Sciences and Engineering, Nanjing University, China
**Corresponding author: peini@nju.edu.cn*

INTRODUCTION

The Jinshan gold deposit, located in the northeast of Jiangxi Province, South China, is a world-class ductile shear zone-hosted gold deposit (see Figure 1), which is located in the Neoproterozoic Shuangqiaoshan Group. Two types of gold mineralisation can be distinguished in this deposit: (1) auriferous ultra-mylonite, and (2) quartz vein-type within ductile shear zones. Previous studies mainly focused on ore deposit geology (Wei, 1996), ore formation ages (Mao et al., 2008), and He-Ar isotope of ore-forming fluids (Li et al. 2010). However, the characteristics and evolution process of ore-forming fluids is poorly investigated. In this paper, we show systematic fluid inclusion data to constrain the genetic type and origin of this ore deposit.

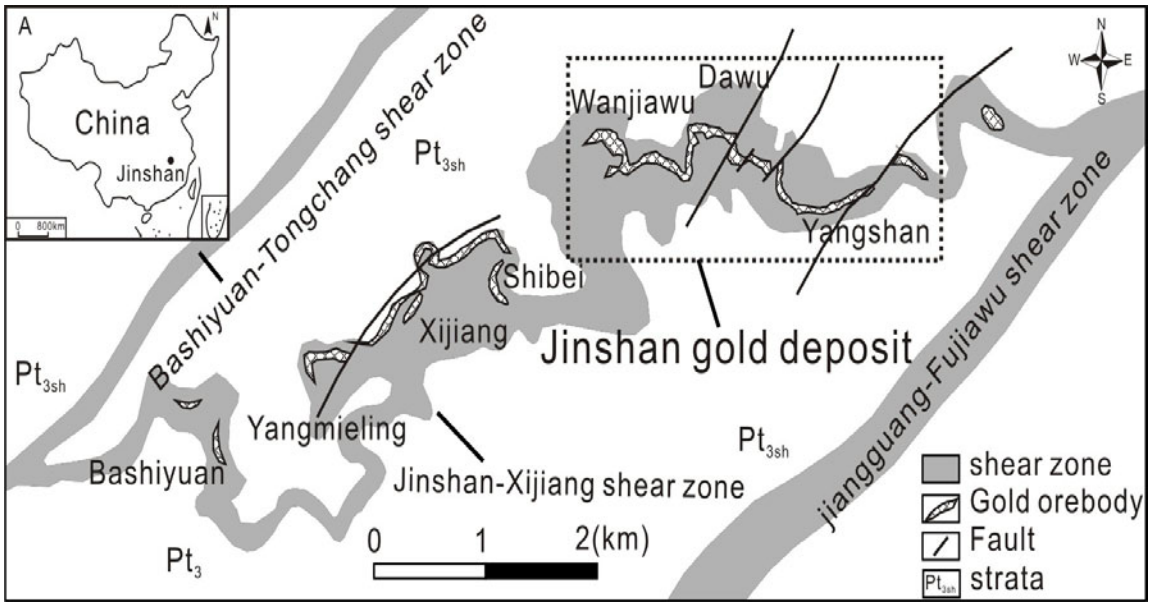

***Figure 1**: Location and simplified geological map of the Jinshan gold deposit.*

FLUID INCLUSION STUDIES

Liquid-rich, two phase aqueous inclusions (type I) and two/three phase CO_2–bearing inclusions (type II) can be recognised in auriferous quartz veins of the Jinshan gold deposit (see Figure 2).

The type I fluids show homogenisation temperatures from 242 to 289 ^{o}C and salinities from 2 to 5.3 wt. % NaCl equivalent. The vapour-rich type II inclusions with vapour/liquid ratio between 0.7 and 0.9 yield homogenisation temperatures between 241 and 261 ^{o}C and salinities from 3.7 to 7.6 wt. % NaCl equivalent.

CONCLUSIONS

The above mentioned two types of coexisting fluid inclusions have similar homogenisation temperatures and contrasting salinities, indicating immiscibility had occurred during gold ore

formation. Stable isotope data show that the ore fluids are of metamorphic origin. The occurrence of ductile shear zone controlled ore-bodies and fluid immiscibility during ore formation, are consistent with the stable isotope data, and demonstrate that the Jinshan gold deposit is a typical orogenic gold deposit.

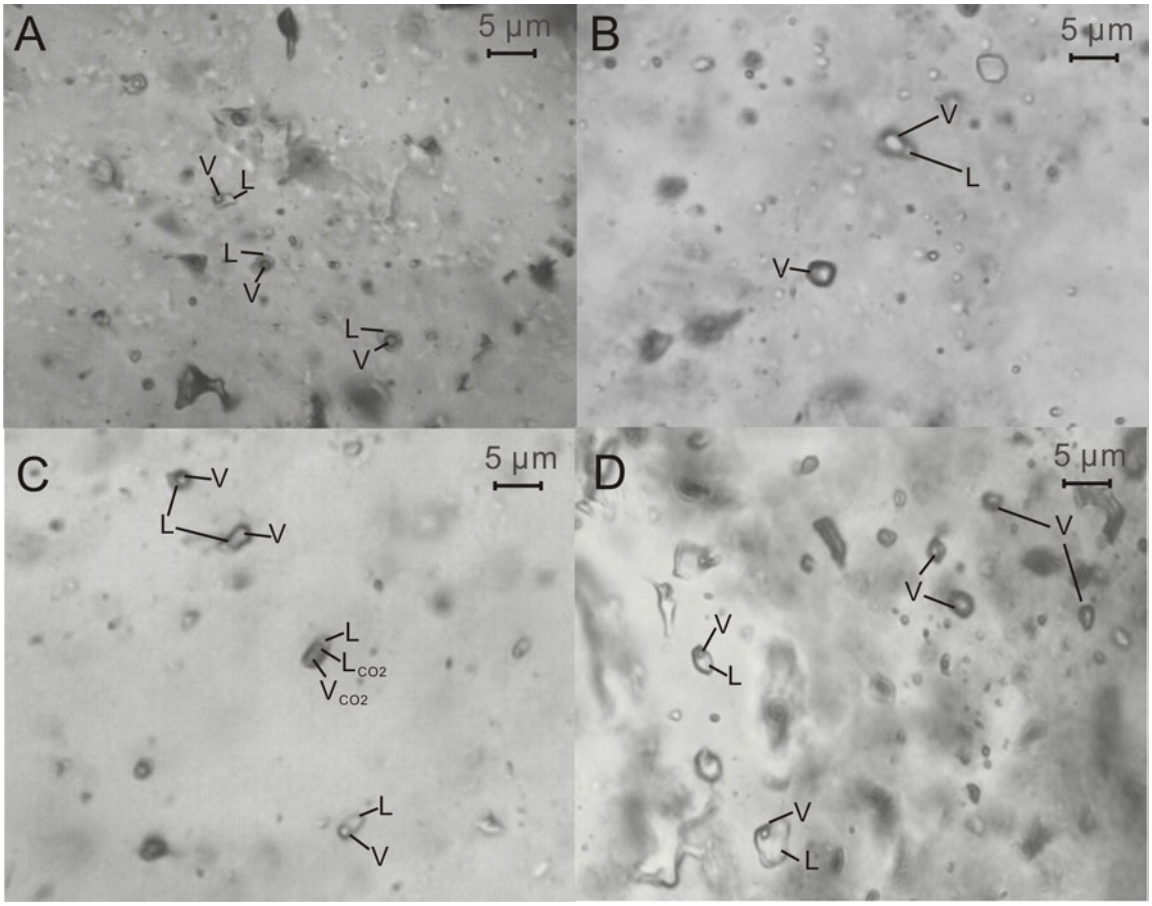

***Figure 2**: Photomicrographs of fluid inclusions from an auriferous quartz vein in the Jinshan gold deposit. (A) type I inclusions, (B) type II inclusions, (C-D) type I and type II fluid inclusion assemblage.*

REFERENCES

Li, X., Wang, C., Hua, R., Wei, X., 2010. Fluid origin and structural enhancement during mineralization of the Jinshan orogenic gold deposit, South China. *Mineralium Deposita*, **45**, 583-597.

Mao, G., Hua, R., Gao, J., Long, G., Lu, H., 2008. Rb-Sr age of gold-bearing pyrite in the Jinshan Gold Deposit, Jiangxi Province. *Acta Geoscientica Sinica*, **29**, 599-606.

Wei, X.L., 1996. The geological characteristics of Jinshan ductile shear zone-type gold deposit in Jiangxi. *Jiangxi Geology*, **10**, 52-64